Biogeochemical Signatures of the Great Lakes Watersheds

by

Qualbe Shadman T. Chowdhury

A thesis

presented to the University of Waterloo

in fulfilment of the

thesis requirement for the degree of

Master of Applied Science

in

Civil Engineering

Waterloo, Ontario, Canada, 2018

Author's Declaration

I hereby declare that I am the sole author of this thesis. This is a true copy of the thesis, including any required final revisions, as accepted by my examiners.

I understand that my thesis may be made electronically available to the public.

Abstract

Water quality in many regions of the Great Lakes Basin (GLB) has deteriorated due to numerous anthropogenic drivers, including increases in agricultural area, increased fertilizer use, intensive livestock production, and increases in human population densities. Excessive nutrient inputs from both point and non-point sources have accelerated eutrophication in inland watersheds and in receiving water bodies, and policy goals have recently been set to reduce phosphorus loading to Lake Erie by as much as 40%. Under such pressures, it is crucial to better our understanding of nutrient transport across the GLB and to identify key watershed drivers of both seasonal and annual nutrient loading from watersheds to the lakes. In this research study, I have utilized numerous metrics to characterize nutrient dynamics in Great Lakes Watersheds across a gradient of human impacts and have attempted to identify key controls on biogeochemical signatures. As a part of this work, I paired water quality data from over 200 Great Lakes watersheds with land use and climate data to identify dominant controls on stream nutrient concentrations at the annual, seasonal, and event scales. At the annual scale, standardized regression analysis identified significant relationships between flow-weighted concentration (FWCs) and selected catchment characteristics. FWCs were found to be strongly linked to land-use variables such as combined agricultural and urban land, wetlands and tile drainage. Our quantification of these relationships was used to create spatial maps of annual nutrient concentrations and loads and to identify nutrient hotspots across the GLB. Specifically, high nutrient concentrations and export were observed in the Maumee and Sydenham River catchments, whereas lower concentrations and loads were found in Lake Superior catchments. At the seasonal scale, three primary seasonal nutrient regimes were identified: (1) 'in-phase' (positive correlation between monthly concentrations and discharge), (2) 'out-of-phase' (negative correlation), and (3) 'stationary' (no significant relationship). While in-phase seasonality was found to be the most common concentration regime for watersheds with higher levels of agricultural land use, nitrate seasonality in particular was found to be muted in watersheds with the highest agricultural land use, but to be more extreme in watersheds with less agriculture but higher amounts of forested area and higher wetland densities. Out-of-phase seasonality was found to be significantly associated with higher population densities and higher percent urban areas. At the event-scale, concentrations were found to be more variable with discharge for phosphorus than for nitrate. Additionally, Lake Erie showed significantly lower concentration variability in relation to discharge compared to all the other Lakes. As the Lake Erie basin also has higher agricultural land use than the other lakes, the more chemostatic concentration dynamics in these watersheds appears to be linked to agricultural nutrient use and suggests that agricultural nutrient legacies may be an important driver of current patterns in nutrient delivery to the lakes.

Acknowledgements

Ever since I began my work on this research project, I was constantly reminded of a quote that was said by the legendary civil rights leader Malcom X: “There is no better than adversity. Every defeat, every heartbreak, every loss, contains its own seed, its own lesson on how to improve your performance next time.”

Firstly, I wish to thank Dr. Nandita Basu for the opportunity, support and guidance of my master’s research project. I also wish to thank Dr. Kimberly Van Meter for her extensive help and guidance throughout the course of this work. Both Dr. Basu and Dr. Van Meter have been instrumental in helping me develop and improve my academic skills. I also want thank Dr. Bryan Tolson and Dr. Robert Gracie for reviewing my thesis, as well as providing improvements and constructive feedback towards my thesis.

To Dr. Mahyar Shafii, I want to thank you for not only continuing to be an incredible mentor, but also providing a constant beacon of support during the most trying of times. Thank you for being patient with me, for teaching me invaluable lessons not just in statistics, but the pursuit of happiness, and for believing in my ability to achieve.

The staff and co-op students at the Geospatial Center in Dana Porter library were all very kind and helpful, especially during the early stages of my work when my GIS experience was non-existent. Thank you for instilling the teachings and lessons of GIS onto me and I hope students continue to appreciate the invaluable resources you provide.

To the individuals I can proudly call my close friends, I am grateful to Idhaya and Tejasvi for their help and support. From sharing our grad student woes, to engaging in thought-provoking discussions regarding the meaning of life, and everything in between, I will treasure the memories.

Finally, I want to thank my mom for her unyielding love and support throughout this eventful journey, and hope that the strength, courage, and prayers that she continuously provides will take me where I need to be next. Thank you for always being by my side.

Table of Contents

List of Figures

List of Tables

1.0 Introduction

1.1 Background

Eutrophication can be defined as the excessive growth of plants and algae from increased nutrient inputs such as phosphorus (P) and nitrogen (N), resulting in the depletion of dissolved oxygen in rivers, streams, lakes, and other water bodies (D.W. Schindler, 2006; Yang, Wu, Hao, & He, 2008). Although eutrophication can occur naturally in aquatic ecosystems, excessive nutrient inputs from anthropogenic sources can cause great ecological harm to receiving water bodies (Smith, Joye, & Howarth, 2006). Furthermore, the acceleration of eutrophication from additional nitrogen and phosphorus inputs can result in harmful algal blooms (HABs), which are typically dominated by cyanobacteria (Downing, Watson, & McCauley, 2001; Smith et al., 2006). Cyanobacterial blooms in eutrophic waters can severely degrade aquatic ecosystems by generating toxins that can kill aquatic species, promote anoxic (oxygen-depriving) conditions in aquatic environments, reduce species diversity, and produce undesirable taste and odour in drinking water (Downing et al., 2001). Cyanobacterial blooms have been observed both locally and globally in eutrophic water bodies. For example, in May 2007, Lake Taihu, China's third largest freshwater lake, experienced severe toxic cyanobacterial blooms, which were caused by nutrient enrichment from urban and agricultural development, as well as warm spring temperatures (Qin et al., 2010). In Canada's Lake Winnipeg, notable increases in cyanobacteria have been observed since the mid-1990s as a result of P loadings from increased production of livestock and fertilizer application, as well as larger and more frequent spring floods in the Red River watershed (David W. Schindler, Hecky, & McCullough, 2012). Although many studies have explored the causes and effects of eutrophication, remediation and efforts to prevent the production of harmful algal blooms are still ongoing in many regions, including some of the Great Lakes (i.e. Lake Erie) in North America.

The Laurentian Great Lakes house almost 21 percent of the world's supply of surface fresh water and are an indispensable source of clean drinking water to over 24 million individuals across Canada and the United States (Environment Canada & U.S. Environmemntal Protection Agency, 2014). In the 1960s, excessive algal blooms were identified as a major threat to the water quality of the Great Lakes (Beeton, 2002). Algal bloom occurrences and eutrophication have also been

noted in tributary watersheds within the basin (Scavia et al., 2014). Eutrophication in the Great Lakes regions has been attributed to increases in P export from agricultural watersheds, population increase, and excessive use of phosphorus-laden detergents (Dove & Chapra, 2015), and is considered a threat to public health, recreational activities, tourism, fisheries, and drinking water across many communities. To address these problems, the Great Lakes Water Quality Agreement (GLWQA) was signed in 1972 between Canada and the United States (IJC, 1972). This agreement set water quality objectives for the Lakes and emphasized the assurance of Canada and the United States in implementing pollution control programs that target municipal and industrial sectors (IJC, 1972). Revisions to the agreement have since been made to expand the objectives of protecting the Great Lakes Basin by focusing on the 'restoration of the Great Lakes Basin Ecosystem' rather than just improving water quality through pollution control (IJC, 1978). In particular, a requirement to reduce P loadings and to meet specified concentration targets has been added to the 1978 GLWQA. This mandate has prompted regulatory authorities within Canada and the United States to develop control measures to reduce point-sources of P from sewage treatment plants (IJC, 1972; Dove & Chapra, 2015). Legislation to reduce the P content in detergents was first introduced in Canada during the 1970s, and was later followed by many U.S. States, including Illinois (the first State to limit phosphorus content in detergents), New York, Ohio, Michigan, and others (Litke, 1999). The policy change resulted in a reduction in total P loading and improved water quality conditions in the lakes up to the late 1980s (De Pinto, Young, & McIlroy, 1986; Dolan & Chapra, 2012). Since the mid-1990s however, there has been a resurgence of algal blooms, particularly from Lake Erie, which has become more eutrophic, as evident by the increases in cyanobacteria (Scavia et al., 2014).

In 2011, Western Basin of Lake Erie experienced one of its largest algal blooms, potentially caused by intense precipitation events during the spring season, in combination with long-term agricultural and land-use practices, resulting in large bioavailable dissolved reactive phosphorus (DRP) export to the lake (Michalak et al., 2013). The re-eutrophication of Lake Erie, as well as the degradation of water quality in streams and rivers have led to revisions in the GLWQA to target present ecological issues in the Great Lakes Basin (Fryefield, 2013). For example, Annex 6 (Aquatic Invasive Species) highlights control strategies to reduce populations of existing invasive species such as Dreissenid Mussels that may harm the Great Lakes (Canada & USA, 2013). Annex 9 (Climate Change Impacts) has also been added to address the impacts of climatic

conditions in the Great Lakes Ecosystem (Canada & USA, 2013). Annex 4 (Nutrients) emphasizes the importance in reducing nutrient loads (specifically P) and improving regulations of point source and non-point source loading in open waters (Canada & USA, 2013; Fryefield, 2013). The commitment of meeting phosphorus targets was further evident in 2015 with the agreement between the Canadian and U.S. government agencies to reduce phosphorus loadings by 40 percent (IJC, 2016). Addressing these present challenges requires identifying hotspots of pollution, assessing non-point sources of nutrient pollution, and quantifying seasonality and dominant controls of nutrient concentrations to effectively manage efforts in restoring water quality in the Great Lakes watersheds.

1.2 Watershed Signatures

In the recent past, there has been increasing interest in characterising watersheds based on easily identifiable metrics or "signatures" (Sivapalan, 2005). Such signatures can be used to describe, in a meaningful and practical manner, the hydrological variability that may be observed both spatially and temporally, and can potentially be linked with a range of catchment properties, including climate, soils, and land-use inputs (Sivapalan, 2005). Hydrographs, for example, provide temporal observations of discharge within a catchment. Metrics associated with visualized data such as hydrographs provide different and more organized ways of understanding catchment functionality, and can be easily compared across catchments at different scales, in different landscapes, and across varied climate conditions. Commonly used signatures that focus on streamflow response include inter-annual (e.g. year-to-year) streamflow patterns, regime curves (i.e. monthly-average streamflow behaviour), flow duration curves, and rainfall-runoff relationships such as the runoff coefficient (McMillan et al., 2014; Merz & Blöschl, 2009; Sivapalan, 2005). Hydrological signatures that focus on temporal or seasonal variability provide insights into different processes occurring within the catchment during specified time periods (Sivapalan, 2005). For example, south-eastern catchments in the U.S. (e.g. Georgia and Florida) have been shown to have strong seasonal precipitation that is 'in-phase' with potential evapotranspiration, whereas precipitation in western catchments of the U.S. (e.g. California and Idaho) exhibits 'out of phase' behaviour with potential evapotranspiration (Ye, Yaeger, Coopersmith, Cheng, & Sivapalan, 2012). Linking climate characteristics (that are spatially

consistent) to seasonal streamflow patterns becomes important when establishing a classification system for dominant processes, and relating catchments at a regional scale (Ye et al., 2012).

Other hydrological signatures have also been used to identify key hydrologic patterns of watersheds. Some of these signatures include the time of concentration, defined as the time required for a droplet of water to travel from the most remote part of the catchment to the outlet (Aronica & Candela, 2007; Grimaldi, Petroselli, Tauro, & Porfiri, 2012); recession curves, defined as the decrease in measured discharge after a storm event (Brutsaert & Nieber, 1977; Harman, Sivapalan, & Kumar, 2009; Kirchner, 2009; Stoelzle, Stahl, & Weiler, 2013; Vogel & Kroll, 1992); and water age and residence time distributions (Sivapalan, 2005). These signatures help further our understanding of hydrological processes and can be used to estimate flood frequencies (Merz & Blöschl, 2009), improve the accuracy of hydrological models for streamflow estimation in ungauged basins (Grimaldi et al., 2012; Gupta, Wagner, & Yuqiong, 2008), and assist in classifying watersheds based on land-use and climatic characteristics (Price, 2011; Stoelzle et al., 2013).

Work regarding the identification of biogeochemical signatures is relatively limited compared to hydrologic signatures; however, many studies within the past decade or more have begun to explore explicit linkages between hydrology and biogeochemical processes (Asano, Uchida, Mimasu, & Ohte, 2009; Burt & Pinay, 2005; Cirmo & McDonnell, 1997; P. M. Haygarth, Condron, Heathwaite, Turner, & Harris, 2005; Seibert et al., 2009). More recently, studies have explored controls on nutrient export at larger spatial scales using regression-based models in order to determine the source of these problems such as excessive eutrophication, and to establish effective remediation options to restore water quality (Robertson & Saad, 2011; Sinha & Michalak, 2016).

One of the simplest biogeochemical signatures for a watershed could be considered to be the mean annual concentration or average annual loads of important solutes. Prediction of average nutrient loads, however, can be challenging due to the large temporal and seasonal variability in nutrient export, as well as the common use of sparse concentration datasets as a basis for the load estimation. Furthermore, exploring the spatial variability of mean annual concentrations across multiple catchments, without accounting for flow variability, can be misrepresentative when identifying dominant controls from catchment properties such as land-use, soil characteristics,

and climate. A simple alternative is the use of *flow-weighted* concentrations (FWC) as a metric (Basu, Thompson, & Rao, 2011). Flow-weighted concentrations are calculated as the sum of the product of concentration and discharge divided by the total sum of discharge (Godsey, Kirchner, & Clow, 2009). Use of flow-weighted concentrations rather than simple mean values for concentration or annual loads allows us to avoid issues related to high flow-variability across years while still adequately accounting for discharge-driven differences in concentration.

1.2.1 Statistical Methodologies to estimate seasonal and annual loads from sparse concentration data

As mentioned above, one of the continuous challenges in studying water quality is estimating stream solute loads. Specifically, the problem involves estimating average load based on sparse concentration measurements taken a few times during a year, coupled with daily mean discharge magnitudes. Many methodologies have been developed to estimate load, including simple averaging methods based on field measurement data, ratio estimators, and multiple regression models (or rating curves), which estimate concentration as a function of selected explanatory variables (Aulenbach & Hooper, 2006; Cochran, 1977; Cohn, 2005; Dolan, Yui, & Geist, 1981; Hirsch, Alexander, Smith, & Geological, 1991; Hirsch, Moyer, & Archfield, 2010; Preston, Bierman, & Silliman, 1989; Runkel, Crawford, & Cohn, 2004; and others). A common regression approach used in many studies is the LOAD ESTimator (LOADEST) model (Cohn, 2005; Runkel et al., 2004). The LOADEST model estimates the natural-log of concentrations as a function of explanatory variables such as time, season, and discharge. Additional explanatory variables can also be added or removed from the model. For example, the L7 model is seven-parameter LOADEST model that estimates the natural-log concentration as a function of the natural-log of discharge (in quadratic form), time (in quadratic form), and season (as a sinusoidal function) (Cohn, Caulder, Gilroy, Zynjuk, & Summers, 1992; Hirsch, 2014). Estimated natural-log concentrations are transformed back by taking the exponent and multiplying by a bias correction factor (BCF). This correction factor is applied in order to take into account that the expected value of concentration is not the exponent of the expected value of natural-log concentration (Cohn, 2005; Hirsch, 2014). Although the LOADEST model provides unbiased estimates of solute flux when model assumptions are met (Cohn, 2005), the accuracy of load

estimates is reduced when conditions move away from the model assumptions. These issues include 1) lack of a quadratic fit between concentration and discharge, 2) changes in seasonal patterns between concentration and discharge over time, 3) changes in concentration patterns with respect to high or low flows, and 4) lack of homoscedasticity in the residuals of the LOADEST model (Hirsch, 2014). Many studies that have relied upon the LOADEST model have led to poor estimation of nutrients loads, including catchments draining into Lake Decatur in Illinois (Guo, Markus, & Demissie, 2002), major river systems in Iowa and the Des Moines Lobe (Stenback, Crumpton, Schilling, & Helmers, 2011), and several watersheds draining into the Chesapeake Bay basin (Moyer, Hirsch, & Hyer, 2012).

A more recent regression model developed by Hirsch et al., 2010 called the Weighted Regression on Time, Discharge and Seasons (WRTDS), was developed to address the issues found in the LOADEST model. The model equation for WRTDS is in some ways similar to the LOADEST model, as it relies upon time, discharge, and season as explanatory variables. WRTDS, however, estimates a unique set of coefficients at every estimation point. This is achieved by applying weighted regressions, where the weights are calculated as function of the 'distance' between the estimated point and the sample points in time, discharge, and seasons (Hirsch et al., 2010). A key advantage of WRTDS over LOADEST is its ability to create many unique models of concentration, in which the coefficients vary based on time, discharge, and seasons across the period of record (Hirsch et al., 2010; Qian Zhang, Harman, & Ball, 2016). In contrast, concentration estimates from LOADEST assume fixed coefficients over all times, discharges and seasons, making it less dynamic and adaptable versus the WRTDS model (Hirsch, 2014; Qian Zhang et al., 2016). Numerous recent studies have utilized WRTDS for load estimation, including those carried out for the Mississippi River (Sprague, Hirsch, & Aulenbach, 2011), Lake Champlain tributaries (Medalie, Hirsch, & Archfield, 2012), and the Susquehanna River Basin (Q. Zhang, Brady, & Ball, 2013; Qian Zhang et al., 2016).

1.2.2 Dominant Controls on Stream Nutrient Concentrations

Numerous important controls on nutrient concentrations and loads have been identified, including annual and seasonal precipitation (Piñol, Ávila, & Rodà, 1992; Sinha & Michalak, 2016), antecedent moisture conditions (Biron et al., 1999) and nutrient uptake (Ensign & Doyle,

2006; Von Schiller et al., 2008). In addition, human-impacted watersheds (with primarily agricultural or urban activity), has been shown to be a key driver of stream water quality and nutrient export. The influences of land use on stream ecosystems range from increases in sedimentation and nutrient concentrations, to changes in hydrologic conditions and a loss of riparian vegetation (Allan, 2004). Many studies have explored the impacts of land use on stream water quality as well as the impacts of nutrient export in relation to geomorphology, soil characteristics and climate (Arheimer & Lidén, 2000; Carpenter et al., 1998; Hill, 1978; Johnson, Richards, Host, & Arthur, 1997; Sharpley et al., 1994; and others). Quantifying land use as a dominant control on stream water quality is important for the mitigation of excessive eutrophication and the development of effective watershed management practices for healthy stream ecosystems across the Great Lakes Basin.

Stream nutrient concentrations are highly influenced by land use, particularly with regards to increases in agricultural activities and urbanization. Many studies have found the application of N and P fertilizers, which can lead to non-point source runoff, to be a dominant source of nutrient export in streams and rivers (e.g. Arheimer & Lidén, 2000; Han & Allan, 2008; Hill, 1978; Johnson et al., 1997; Tian et al., 2016). Accordingly, the development of new conservation measures or management practices to mitigate issues of nutrient pollution, leads to the importance of mitigation efforts regarding stream water quality by addressing best management practices (BMP), which includes reducing the amount of fertilizers used in the landscape, adopting conservative tillage practices and minimizing anthropogenic impacts at a watershed level (Allan, 2004).

Artificial and subsurface drainage systems can also be a significant control on nutrient concentration-discharge dynamics within a catchment by reducing surface flow and transferring excess precipitation to subsurface flow (Blann, Anderson, Sands, & Vondracek, 2009; Tian et al., 2016). The presence of these drainage systems may lead to further degradation of water quality in streams, rivers and lakes, as subsurface flow bypass riparian vegetation, which allows for the uptake of nutrients and overall reduction of nutrient export in lotic ecosystems (Blann et al., 2009). Poorly managed drainage ditches, created as a result of nutrient transport from tile and subsurface drainage, can impact stream water quality. Specifically, nitrogen and phosphorus

losses from drainage ditches can result in increased cultural eutrophication and degradation of stream ecosystems within the Great Lakes Basins (Ahiablame, Chaubey, Smith, & Engel, 2011).

Urbanized landscapes also significantly affect hydrology and water quality in catchments across the Great Lakes. Increased development of impervious areas can cause major alterations in hydrology, including higher degrees of surface runoff from storm events (Paul & Meyer, 2001). More surface runoff may lead to poor nutrient filtration due to decreased hydraulic residence time (HRT), a lack of biological activity, and the removal of plants and vegetation that facilitate nutrient uptake (Allan, 2004; Paul & Meyer, 2001; Tian et al., 2016). Sources of nutrient export from urban (non-point source) runoff may include lawn fertilizers, pet waste, and poor operation of septic systems. (S. Carpenter et al., 1998). Additionally, wastewater and sewage treatment plants act as point sources and can be a major contributor to water quality degradation in streams, rivers and lakes (S. Carpenter et al., 1998; Paul & Meyer, 2001). Understanding the impacts of biogeochemical processes in relation to extensive urbanization of catchments is critical to reducing eutrophication in streams and receiving water bodies.

1.2.3 Relationship between concentration and discharge

Quantifying the relationship between concentration and discharge is important in understanding catchment behaviour (Musolff, Schmidt, Selle, & Fleckenstein, 2015; Thompson, Basu, Lascurain, Aubeneau, & Rao, 2011). Soil erosion, dynamic fluctuations in climate, and the continuous growth of agricultural, and urban development can affect both biogeochemical processes and the hydrological conditions of catchments (Musolff et al., 2015). Concentration-discharge relationships for a range of nutrients and solutes have been studied over decades in landscapes that range from forested basins (Band, Tague, Groffman, & Belt, 2001; Creed & Band, 1998; Fiorentino et al., 2003; P. Haygarth et al., 2004; Hedin, Armesto, & Johnson, 1995; Valett, Crenshaw, & Wagner, 2002) to more recent agricultural and humanly impacted catchments (Basu et al., 2010; Musolff et al., 2015; Schwientek, Osenbrück, & Fleischer, 2013; Thompson et al., 2011). Additionally, hysteresis loops extrapolated from concentration-discharge plots have been used to construct mixing models based on different flow components (e.g. event water, soil water and groundwater) in order to determine the timing of solute mixing (Chanat, Rice, & Hornberger, 2002; Evans & Davies, 1998; Godsey et al., 2009). Analysis of

concentration-discharge patterns across larger spatial areas are beneficial in determining the effects of vegetation, soil type, and climate within the landscape (Likens & Buso, 2006). Although many studies have explored event-scale concentration-discharge dynamics, very little has been done in conjunction with seasonal and annual time scales. Additionally, studies focusing on biogeochemical processes have primarily been carried out at local scales (Likens & Buso, 2006). Therefore, there is a need to characterise and understand concentration-discharge dynamics at larger scales to clarify the nature of anthropogenic impacts on the environment, to assist in the prediction and forecasting of biogeochemical patterns, and to expand the role of policy and decision-making (S. R. Carpenter, 2002; Clark et al., 2001; Likens & Buso, 2006).

Watersheds are generally considered to be either 'chemostatic' or 'chemodynamic' depending upon the nature of event-scale relationships between concentration and discharge. A chemostatic response occurs when concentrations remain relatively constant in time over significant fluctuations in discharge. Conversely, chemodynamic behaviour occurs when concentrations increase or decrease with discharge (Basu et al., 2010; Godsey et al., 2009; Thompson et al., 2011). Chemostatic solute dynamics were first identified for geogenic species such as calcium, magnesium, and silica and have been explained by the nearly unlimited supply of these weathering-related solutes across a range of landscape types (Godsey et al., 2009; Thompson et al., 2011). More recently, it has been noted that nutrients in anthropogenic landscapes, where decades of fertilizer application and intensive livestock production have led to an accumulation of legacy stores of nutrients in soils and groundwater (Basu et al., 2010; Musolff et al., 2015; Thompson et al., 2011; Van Meter & Basu, 2015), may also exhibit chemostatic behavior. This phenomenon is considered parallel to the chemostatic response of geogenic solutes. For phosphorus species, although legacy stores can also develop under intensive agriculture (Bruland, Grunwald, Osborne, Reddy, & Newman, 2006), chemodynamic responses have frequently been observed in agriculturally dominated catchments (Musolff et al., 2015; Thompson et al., 2011). This chemodynamic response can potentially be attributed to threshold-driven transport of phosphorus such as the erosion of stream banks. Additionally, concentration-discharge dynamics of soluble and total phosphorus may likely be influenced by the degree of sorption onto soil particles, particularly from sediments that reside at the channel bottom of streams and rivers (Thompson et al., 2011).

The relationship between concentration C and discharge Q identified in the literature has been found to follow a power law relationship:

$$C = aQ^b \tag{1}$$

in which a and b are constants (Godsey et al., 2009). Concentration data are typically sparse, whereas discharge measurements are more continuous (e.g. instantaneous or daily averages) throughout the period of record (Hirsch, 2014; Lee et al., 2016). The exponent of the power law relationship (or equivalently, the slope of the C-Q relationship on log-log scale) provides a physical interpretation of the catchment. A slope of near-zero indicates that the catchment behaves 'chemostatically' (i.e. concentrations remain constant under variable discharge). A negative b-slope indicates a dilution signal and a positive slope shows an accretion pattern. Transforming the power law relationship (1) into linear form yields the following:

$$\ln C = \ln a + b \ln Q + \varepsilon \tag{2}$$

in which ε is a random error term. Slope-*b* magnitudes near zero (with a dilution signal) have been observed for geogenic solutes such as calcium, magnesium, sodium and silica in minimally human impacted catchments (Godsey et al., 2009). These slope-*b* values, however, are not a sufficient metric for characterizing watershed solute behavior as chemostatic or chemodynamic because concentration variability can still be present with near-zero slope values. In particular, changes in solute concentrations may not be significantly associated with changes in discharge, and concentrations may still show considerable variability due to a range of factors, from fluctuations in temperature and plant nutrient uptake (Duncan, Welty, Kemper, Groffman, & Band, 2017) to the presence of intermittent anthropogenic point sources. An alternative metric that has proven useful (Musolff et al., 2015; Thompson et al., 2011) is the ratio between the coefficient of variation for concentration, (CV_C) and the coefficient of variation for discharge (CV_Q), as defined below:

$$\frac{CV_C}{CV_Q} = \frac{\mu_Q}{\mu_C}\frac{\sigma_C}{\sigma_Q} \quad (3)$$

The CV ratio (CV_C/CV_Q) provides a robust measure of variations in concentration in relation to variations in discharge, with smaller CV ratio values being indicative of chemostatic behavior. Low CV ratios for geogenic compounds, and consequently chemostatic behaviour, have been consistently observed in multiple catchments within the U.S. and Germany (Musolff et al., 2015; Thompson et al., 2011). In contrast, higher CV ratios and hence more chemodynamic export have generally been found for phosphorus species in agriculturally dominated watersheds (Musolff et al., 2015; Thompson et al., 2011). The CV ratio describes the variability of concentration with respect to the variability of discharge, whereas the slope-*b* identifies the type of chemodynamic behaviour, which can range from dilution (slope-b < 0) to accretion (slope-b > 0) patterns (Musolff et al., 2015).

1.3 Research Objectives

In this research study, I focused on three temporal scales of aggregation to understand the dominant controls on stream nutrient concentrations. Our specific objectives are as follows:

A) Annual Scale
    a. Quantify mean annual flow-weighted concentrations for selected watersheds within the Great Lakes Basin.
    b. Quantify dominant controls on flow-weighted concentrations, and use a multiple linear regression approach to predict flow-weighted concentrations for ungauged watersheds.
    c. Develop maps and loading estimates for nutrients across all five Great Lakes.

B) Seasonal Scale

   a. Identify dominant controls on seasonal patterns in flow-weighted nutrient concentrations.

C) Event Scale

   a. Understand how concentration varies with discharge across a range of watersheds and land-use types, and determine key controls on the C-Q relationship.

2.0 Materials and Methods

2.1 Site Description

The five Great Lakes covers approximately 240,000 km^2 of surface water, with a total volume greater than 20,000 km^3 (Macdonagh-Dumler, Pebbels, & Gannon, 2005). Fifty-nine percent of the watersheds draining into the Great lakes are in the US, while the remaining area is in Canada (Neff, Day, Piggott, & Fuller, 2005). Precipitation across the Great Lakes basin ranges from less than 680 mm of rainfall west of Lake Superior to greater than 1100 mm east of Lake Ontario (Neff et al., 2005). Land use across the basin varies from forested areas in the Lake Superior watersheds, to more agricultural and urban areas in the southern parts of the basin. Urban areas are concentrated along Lake Michigan in the metropolitan areas of Chicago and Milwaukee, as well as around Lake Ontario near the cities of Hamilton and Toronto. Metropolitan areas in the catchment area for Lake Huron include Flint and Saginaw-Bay City.

Soil and geological characteristics vary spatially across the Great Lakes Watersheds. The more northern parts of the Great Lakes (e.g. Lake Superior) have a cooler climate and contain large amounts of granite bedrock, forested area and poor soil conditions including lack of nutrients to sustain healthy microbial activity (US Environmental Protection Agency & Government of Canada, 1995). The southern regions of the Great Lakes (Lake Erie, southern Lake Michigan, and Lake Ontario) have warmer climates and fertile soils which are readily used for agricultural development, particularly for watersheds draining to Lake Erie (US Environmental Protection Agency & Government of Canada, 1995).

2.2 Data Sources and Site Selection Criteria

The Great Lakes watersheds include the Canadian provinces of Ontario and the U.S. States of Illinois, Indiana, Michigan, Minnesota, New York, Ohio, Pennsylvania and Wisconsin. Water quality data for Ontario and the eight Great Lake states were obtained from the Provincial Water Quality Monitoring Network (PWQMN) and the United States Geological Survey (USGS), respectively. Additionally, some water quality stations for NO_3-N were obtained via the Water Quality eXchange (WQX) and Storage and Retrieval Data Warehouse (STORET) databases. Daily streamflow data was obtained from Environment Canada (EC) and USGS. Watersheds draining to the selected gauged stations were delineated using the hydrology toolbox in ArcMap v10.3. Watersheds in Ontario were separately delineated using the Ontario Flow Assessment Tool (OFAT) accessed from the Ontario Ministry of Natural Resources and Forestry. Streamflow and water quality stations were not always co-located. To address this issue, I selected streamflow stations that were sufficiently close to the water quality stations, based on the two following decision criteria: 1) The water quality and streamflow station lay on the same river stem; 2) the percent difference in drainage area between the water quality and streamflow station was less than 15%. Stations with data between 2000 and 2016 were selected. Using these criteria, I selected 179, 174 and 206 stations with water quality data for nitrate + nitrite-nitrogen (nitrate-N), reactive orthophosphate-P (SRP) and total phosphorus-P (TP), respectively.

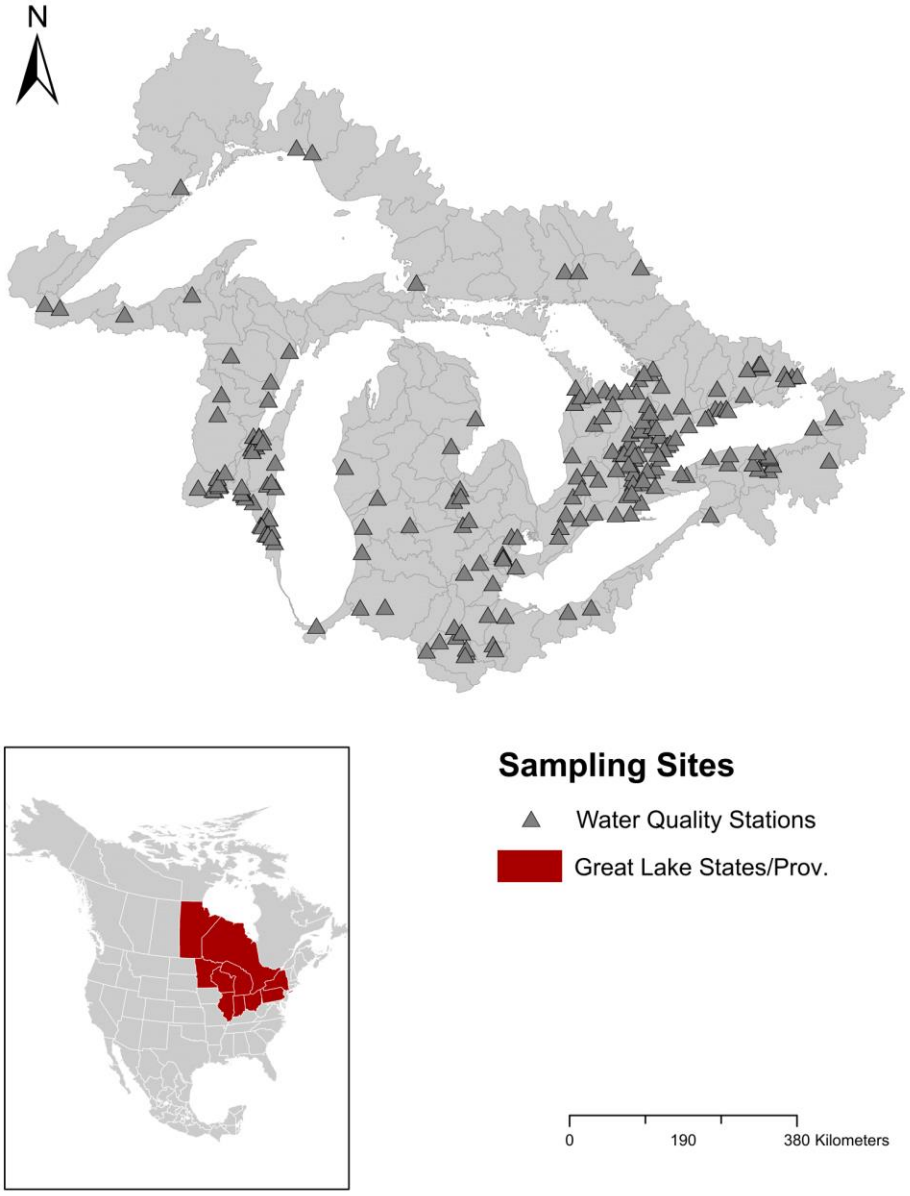

Figure 2.1. Map of selected Water Quality sites within the Great Lakes Region.

Gridded data representing catchment variables (e.g. percent clay, tile drains, etc.) were extracted from various gridded databases, as described in subsequent paragraphs and summarized in Appendix B, using ArcMap v10.3 tools. To obtain mean numerical values for a watershed based on the accumulation of gridded cells, the area-weighted average was computed as follows:

$$X_{avg}\frac{\sum_{i=1}^{n} XG_i A_i}{\sum_{i=1}^{n} A_i} \quad (4)$$

in which X_{avg} is the area-weighted average of a catchment variable for a particular watershed, XG_i is the numerical value associated for the gridded cell in row i, A_i is the area of the gridded cell in row i, and n is the number of gridded cells appearing in the catchment.

Canadian land-use data pertaining to agricultural, forested, urban and wetland areas were obtained from the 2015 Agriculture and Agri-Food Canada (AAFC) annual crop inventory. U.S. land-use data was obtained from the 2011 National Land Cover Database (NLCD). Land-use classifications of different land types (ex. agricultural, forested, etc.) were simplified, in that grid-codes identifying crops such as oats, wheat, corn, etc. were grouped to represent agricultural land. The recommended classification of land-types from the AAFC and NLCD were adopted in the analysis.

Tile drainage data for the Canadian province of Ontario was obtained from Ontario Ministry of Agriculture, Food and Rural Affairs (OMAFRA, 2015). U.S. tile drainage data was obtained from the United States Census of Agriculture, National Agricultural Statistics Services (USDA, NASS, 2012).

Global precipitation and temperature gridded data (at 1 km spatial resolution) were obtained from the WorldClim database (Fick & Hijmans, 2017). Gridded slope data for the U.S. Great Lakes area was extracted from the hydrologic landscape regions of the United States dataset (Wolock, Winter, & McMahon, 2004). Slope data pertaining to Canadian Great Lakes catchments were processed using the slope tool in ArcMap from a 30-meter digital elevation model (DEM), as well as extracted from OFAT after delineation.

Gridded soil data were extracted from the National Soil Database (NSDB) for Ontario, Canada and the Soil Survey Geographic Database (SSURGO) for the United States. Additionally, the Harmonized World Soil Database (HWSD) was used to process percent sand, silt and clay data in the northern areas of Ontario due to large amounts of missing data from the NSDB surrounding those regions.

2.3 Estimation of Flow-Weighted Concentrations (FWC)

The Weighted Regressions on Time, Discharge and Seasons (WRTDS) method developed by Hirsch et al (2010), is a non-linear model which was used to estimate seasonal and annual flow-weighted concentrations from intermittently measured concentration and continuously measured flow data. Daily concentration values are estimated in WRTDS by:

$$\ln(c) = \beta_0 + \beta_1 t + \beta_2 \ln(Q) + \beta_3 \sin(2\pi t) + \beta_4 \cos(2\pi t) + \varepsilon \quad (5)$$

in which $\ln(c)$ the natural logarithm of concentration, β_is values are fitted regression coefficients using weighted least squares, $\ln(Q)$ is the natural logarithm of daily mean streamflow Q, t is decimal time and ε is unexplained variation (Hirsch et al., 2010; Sprague et al., 2011). WRTDS is a highly flexible model that can be used to estimate daily concentrations and fluxes by utilizing and expanding on regression-based techniques. From (5), WRTDS combines the explanatory variables of time, discharge and seasons to estimate daily nutrient concentrations.

In order to estimate a daily concentration point at t_i, WRTDS selects neighboring points that are sufficiently close to the estimation point and calculates three distances in time, discharge and seasons (Hirsch et al., 2010; Sprague et al., 2011). The first distance is the time difference between t_0 and t_i; the second distance is the seasonal difference between the time of the year at t_o and the time of the year at the estimation point, t_i in decimal years (for example, the seasonal difference between March 1, 2007 and March 1, 2011 is zero); the third distance is the difference between $\ln(Q_0)$ and $\ln(Q_i)$. The weight for each distance is calculated using the tri-cube weight function defined by Tukey as:

$$w = \begin{cases} \left(1 - \left(\frac{d}{h}\right)^3\right)^3 \; if \; |d| \leq h \\ 0 \; if \; |d| > h \end{cases} \quad (6)$$

in which w is the weight, d is the distance in either time, discharge or seasons, and h is the half-window width (Hirsch et al., 2010).The overall weight (6) for each observation is calculated as the product of the three individual weights (Hirsch & De Cicco, 2015; Hirsch et al., 2010; Sprague et al., 2011). Recommended half-window widths for time, discharge, and seasons were reported as 7 years, 0.5 years, and 2 natural log units (Hirsch & De Cicco, 2015). In this analysis, a half-window width of 100 years for the 'time distance' was used in order to make the weights for all observations near the estimation point equal. Setting a half-window width of 100 years yields weights of approximately 1 for all observations that fall near the estimation point. This approach provides greater influence of weights estimated from the seasonality and discharge 'distances' of WRTDS. Average β_1 estimates were greater than -1 or less than 1 for nearly all stations. Additionally, the differences in the flux bias static (described in more detail below) when setting the half-window widths for 7 years and 100 years were less than 5 percent for most stations.

A key advantage in using WRTDS is its ability to provide unbiased estimates of daily concentrations and fluxes (Sprague et al., 2011). Namely, the coefficients β_i from (5) are unique for each daily estimated concentration point based on weights derived from streamflow magnitude and its corresponding time (in years and seasons). Additionally, a unique bias correction factor for each estimation point was applied before transforming the natural-log concentration back to the original units in order to reduce the re-transformation bias (Duan, 1983; Sprugel, 1983). Having unique coefficients to estimate a daily concentration value provides a dynamic approach to estimating nutrient export versus having a constant array of coefficients over the entire period of record (Sprague et al., 2011).

In order to assess the accuracy of the WRTDS estimates, the flux bias statistic was computed for all stations. The following equations were used to compute the flux bias statistic:

$$P = \left(\sum_{i=1}^{n} k * c_{i,EGRET} * Q_i \right) \quad (7)$$

$$O = \left(\sum_{i=1}^{n} k * c_{i,OBS} * Q_i \right) \quad (8)$$

$$B = \frac{P - O}{P} \quad (9)$$

in which B is the flux bias statistic, P is the sum of the estimated WRTDS flux on the sampled days, O is the sum of the estimated fluxed from measured concentration and discharge data, k is a units conversion factor = 86.4, $c_{i,EGRET}$ is the estimated concentration on the ith sampled day in mg/L, $c_{i,OBS}$ is the measured concentration on the ith sampled day in mg/L, Q_i is the discharge on the ith sampled day in m^3/s, and n is the number of sampled days (Hirsch & De Cicco, 2015). A positive flux bias indicates over-predictions of WRTDS concentrations, whereas a negative flux bias indicates under-predictions of WRTDS concentrations during sampled day periods. Water quality stations with at least 40 data points between 2000 and 2016 were considered in the WRTDS analysis. Stations with flux bias estimates less than -0.15 or greater than 0.15 were omitted from further analysis.

Seasonal and annual flow-weighted concentrations (FWC or C_f) were calculated from measured daily discharge and WRTDS-estimated daily concentrations using the following equation:

$$C_f \frac{\sum_{i=1}^{n} C_i Q_i}{\sum_{i=1}^{n} Q_i} \quad (10)$$

in which C_f is the flow-weighted concentration, C_i and Q_i are the concentration and discharge on the ith day respectively, and n is the number of days. In the above equation, the numerator is the annual nutrient load, and the denominator is the total annual discharge.

2.4 Metrics

2.4.1 Seasonality Index (SI)

The Seasonality Index (SI), a metric that has traditionally been used to assess the seasonality of precipitation (Walsh & Lawler, 1981), was used in the present analysis to quantify seasonal variations in monthly flow-weighted concentrations. SI is calculated according to the following equation:

$$SI_{C_f} = \frac{1}{M}\sum_{i=1}^{12}\left|M_i - \frac{M}{12}\right| \quad (11)$$

in which M is the monthly sum of the flow-weighted concentrations and M_i is the average flow-weighted concentration in month i. The SI index was similarly used to calculate seasonal index values for flow-weighted concentrations. The SI index is theoretically bound between 0 (if all months have the same export) and 1.83 (if all export occurs in one month) (Walsh & Lawler, 1981). $SI \leq 0.2$ describes even seasonal distribution, $0.2 < SI \leq 0.4$ describes an essentially even seasonal distribution with larger values in some months, $0.4 < SI \leq 0.6$ describes a seasonal distribution with small values in some months, and $SI > 0.6$ describes strong seasonal variation (Tian et al., 2016; Walsh & Lawler, 1981). The seasonality index was computed using monthly concentrations based on aggregating the daily water quality data estimated from the WRTDS model.

2.4.2 Slope-b and the Coefficient of Variation of Concentration-Discharge Relationships:

Event scale concentration-discharge dynamics were captured using the slope-*b* and CV ratio (3) metrics. Slope-*b* was estimated from the C-Q relationships by equating the natural logarithm of concentration as a function of the natural logarithm of discharge (2). Linear regression was then applied to extract the slope-*b* value for each water quality station, using a p-value threshold less

than 0.05. Sampled (i.e. measured) water quality and daily discharge data were analysed to estimate the slope-b and CV ratio.

2.5 Multiple Regression Model to Understand Dominant Controls:

In order to understand dominant controls on biogeochemical signatures, generalized linear models describing flow-weighted nutrient concentrations as a function of catchment characteristics were developed and applied to the ungauged basins of the Great Lakes. A major concern when conducting multiple regression analysis is the presence of multicollinearity, where one explanatory variable may be correlated with one or many other explanatory variables. The inclusion of highly correlated explanatory variables can result in negative consequences in the multiple regression analysis, including signs and magnitudes in the slope coefficients that may not make sense, high sensitivity in the slope coefficients (ex. small changes in data points drastically alters coefficient magnitudes), and the removal of significant variables when using stepwise regression techniques (Graham, 2003; Helsel & Hirsch, 1992). A commonly used diagnostic to assess multicollinearity is assessing the variance inflation factor (VIF) and eliminating explanatory variables with VIFs > 10 in the multiple regression analysis that may otherwise cause problems (Chatterjee & Hadi, 2006).

Model selection was carried out using the Akaike information criterion (AIC):

$$AIC = 2k - 2ln(\hat{L}) \tag{12}$$

in which $\hat{L}$ is the maximum value of the likelihood function of the model and k is the number of estimated parameters in the model. Techniques such as stepwise regression which utilizes computer algorithms have been developed to automatically determine the most preferred model (Helsel & Hirsch, 1992). The main limitation when using procedures such as the forwards or elimination method is that not all models are evaluated and therefore, the best model may not be selected by the computer algorithm. Because techniques such as stepwise regression do not always guarantee the best model, every possible model combination was evaluated. For example, if five x-variables were selected to estimate flow-weighted nitrate-N concentrations, then 31 (i.e.

$2^5 - 1$) models are evaluated and the best model (based on lowest AIC and highest r-squared value) is selected. In total, 127 models were evaluated for nitrate-N and 255 models were evaluated for phosphorus. Multiple regression equations were constructed based on the annual-average FWC as a function of the (significant) catchment variables (see Appendix B for list of catchment variables). The best MLR model was chosen according to the lowest AIC value.

2.6 Developing maps of flow-weighted concentrations across the Great Lakes Basin

Spatial maps of flow-weighted concentrations (10) for nitrate-N, SRP, and TP were developed to identify regional patterns and hotspots across the Great Lakes Basin. Single standardized regression was first applied between WRTDS-estimated FWC and catchment variables in order to identify dominant controls that would later be used to develop MLR models. Prior to the regression analysis, flow-weighted concentrations were natural-log (LN) transformed to strengthen the normality and linearity of the relationships. Catchment characteristics such as soil texture, land use, average temperature, and other variables were used based on area-weighted averages for the selected gauged watersheds (4). Once the watershed characteristics (i.e. catchment variables) exerting dominant controls were identified, and the best MLR model to estimate FWC was constructed as described in section 2.5, the MLR model was applied for all ungauged watersheds across the Great Lakes Basin.

2.7 Estimating tributary loads to the Great Lakes

Annual average tributary loads from gauged and ungauged basins were estimated across the Great Lakes region. The St. Lawrence basin was omitted from the analysis, as our goal was to estimate tributary load exports directly to the five Great Lakes. For this purpose, inland watersheds were also merged with their respective nearshore watersheds. Merging inland watersheds with the correct nearshore watersheds was achieved by utilizing stream network shapefiles (derived from a DEM) in order to identify the appropriate drainage point for which the inland and nearshore watersheds meet. Flow-weighted concentrations as well as annual average discharge were recalculated to account for the larger watershed areas. Loads from gauged stations were estimated using the following equation:

$$L_{N,annual} = C_f * Q_{annual} \quad (13)$$

in which $L_{N,annual}$ is the annual-average nutrient load (i.e. nitrate-N, SRP and TP), C_f is the flow-weighted concentration (FWC), and Q_{annual} is the annual averaged discharge. For gauged watersheds, C_f is the flow-weighted concentration calculated using the WRTDS model, and Q_{annual} is the annual-average discharge calculated from the measured data. For ungauged watersheds, C_f is the flow-weighted concentration using the MLR model, and Q_{annual} is the annual-average discharge estimated from the single regression model (Figure 2.2).

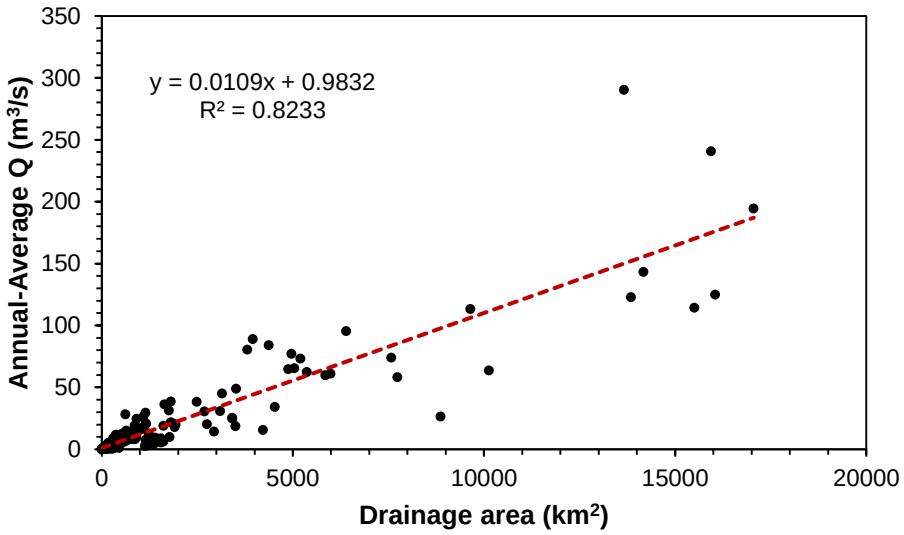

Figure 2.2. Annual-average discharge as a function of drainage area (p-value < 0.001). Annual Q is the annual-average discharge estimated from selected gauged streamflow stations across the Great Lakes.

Figure 2.2 shows a strong correlation between drainage area and average annual discharge (R^2 = 0.82). By applying the single and multiple regression models for discharge and flow-weighted concentrations respectively, loads from ungauged tributaries in the Great Lakes were estimated.

3.0 Results and Discussion

3.1 Mean Annual Flow-weighted Concentrations

3.1.1 Dominant controls on the mean annual FWC

The mean annual FWC values across the Great Lakes watersheds ranged from 0.04 – 11 mg/L for nitrate, 1–275 ug/L for SRP, and 9 – 1100 ug/L for TP. Of the 223 stations analyzed in the study across all nutrients, 136 stations for nitrate, 124 stations for SRP, and 158 stations for TP had flux-biases (9) between ±0.15 and were used for further analysis. A flux bias near zero means the WRTDS model is generally unbiased with respect to high or low fluxes.

Regression analysis was used to quantify dominant controls on the mean annual FWC. The results of the regression analysis indicate that land use is a primary driver of flow-weighted nutrient concentrations in the Great Lakes watersheds. As shown in Fig. 3.1 (and subsequently Table 3.1), percent agricultural and urban land had the highest standardized coefficient and r-square values of all the variables evaluated, explaining around 76% of the variability (on average) across all three constituents. The strong positive correlation between FWC and percent agricultural and urban land is consistent with the understanding that nonpoint source pollution is the major contributor of high nutrient concentrations in streams (S. Carpenter et al., 1998; Sharpley et al., 1994). A negative correlation was observed between FWC and percent wetland cover, highlighting the significant role of wetlands in reducing the nutrient concentrations in human impacted watersheds. Of course, it should be acknowledged that there is significant cross correlation with the agricultural land cover and the wetland cover.

Significant positive relationships were observed between FWC and percent tile-drained area across all nutrients, illustrating the role of subsurface drainage networks in bypassing the nutrient filtering abilities of the soil and thus contributing to enhanced nutrient export (Basu et al., 2011). It is interesting to note that the standardized regression coefficient (SRC) between FWC and percent tile drainage is the highest for nitrate, and lowest for TP, while that for SRP lies in between. This is possibly because N is transported primarily through the subsurface pathway, and is thus most strongly affected by tile-drains, while P is transported in particulate and

dissolved forms through both surface and subsurface pathways and is thus less impacted by tile-drains. This is further corroborated by the fact that the more soluble form of P (SRP) has a higher SRC value than TP, which also includes the particulate form. Strong significant (p-value < 0.001) relationships between FWC and the percent silt and clay fraction of the soil was observed as well. This can be attributed to the fact that a greater fraction of silt and clay indicates more surface runoff and thus a lower potential for nutrient attenuation within the subsurface.

Table 3.1. Individual regression analysis of flow-weighted nutrient concentrations. Concentration variables were natural-log transformed to increase linearity and normality. AGRIURB is the combined percent agricultural and urban land; FOR is the percent forest; WET is the percent wetlands; TD is the percent tile drains; PD is the population density (persons/km^2); SLP is the percent slope; SILTCLAY is the combined percent silt and clay content; PRECIP is the annual average precipitation (mm/yr); TAVG is the annual average temperature (^{o}C).

	Nitrate-N		SRP		TP	
	p-value	r^2	p-value	r^2	p-value	r^2
AGRIURB	$p < 0.001$	0.66	$p < 0.001$	0.54	$p < 0.001$	0.53
FOR	$p < 0.001$	0.55	$p < 0.001$	0.53	$p < 0.001$	0.42
WET	$p < 0.001$	0.56	$p < 0.001$	0.30	$p < 0.001$	0.41
TD	$p < 0.001$	0.42	$p < 0.001$	0.32	$p < 0.001$	0.18
PD	0.42	0.00	0.04	0.03	0.02	0.04
SLP	$p < 0.05$	0.07	$p < 0.001$	0.28	$p < 0.001$	0.33
SILTCLAY	$p < 0.001$	0.32	$p < 0.001$	0.38	$p < 0.001$	0.45
PRECIP	0.01	0.04	0.03	0.04	$p < 0.001$	0.17
TAVG	$p < 0.001$	0.29	$p < 0.001$	0.29	$p < 0.001$	0.31

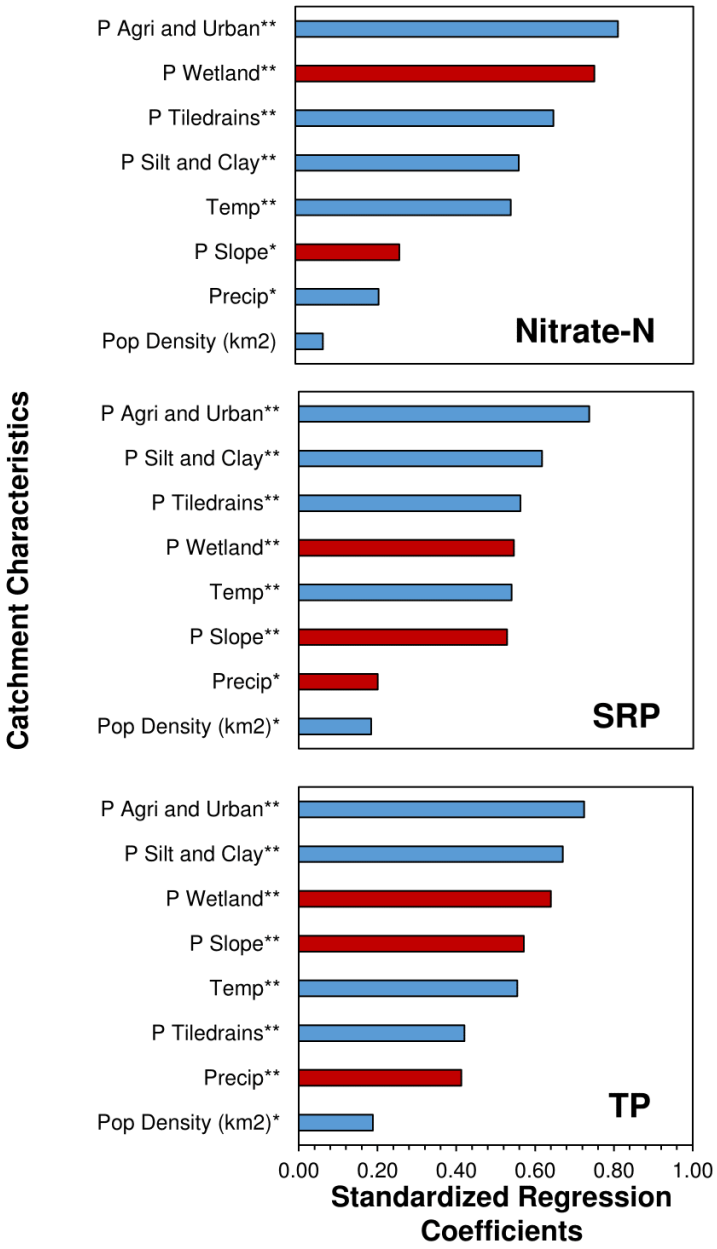

Figure 3.1. Bar plots representing standardized individual regression coefficients for flow-weighted concentrations against selected catchment characteristics. Blue and red bars indicate positive and negative relationships, respectively. P Agri and Urban, P Wetland, P Tile drains, P Silt and Clay, and P Slope are fractional areas (in %) of land-use and soil; Tavg is the annual average temperature in ^{o}C; Precip is the annual average precipitation (mm/yr); Pop Density is the population density (persons/km^2). *: $p < 0.05$; **: $p < 0.001$.

3.1.2 Multiple Linear Regression Model between FWC and Catchment Characteristics

Multiple linear regression models were developed to estimate FWC in the ungauged areas of the Great Lakes, as a function of catchment characteristics. A collinearity analysis was used to eliminate some of the variables identified in the previous section. Pearson's correlation coefficients and VIFs were computed to determine the degree of collinearity between catchment (i.e. explanatory) variables (Table 3.2). The collinearity table only includes catchment variables found to be significant (p-value < 0.05) based on individual regression analyses for each nutrient. For example, drainage area was found to be insignificant (p-value > 0.05) when regressed individually against (natural-log transformed) flow-weighted nitrate-N, SRP, and TP concentrations, and were therefore removed from the VIF analysis. This elimination allowed for better interpretation of the VIF values for each variable and aided in the selection of variables appropriate for the multiple regression analysis.

Table 3.2. Pearson's correlation coefficients of catchment variables. P Agri and Urban (AGRIURB), P Forest (FOR), P Wetland (WET), P Tile drains (TD), P Silt and Clay (SILTCLAY), and P Slope (SLP) are fractional areas of land-use and soil; TAVG is the average temperature in °C; PD is the population density in persons/km^2; Red values represent insignificant (p-value > 0.05) correlation between catchment variables.

	AGRIURB	FOR	WET	TD	PD	SLP	SILTCLAY	PRECIP	TAVG	VIF	VIF without FOR
AGRIURB	1	-0.91	-0.81	0.48	0.30	-0.38	0.73	-0.01	0.68	24.6	4.7
FOR	-0.91	1	0.58	-0.39	-0.27	0.46	-0.65	0.14	-0.58	12.3	-
WET	-0.81	0.58	1	-0.49	-0.29	0.23	-0.62	-0.15	-0.61	5.4	3.5
TD	0.48	-0.39	-0.49	1	-0.21	-0.28	0.46	0.30	0.39	1.9	1.9
PD	0.30	-0.27	-0.29	-0.21	1	-0.07	0.17	-0.19	0.23	1.4	1.4
SLP	-0.38	0.46	0.23	-0.28	-0.07	1	-0.39	0.37	-0.58	2.4	2.1
SILTCLAY	0.73	-0.65	-0.62	0.46	0.17	-0.39	1	0.07	0.46	2.4	2.4
PRECIP	-0.01	0.14	-0.15	0.30	-0.19	0.37	0.07	1	-0.09	1.6	1.5
TAVG	0.68	-0.58	-0.61	0.39	0.23	-0.58	0.46	-0.09	1	2.8	2.7

Results from the collinearity table indicate percent combined agricultural and urban land, as well as percent forested land having the highest correlations with respect to all other catchment variables (VIF > 10). The percentage of forested land-variable was therefore excluded in the multiple regression analysis because the percent combined agricultural and urban land-variable is

more important when assessing human impacts on flow-weighted nutrient concentrations. Tables 3.3 and 3.4 provides a summary of the p-values and coefficients for the top 3 selected multiple regression models based on lowest AIC (12). Model 1 for each nutrient was used to estimate flow-weighted concentrations for the entire Great Lakes Basin. FWC estimated from the top MLR models were compared with WRTDS-estimated FWC to assess the accuracy of the regression models (Figure 3.2).

Table 3.3. Summary of p-values of the three top multiple regression models for (natural-log transformed) nitrate-N, SRP, and TP. INT is the intercept; AGRIURB is the combined percent agricultural and urban land; WET is the percent wetlands; TD is the percent tile drains; SLP is the percent slope; SILTCLAY is the combined percent silt and clay content; PRECIP is the annual average precipitation (mm/yr); TAVG is the annual average temperature (°C).

Nitrate-N	AGRIURB p-value	WET p-value	TD p-value	SLP p-value	SILTCLAY p-value	PRECIP p-value	TAVG p-value
Model 1	p < 0.001	p < 0.05	p < 0.001	-	-	-	0.04
Model 2	p < 0.001	p < 0.05	p < 0.001	-	-	-	-
Model 3	p < 0.001	-	p < 0.001	-	-	-	-

SRP	AGRIURB p-value	WET p-value	TD p-value	SLP p-value	SILTCLAY p-value	PRECIP p-value	TAVG p-value
Model 1	p < 0.001	-	p < 0.001	p < 0.05	-	p < 0.001	-
Model 2	p < 0.001	-	p < 0.001	0.03	-	p < 0.001	-
Model 3	p < 0.001	-	p < 0.001	-	-	p < 0.001	-

TP	AGRIURB p-value	WET p-value	TD p-value	SLP p-value	SILTCLAY p-value	PRECIP p-value	TAVG p-value
Model 1	-	p < 0.001	p < 0.05	p < 0.05	p < 0.001	p < 0.001	-
Model 2	-	p < 0.001	p < 0.05	-	p < 0.001	p < 0.001	0.04
Model 3	-	p < 0.001	-	p < 0.001	p < 0.001	p < 0.001	-

Table 3.4. Summary of coefficients and model evaluation estimates of the three top multiple regression models for (natural-log transformed) nitrate-N, SRP, and TP. INT is the intercept; AGRIURB is the combined percent agricultural and urban land; WET is the percent wetlands; TD is the percent tile drains; SLP is the percent slope; SILTCLAY is the combined percent silt and clay content; PRECIP is the annual average precipitation (mm/yr); TAVG is the annual average temperature (°C). AIC is the Akaike information criterion. The Model 1 for each nutrient was used to estimate flow-weighted concentrations in the ungauged basins.

Nitrate-N	INT	AGRIURB	WET	TD	SLP	SILTCLAY	PRECIP	TAVG	AIC	rsq
	β_0	β_1	β_2	β_3	β_4	β_5	β_6	β_7		
Model 1	-0.8	0.03	-0.03	0.02	-	-	-	-0.10	259	0.76
Model 2	-1.27	0.02	-0.02	0.02	-	-	-	-	262	0.75
Model 3	-2.05	0.03	-	0.02	-	-	-	-	266	0.74

SRP	INT	AGRIURB	WET	TD	SLP	SILTCLAY	PRECIP	TAVG	AIC	rsq
	β_0	β_1	β_2	β_3	β_4	β_5	β_6	β_7		
Model 1	-2.14	0.02	-	0.03	-	0.02	0.00	-	277	0.71
Model 2	-2.20	0.03	-	0.03	-0.09	-	0.00	-	283	0.70
Model 3	-2.02	0.03	-	0.03	-	-	0.00	-	286	0.69

TP	INT	AGRIURB	WET	TD	SLP	SILTCLAY	PRECIP	TAVG	AIC	rsq
	β_0	β_1	β_2	β_3	β_4	β_5	β_6	β_7		
Model 1	0.04	-	-0.04	0.01	-0.10	0.02	0.00	-	279	0.74
Model 2	0.34	-	-0.03	0.01	-	0.02	0.00	0.08	285	0.73
Model 3	0.16	-	-0.05	-	-0.13	0.02	0.00	-	286	0.72

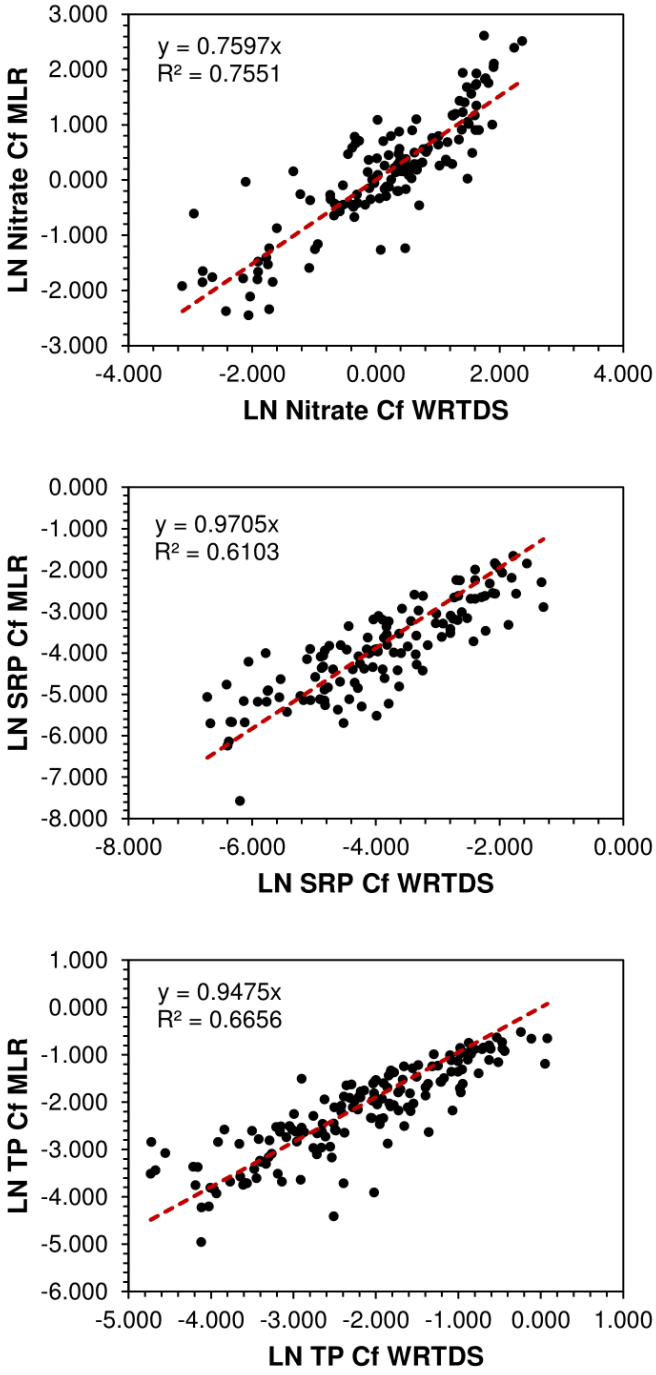

Figure 3.2. Predictive (1:1) measure of (natural-log transformed) MLR flow-weighted concentrations against WRTDS-estimated flow-weighted concentrations for nitrate-N, SRP, and TP.

MLR estimates of (natural-log transformed) flow-weighted concentrations for nitrate-N, SRP and TP show moderate predictive power with R^2 values of 76%, 61%, and 67%, respectively.

3.1.3 Spatial Patterns in Mean Annual FWC

Using the multiple regression equations developed for nitrate-N, SRP and TP, FWC were estimated across the Great Lakes Area (Figures 3.3 – 3.5). The northern watersheds of Lakes Superior, Michigan, Huron and Ontario all display low-to-moderate FWC levels, with nitrate-N concentrations below 1 mg/L, soluble phosphorus concentrations ranging between 1 and 15 µg/L, and total phosphorus concentrations ranging between 9 and 90 µg/L. The majority of Lake Erie watersheds showed much higher FWC for all three nutrients compared with watersheds draining into Lake Superior and the northern watersheds of Lake Huron and Ontario. In particular, hotspots (nitrate-N > 5 mg/L; SRP > 70 µg/L; TP > 200 µg/L) can be identified near the lower-west region of Lake Erie, specifically in the Lower Maumee watershed, as well as in the Thames and Sydenham River that drains into Lake St. Clair. These watersheds are largely impacted by human activities which is reflected by their high levels of agricultural land-use and tile-drainage densities. The nearshore watersheds of Humber-Don, Niagara, Genesee, and Oswego surrounding the urban regions of Lake Ontario show moderate FWC levels for nitrate-N (0.1 – 3 mg/L), SRP (10 – 35 µg/L), and TP (50 – 200 µg/L). The Saginaw watershed draining to the Saginaw Bay in Lake Huron shows moderate nitrate-N (0.5-2 mg/L), SRP (20-30 µg/L) and TP (100-120 µg/L) FWC. Hotspots were consistently shown in the Ausable, Pigeon-Wiscoggin, and Birch-Willow watersheds in Lake Huron, where the combined fraction of agricultural and urban land, as well as tile drainage densities exceeded 70%, and 40%, respectively. The lower western catchments of Lake Michigan (e.g. Lower Fox, Milwaukee, and St. Joseph), which have high urban and agricultural land use, displayed moderate nitrate-N FWC ranging between 0.5 and 3 mg/L. Here, SRP and TP FWC are relatively higher, ranging from 30-70 µg/L and 140-200 µg/L, respectively.

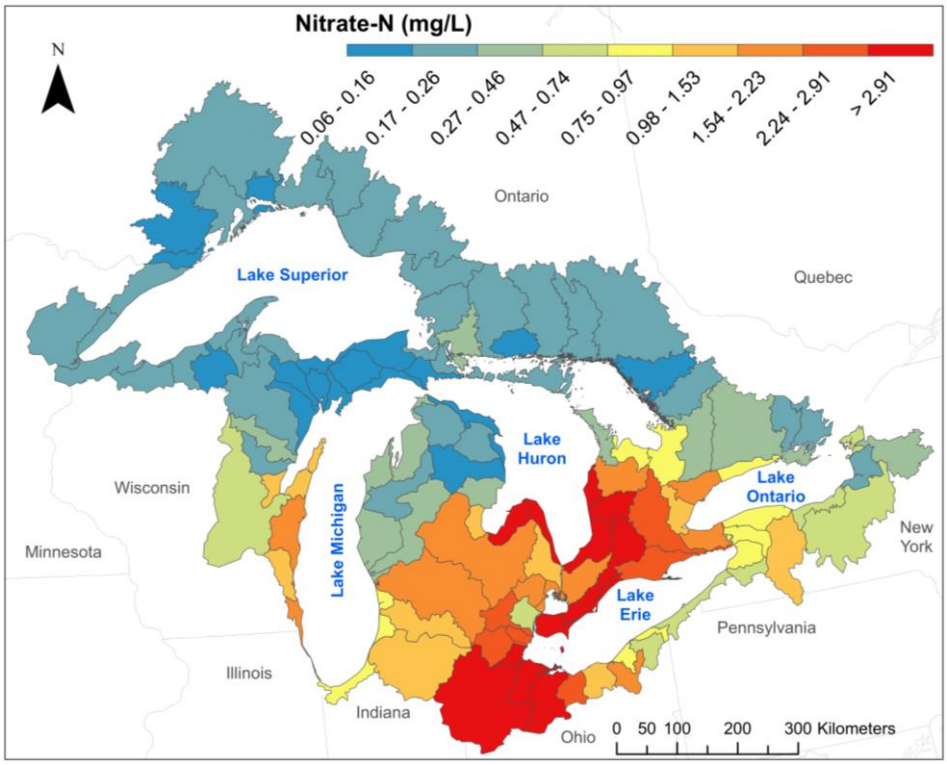

Figure 3.3. Flow-weighted concentrations for nitrate-N across the Great Lakes Watersheds.

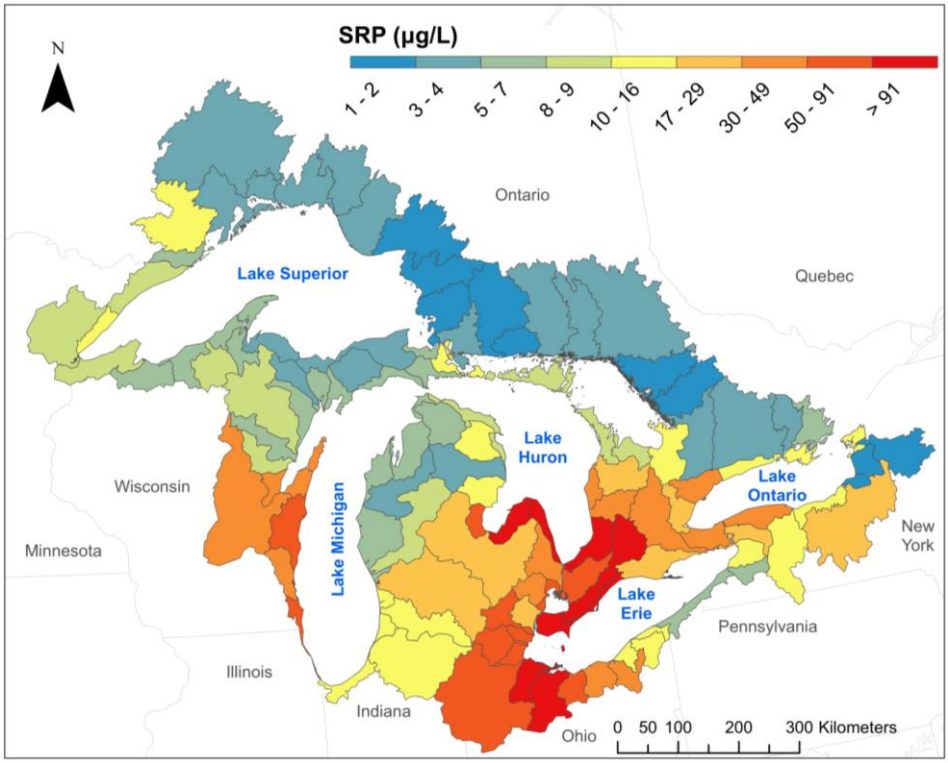

Figure 3.4. Flow-weighted concentrations for SRP across the Great Lakes Watersheds.

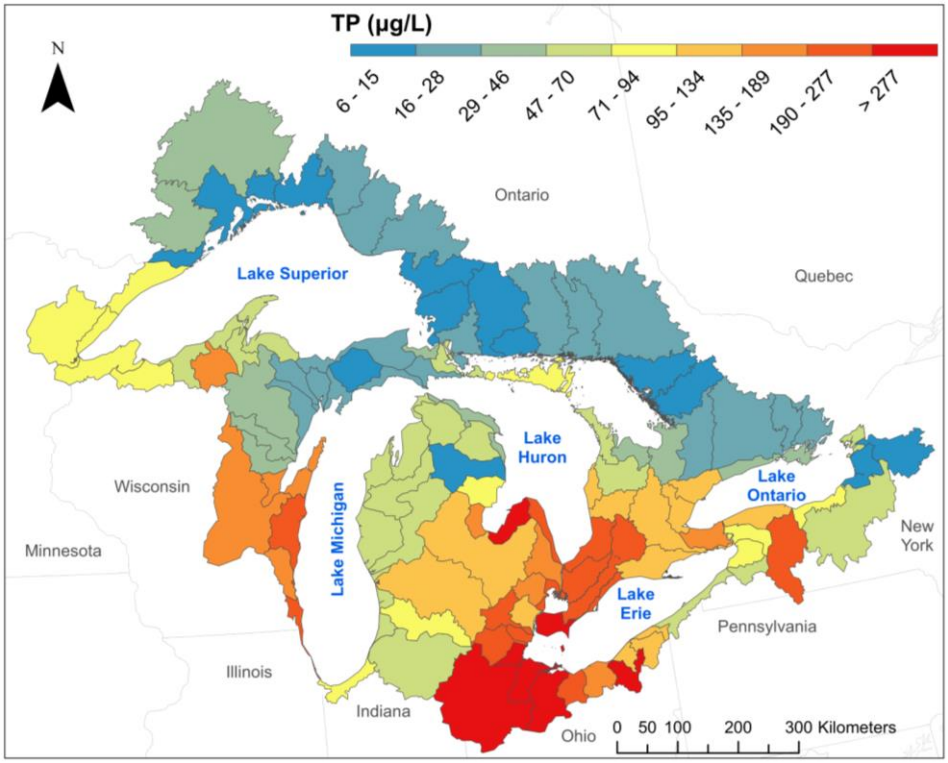

Figure 3.5. Flow-weighted concentrations for TP across the Great Lakes Watersheds.

3.1.4 Nutrient Ratios across the Great Lakes Watersheds

In addition to mapping the annual FWC, I analyzed and mapped nitrate-N to SRP, nitrate-N to TP, and SRP to TP ratios across the Great Lakes Basin (Figures 3.6 – 3.8). Ratios were calculated based on molar values of nitrate-N, SRP and TP.

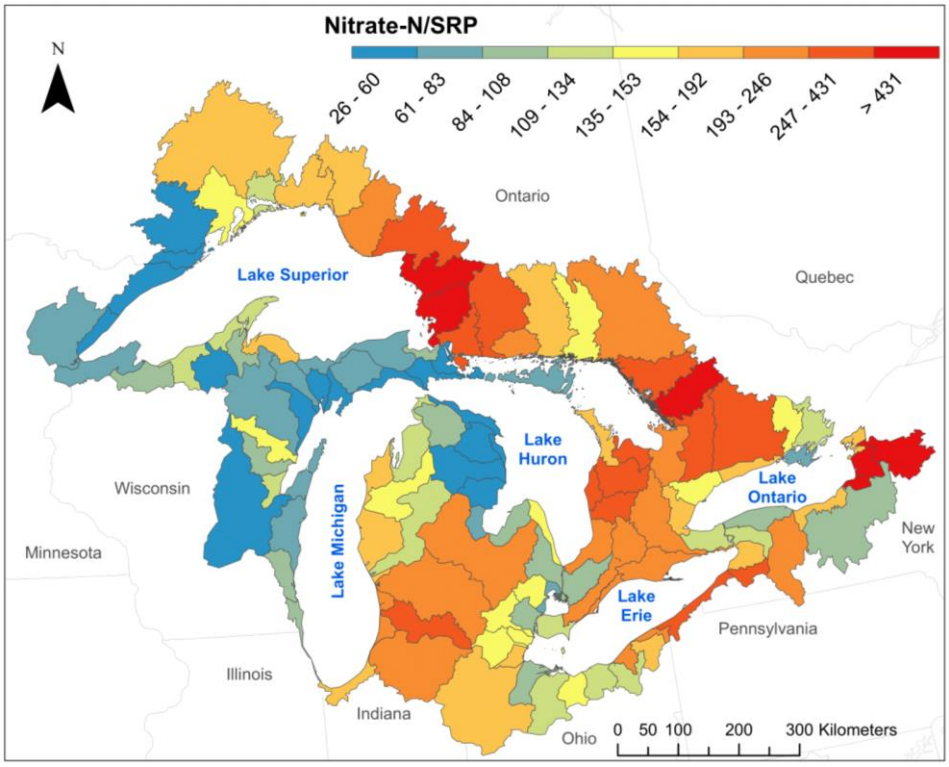

Figure 3.6. Nitrate-N to SRP ratio across the Great Lakes watersheds. Ratios are estimated by using FWC concentrations in mol/L.

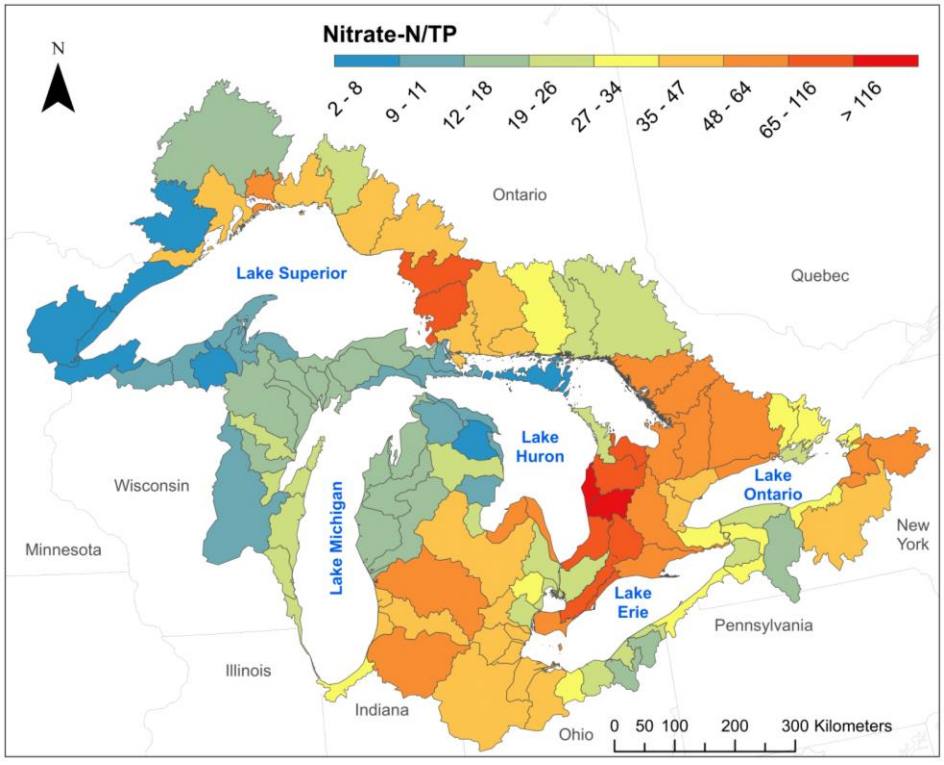

Figure 3.7. Nitrate-N to TP ratio across the Great Lakes watersheds. Ratios are estimated by using FWC concentrations in mol/L.

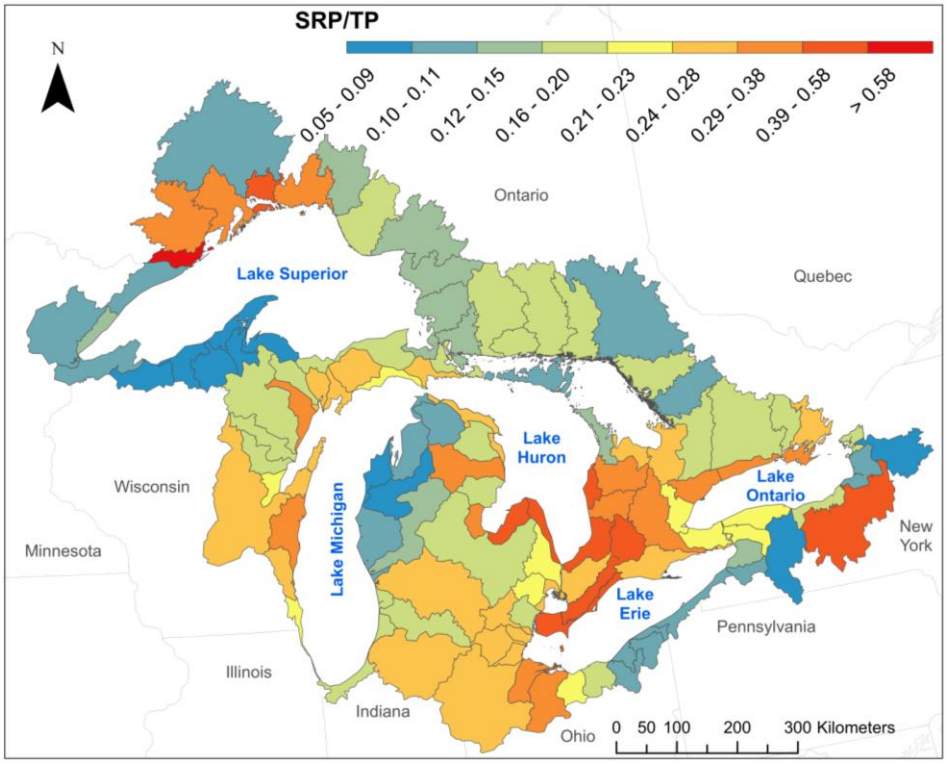

Figure 3.8. SRP to TP ratio across the Great Lakes watersheds. Ratios are estimated by using FWC concentrations in mol/L.

Nitrogen to phosphorus ratios were found to vary across all the Great Lakes, averaging between 160 – 210 for nitrate-N/SRP, 20 – 50 for nitrate-N/TP and 0.2 – 0.3 for SRP/TP. Relatively higher ratios were observed in agriculturally dominated (> 50%) regions of the Lower Thames (SRP/TP > 0.4, nitrate-N/TP > 90) and Cedar (SRP/TP > 0.4, nitrate-N/TP > 50) watersheds in Lake Erie. Low to moderate SRP/TP ratios were observed in the Nipigon watershed (SRP/TP < 0.2) in Lake Superior, as well as the French watershed (SRP/TP < 0.1) in northern Lake Huron. The N/P ratios were also found to be relatively lower in urban areas of Lake Michigan (Lower Fox, Milwaukee) and Lake Ontario (Niagara, Genesee, and Oswego). Interestingly, the Saginaw watershed in Lake Huron displayed very high N/SRP ratios (> 200) compared to N/TP (< 50) and SRP/TP (< 0.2) ratios. Additionally, the Ausable watershed illustrated consistently high ratios for N/SRP (> 200), N/TP (> 90), and SRP/TP (> 0.5).

3.1.5 Nutrient Loads to the Great Lakes

In addition to analysing the spatial variability of nutrient concentrations across the Great Lakes, I also estimated nutrient loads (13) to determine the overall annual-average export to the lakes from tributary sources between 2000 and 2016. Estimating nutrient loads is important because it provides a quantitative understanding of the conditions (and status) of the Great Lakes. Although nutrient loads (specifically total phosphorus) to the Great Lakes were reduced after the implementation of the GLWQA in 1978, the Great Lakes are still experiencing water quality degradation such as excessive eutrophication, high rates of algae production, and hypoxia (Robertson & Saad, 2011). It is therefore important to quantify nutrient loads in the Great Lakes in order to better our understanding of present conditions and develop strategies to mitigate poor water quality in streams and their receiving water body.

Maps of nutrient yields for nitrate-N, SRP and TP are shown in Figures 3.9 – 3.11. Higher nutrient yields were consistently displayed in Lake Erie watersheds for all constituents, averaging 13, 0.3, and 0.8 kg/ha/yr for nitrate-N, SRP and TP, respectively. Total phosphorus yields for Lake Erie ranged from 0.2 to 1.7 kg/ha/yr. In Lake Huron, total phosphorus yields ranged between 0.03 to 1.4 kg/ha/yr. For Lake Michigan, TP yields were estimated between 0.05 and 1 kg/ha/yr. Lake Ontario TP yield estimates ranged from 0.05 to 0.7 kg/ha/yr. Finally, Lake Superior TP yields were between 0.02 – 0.3 kg/ha/yr. Most of Lake Superior watersheds estimated lower average tributary yields (0.7, 0.02, and 0.2 kg/ha/yr for nitrate-N, SRP and TP, respectively) compared to all other Lakes. Hotspots in Lake Erie for SRP and TP were identified in the lower Maumee watershed with nutrient yield estimates of 0.3 and 1.3 kg/ha/yr, respectively. Large nitrate-N yields were also identified in the Lower Thames and Cedar watersheds in Lake Erie (approximately 29 kg/ha/yr), as well as the Sydenham watershed that drains to Lake St. Clair (7 – 10 kg/ha/yr). Consistently high nutrient yields were seen in the lower-eastern watersheds of Lake Huron. Specifically, the Ausable and Pigeon-Wiscoggin watershed yields were both greater than 0.4 and 0.9 kg/ha/yr for SRP and TP, respectively. Watersheds in Lake Ontario (e.g. Niagara, Oak Orchard and Genesse) showed moderate nutrient yields, averaging 4.5, 0.1, and 0.5 kg/ha/yr for nitrate-N, SRP and TP, respectively. Additionally, high SRP and TP yields were observed in the Manitowoc-Sheboygan, Milwaukee, and Pike-Root catchments in Lake Michigan (5 – 9 kg/ha/yr for nitrate-N; 0.1 – 0.3 kg/ha/yr for SRP; 0.6 – 1 kg/ha/yr for TP), which encompass high levels agricultural, urban and tile-drained land.

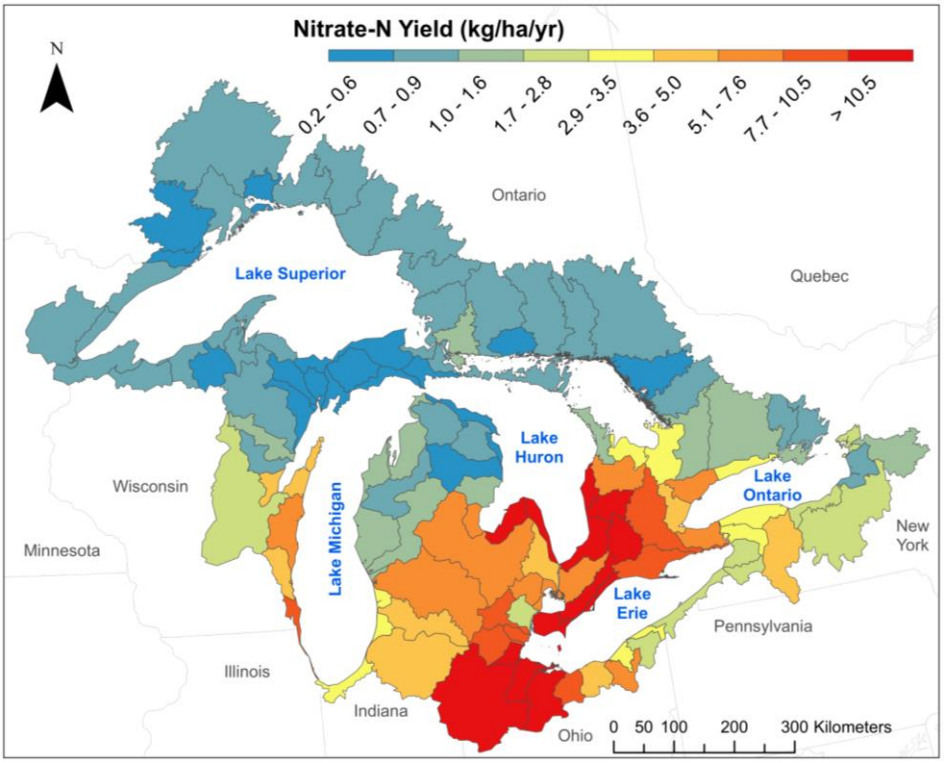

Figure 3.9. Nitrate-N yields across the Great Lakes Watersheds.

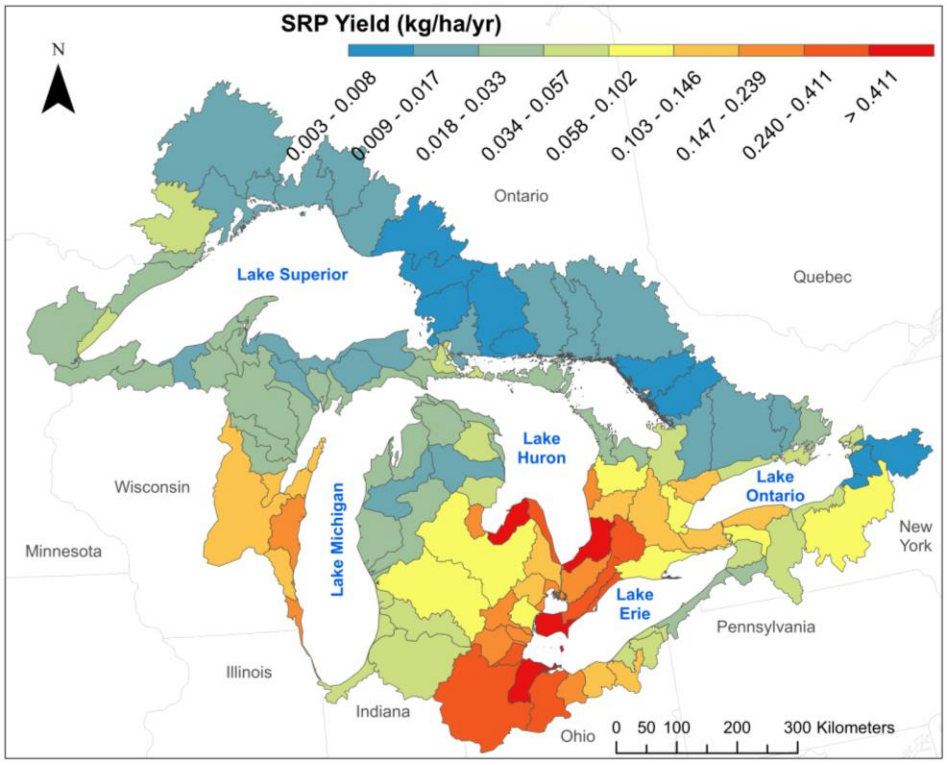

Figure 3.10. SRP yields across the Great Lakes Watersheds.

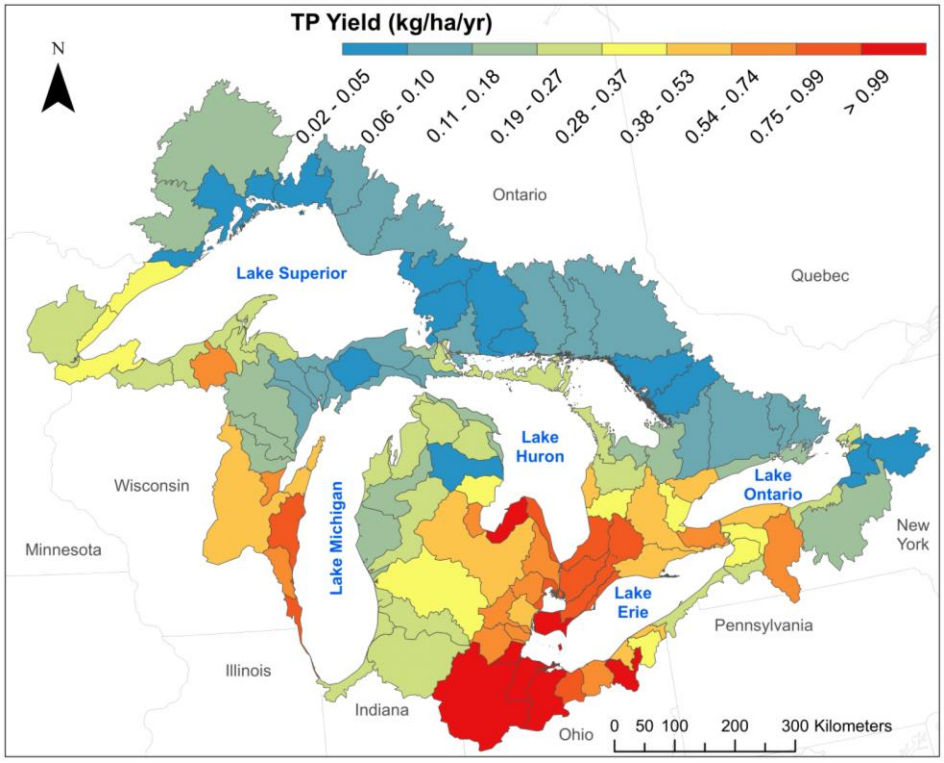

Figure 3.11. TP yields across the Great Lakes Watersheds.

Total annual-average tributary loads for nitrate-N, SRP and TP were calculated for each lake (Figure 3.12). Lake Erie displayed the largest average annual export for all three constituents. Total phosphorus estimates to Lake Erie was approximately 6200 tonnes per annum.

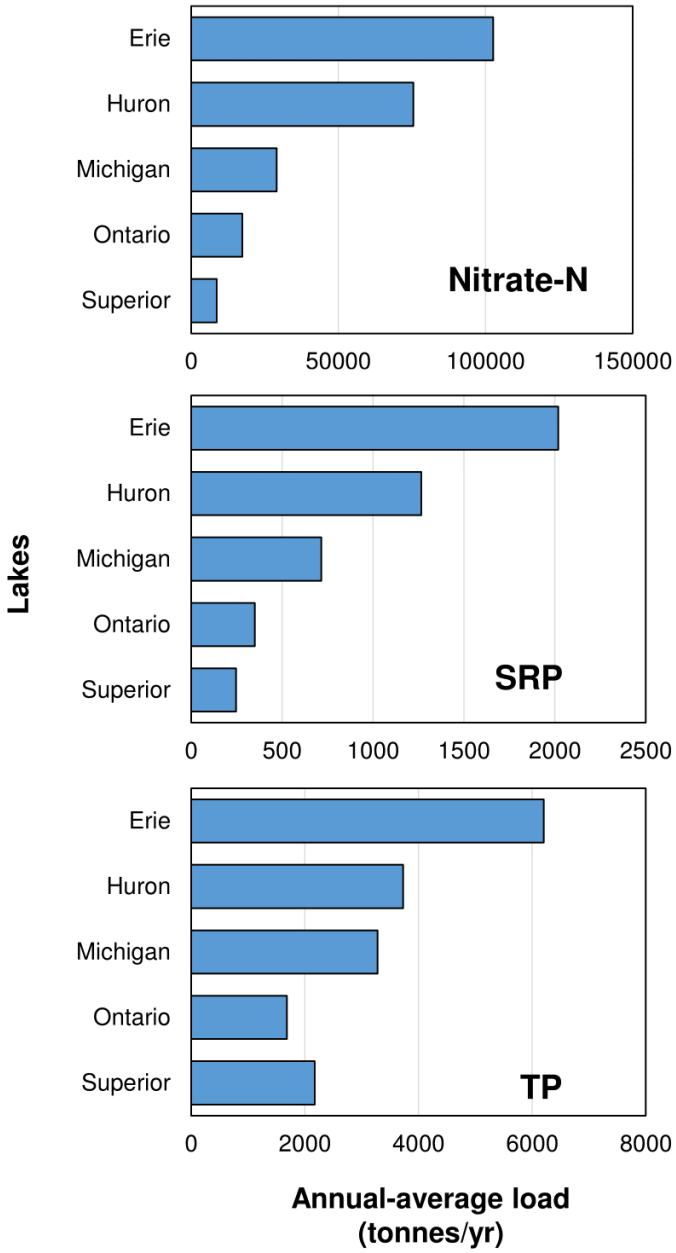

Figure 3.12. Bar plots of annual-average tributary export for each lake.

This is similar to estimates reported by Maccoux et al (2016) and Dolan and Chapra (2012) where Lake Erie TP loads for (only) monitored and unmonitored areas averaged approximately 6690 tonnes per annum between 2003 and 2013 (Maccoux, Dove, Backus, & Dolan, 2016) and 6610 tonnes per annum between 2000 and 2008 (Dolan & Chapra, 2012). Total annual-average SRP export to Lake Erie was estimated to be approximately 2020 tonnes per annum, which is

relatively close to results reported by Maccoux et al (2016), where the average load from the monitored and unmonitored tributary estimates was approximately 1680 tonnes per annum between 2009 and 2013. TP annual-average load estimates for Lakes Michigan and Huron were higher (approximately 3700 tonnes per annum for Lake Huron; 3300 tonnes per annum for Lake Michigan) compared to load estimates reported by Dolan and Chapra (2012) (1920 tonnes per annum for Lake Huron; 2720 tonnes per annum for Lake Michigan). Differences in the load estimations are likely attributed to the methodologies used to calculate nutrient loads from monitored and unmonitored stations across the Great Lakes. Dolan and Chapra (2012) and Maccoux et al (2016) applied the Stratified Beale's Ratio Estimator to estimate monitored tributary loads, in which data are broken into one or multiple strata (or layers) depending on the concentration and flow (Dolan & Chapra, 2012; Dolan et al., 1981; Maccoux et al., 2016). For unmonitored tributaries, a unit area load (UAL) procedure was used, in which the unmonitored catchment loads are calculated based on nearby monitored watersheds (Dolan & Chapra, 2012; Maccoux et al., 2016). One limitation regarding this method is failing to take into account the different land-use types from monitored watersheds when applied to estimate loads in unmonitored areas. Nutrient export to Lake Ontario and Lake Superior were observed to be the lowest for all constituents. In particular, total phosphorus estimates for Lake Ontario and Lake Superior were approximately 1690 and 1870 tonnes per annum, respectively. This was also similar to estimates from Dolan and Chopra (2012) where Lake Ontario and Lake Superior tributary TP load estimates were approximately 2060 and 2320 tonnes per year.

3.2 Intra-annual patterns in flow-weighted concentrations (Seasonality)

Understanding seasonal variability is important for developing sampling and remedial strategies for controlling nutrient export from human-impacted watersheds (Pionke, Gburek, Schnabel, Sharpley, & Elwinger, 1999; Zhu, Schmidt, & Bryant, 2012). An understanding of seasonal variability is also important when attempting to identify key drivers of nutrient processes and can lead to improved model prediction at larger spatial and temporal scales (Von Schiller et al., 2008). In the present work, I have attempted to characterize seasonal variations in flow-weighted concentrations using two different approaches: 1) use of a seasonality index (SI), which allows us to quantify the extent of monthly variations in concentration throughout the year; and 2) pattern identification with regard to relationships between monthly concentrations and monthly

discharge. A non-parametric statistical test, namely the Wilcoxon Rank-Sum (or Mann Whitney U) test, was applied to assess statistically significant differences between two groups. This test assumes independence between the two groups being compared, with no requirement for normality. For the first approach, the two groups that were compared were SI values less than the 25^{th} percentile, and SI values greater than the 75^{th} percentile. For the second approach, the two groups that were compared were the pattern of interest, and the combined remaining patterns. For both approaches, the variables that were compared were the catchment characteristics (e.g. percent agricultural land, percent silt and clay, etc.).

3.2.1 Seasonality Index

The seasonality of the flow-weighted nutrient concentrations, as quantified by the SI values (11), was found to show some variation among the three nutrients (Table 3.5). More specifically, both SRP (SI = 0.35) and TP (SI = 0.32) was found to show significantly greater seasonality (p-value < 0.001 for SRP; p-value < 0.05 for TP) than nitrate. More significant than any of the differences between nutrients, however, is the difference between the seasonality of nutrient concentrations and the seasonality of watershed discharge. SI values for discharge, which range from 0.43 to 0.77, are approximately double the concentration SI values (0.20 – 0.35), suggesting that seasonal concentrations are relatively chemostatic in comparison with seasonal discharge dynamics. Additionally, significant differences between SI groups less than the interquartile range (IQR) and greater than the IQR were compared. Specifically, in the comparison of watersheds with high (SI > IQR) and low (SI < IQR) seasonality in flow-weighted concentrations, SI was found to be significantly associated (p-value < 0.05) with watershed characteristics (Table 3.6), although the watershed drivers appear to vary according to the constituent in question.

Table 3.5. Seasonality Index (SI) Values for nitrate-N, SRP and TP; iq25 and iq75 are the 25th and 75th percentiles, respectively.

SI Values	Nitrate-N		SRP		TP	
	C_f	Q	C_f	Q	C_f	Q
iq25	0.20	0.43	0.25	0.43	0.24	0.45
Median	0.27	0.58	0.35	0.60	0.32	0.62
iq75	0.40	0.72	0.48	0.75	0.41	0.77

Higher nitrate seasonality, for example, is significantly associated with a higher median percent wetland (17%), lower percent urban and agricultural areas (4% urban; 46% agricultural), lower population densities (17 persons/km^2), and lower tile drainage densities (2%). Greater nitrate seasonality is also significantly associated with higher latitudes across the Great Lakes watersheds. These results suggest that seasonal variations in nitrate concentrations are greater in less disturbed landscapes, while the seasonality of more developed landscapes is dampened.

Table 3.6. Median values of selected catchment characteristics based on SI less than 25th and 75th percentiles. Blue values represent medians that are significantly lower, red values represent medians that are significantly higher.

Nitrate-N	AREA	AGRI	URB	FOR	WET	TD	PD	SLP	TAVG	PRECIP	SILTCLAY	LAT	LONG
SI < iq25	568.02	57.22	9.45	16.09	8.28	5.88	63.48	2.24	7.33	902.91	53.94	43.39	-80.38
SI > iq75	789.29	45.56	4.32	22.55	17.10	2.48	17.26	1.26	6.30	827.53	57.08	44.26	-83.53

SRP	AREA	AGRI	URB	FOR	WET	TD	PD	SLP	TAVG	PRECIP	SILTCLAY	LAT	LONG
SI < iq25	617.18	31.87	5.29	26.04	14.61	1.05	18.41	1.87	6.16	889.77	45.77	44.10	-80.79
SI > iq75	201.52	62.50	4.86	17.89	9.85	5.58	33.59	2.93	6.55	969.72	66.21	43.79	-80.40

TP	AREA	AGRI	URB	FOR	WET	TD	PD	SLP	TAVG	PRECIP	SILTCLAY	LAT	LONG
SI < iq25	536.90	50.79	9.38	20.11	14.57	5.35	72.05	1.05	7.07	897.01	51.98	43.51	-80.45
SI > iq75	419.18	64.53	6.56	14.87	9.05	6.88	39.15	2.11	6.72	905.15	65.92	43.69	-80.43

Interestingly, the characteristics of watersheds with high TP and SRP seasonality are quite different, with high seasonality being associated with higher median percent agricultural area (TP, 65%; SRP, 63%), a higher tile drainage density (TP, 7%; SRP, 6%), a higher percent silt and clay content (TP, 66%; SRP, 66%), but lower percent forested area (SRP, 18%). Thus, for P, higher seasonality is observed in more agricultural landscapes and less urban-developed areas. Notably, high discharge seasonality is also significantly associated (p-value < 0.05) with high percent agricultural area and high tile drainage densities, suggesting that the seasonality of P concentrations in both dissolved and particulate forms is more closely linked with discharge dynamics than that of nitrate.

3.2.2 Monthly Regime Curves

As discussed in Section 3.2.1, watershed solute concentrations often exhibit significant seasonality. To better characterize these seasonal patterns, correlations between concentrations and discharge were quantified at the monthly scale. Through this analysis, three primary patterns of seasonal behavior were identified: (1) in-phase; (2) out-of-phase; and (3) stationary. In-phase behavior is characterized by a positive linear relationship (p-value < 0.05) between monthly flow-weighted concentrations and monthly mean discharge, while out-of-phase behavior has a *negative* linear relationship (p-value < 0.05). In contrast, watersheds with biogeochemically stationary behavior exhibit no significant relationship with monthly discharge (p-value > 0.05) and little seasonality (SI < median SI). Table 3.7 summarizes the statistical differences between in-phase, out-of-phase, and stationary watershed groups in relation to individual catchment characteristics.

Table 3.7. Median values of Seasonality Index (SI) and selected catchment characteristics based on in-phase, out-of-phase, and stationary watershed groups for nitrate-N, SRP and TP. Blue values represent medians that are significantly lower, red values represent medians that are significantly higher, and gray values show no significant difference.

Nitrate-N	Percent	AREA	AGRI	URB	FOR	WET	TD	PD	SLP	TAVG	PRECIP	SILTCLAY	LAT	LONG
in-phase	43	748.10	65.02	5.66	18.84	9.85	10.52	35.97	2.23	6.65	957.44	64.74	43.59	-80.47
out-of-phase	7	186.86	50.70	14.62	16.62	8.17	2.27	263.72	1.06	7.75	899.10	50.40	43.06	-80.96
stationary	26	314.47	51.04	12.18	17.01	11.20	1.30	89.93	3.50	7.26	882.89	47.35	43.55	-80.06
other	23	357.68	25.47	4.32	32.25	18.68	0.49	17.26	0.74	6.30	825.56	49.42	44.26	-87.72

SRP	Percent	AREA	AGRI	URB	FOR	WET	TD	PD	SLP	TAVG	PRECIP	SILTCLAY	LAT	LONG
in-phase	24	624.49	61.39	4.29	21.12	10.79	10.52	20.56	2.58	6.09	951.23	52.22	43.96	-80.44
out-of-phase	32	255.88	40.98	10.54	22.44	11.41	3.05	84.14	1.72	7.51	892.70	50.51	43.44	-80.01
stationary	23	748.99	45.29	6.39	21.17	14.04	5.70	23.96	0.74	6.66	896.81	55.55	43.53	-83.36
other	20	253.94	62.12	8.45	11.90	8.59	5.13	47.48	1.90	7.31	840.51	62.82	43.54	-81.10

TP	Percent	AREA	AGRI	URB	FOR	WET	TD	PD	SLP	TAVG	PRECIP	SILTCLAY	LAT	LONG
in-phase	35	550.54	64.80	8.77	14.50	8.28	11.41	47.17	1.63	6.95	890.07	66.24	43.62	-81.33
out-of-phase	9	142.70	51.67	7.09	19.75	12.50	4.26	55.23	2.53	6.91	947.84	54.95	43.48	-79.96
stationary	35	464.82	50.38	10.14	16.75	12.28	5.78	84.17	0.80	7.35	870.59	56.09	43.42	-83.23
other	20	211.66	62.50	7.36	12.01	9.51	5.76	40.98	0.79	7.26	821.48	64.01	43.77	-83.13

As shown in Figure 3.13 (a,b,c), in-phase watersheds commonly show maximum concentration values in winter or early spring, coinciding with increased winter stream flows and periods of spring snowmelt. Notably, the highest discharge months are almost always either March or April (> 90% of watersheds), and watersheds exhibiting in-phase behavior for P also show concentration peaks during these two months (63% SRP; 60% TP). These results suggest that in-phase behavior for P is strongly driven by discharge and landscape dynamics associated with snowmelt and overland flow. For nitrate-N, however, watersheds demonstrating in-phase behavior illustrate a lack of synchronicity between discharge and concentration values during the winter and spring months. More specifically, the in-phase watersheds commonly show concentration peaks in the winter (December, January, and February) months (71% of in-phase watersheds), while only 26% show concentration peaks during March and April, when discharge peaks. Accordingly, although the relationships between monthly concentration and discharge for nitrate are significant for in-phase watersheds, the asynchrony between spring discharge peaks and winter concentration peaks suggests that higher nitrate concentrations are in general less

associated with surface hydrology than with other winter dynamics such as reduced plant uptake (Cambardella et al., 1999), high mineralization rates during freeze-thaw events (Matzner & Borken, 2008), and rising water tables providing connectivity between upland streams and high-nitrate pore water (Molenat, Gascuel-Odoux, Ruiz, & Gruau, 2008).

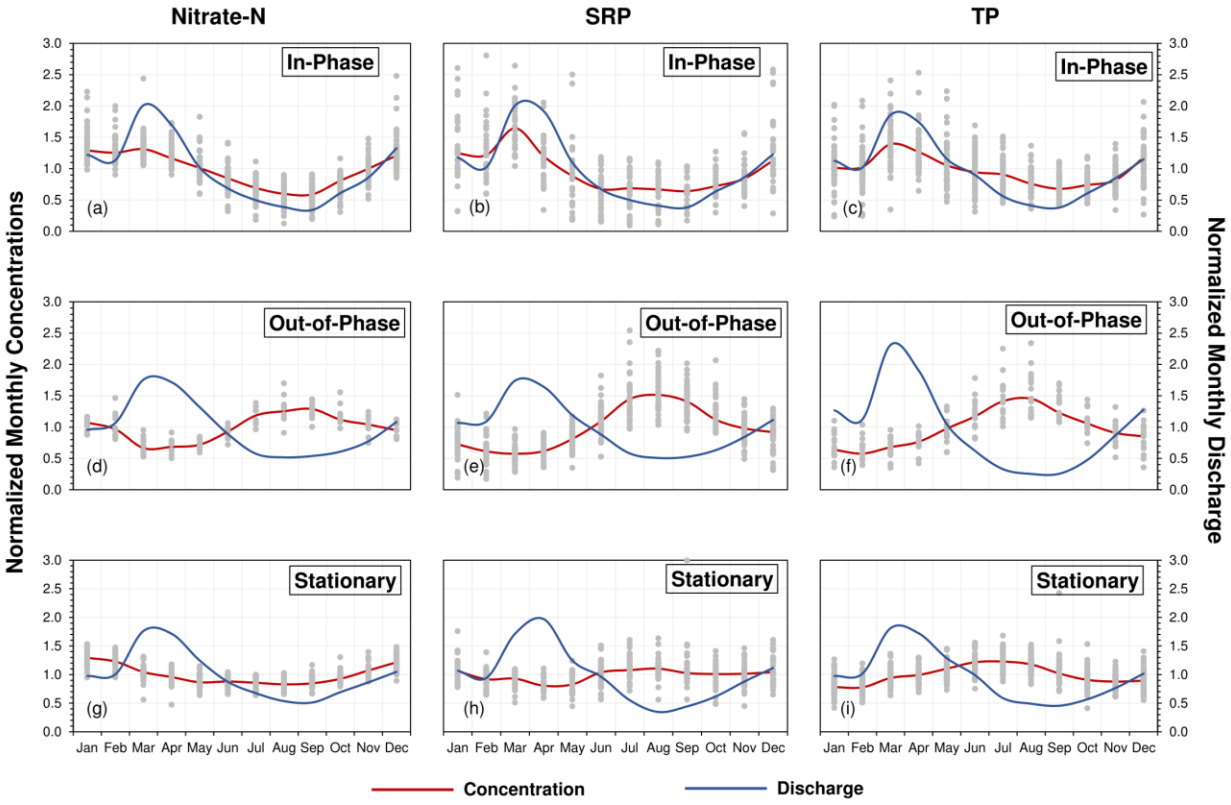

Figure 3.13. Concentration and flow regime curves for nitrate, total P, and soluble reactive P across the Great Lakes Basin. Both concentration and discharge are represented here as normalized values to allow for comparison between watersheds. Our results show three primary patterns of behavior: (1) In-Phase (panels a,b,c), characterized by positive significant relationships (p-value < 0.05) with discharge; (2) Out-of-Phase (panels d,e,f), characterized by negative significant relationships (p-value < 0.05) with discharge; and (3) Stationary (panels g,h,i), characterized by low seasonality (SI < median SI) and no significant relationship with discharge (p-value > 0.05). In all, these three patterns account for 77%, 80%, and 80% of all watersheds for nitrate-N, SRP, and TP, respectively.

For all of the constituents, the in-phase concentration regimes are observed in watersheds with high percent agricultural areas (65%) and high tile drainage densities (>10%), as well as those with higher precipitations rates (>870 mm/year). In contrast, out-of-phase concentration regimes

(Figure 3.14 (d,e,f)) show clear summer concentration peaks, with the majority of out-of-phase watersheds demonstrating maximum concentrations in August (nitrate-N, 40%; SRP, 58%; TP, 60%), a time that coincides with high plant nutrient uptake (Bennett, Mutti, Rao, & Jones, 1989), near-peak temperatures, and low streamflow conditions conventionally not associated with high stream concentrations. For both nitrate-N and TP, the out-of-phase regime is somewhat rare, being observed in only 7% and 9% of the study watersheds, respectively. In contrast, the out-of-phase pattern is the most common concentration regime for SRP, with 30% of watersheds exhibiting this behavior. For nitrate, the out-of-phase watersheds are clearly characterized by significantly higher (p-value < 0.05) population densities (264 persons/km^2) and a higher percent urban area (15%), suggesting that effluent from wastewater treatment plants may be driving summer nitrate concentrations. Out-of-phase SRP behavior is also significantly (p-value < 0.05) linked to higher percent urban areas (11%), but population densities (84 persons/km^2) are lower for the SRP out-of-phase watersheds than for watersheds showing this pattern for nitrate. Out-of-phase TP watersheds, however, show no significant relationship with urban areas. Instead, they are distinguished by their relatively higher watershed slopes (2.5%) and smaller watershed areas (143 km^2). In general, higher concentrations during periods of low summer flow are suggestive of point source contributions. Whether these are conventional point sources such as wastewater treatment plants, as suggested by the nitrate and SRP dynamics, or less conventional point sources such as wetlands or reservoirs, as may be the case with TP, may vary according to not only constituent, but the location of potential sources proximal to water quality sampling stations as well.

The stationary concentration regime occurs in 26% of watersheds for nitrate-N, 23% for SRP, and 35% for TP. As can be seen in Figure 3.13 (g,h,i), the discharge seasonality remains equivalent to that seen in the other concentration regimes, but there is little to no variation in solute concentrations across seasons. For nitrate, stationarity is particularly associated with low tile drainage densities (1.3%) and a somewhat higher urban footprint (population density, 90 persons/km^2; 12% urban area). In this case, lower tile drainage densities are likely reducing the transport of nitrate during the winter months, while higher population densities, through increased N loading from wastewater and industrial discharges, are increasing summer concentrations, resulting in a flattened concentration curve. For SRP, very different drivers seem to be at play, as stationarity is significantly (p-value < 0.05) associated with lower population

densities (24 persons/km^2) but higher percent wetland areas (14%). In these relatively less-impacted areas, wetlands appear to be a major driver of SRP regimes and may reflect seasonal variations in SRP internal loading dynamics, with the wetlands serving as a source during the low-flow summer months but a potential sink during winter and spring (Reddy, Diaz, Scinto, & Agami, 1995).

3.3 Concentration-Discharge Relationships

In Section 3.2, concentration-discharge relationships at a monthly scale were analyzed as a means of understanding linkages between watershed characteristics and varying seasonal concentration regimes for nitrate, total P, and soluble reactive P. In this section, I explore how event-scale concentration-discharge dynamics vary across the Great Lakes Basin?

3.3.1 Quantifying Event-Scale C-Q relationships in the Great Lakes Watersheds

Event-scale concentration-discharge metrics have been developed as a means of classifying nutrient export regimes for catchments (P. Haygarth et al., 2004) and are increasingly becoming valuable tools for understanding catchment functionality (Musolff et al., 2015), simplifying predictions of biogeochemical signatures, and assisting managers to develop and implement strategies in improving water quality (S. R. Carpenter, 2002; Clark et al., 2001). In the present study, I focused primarily on two metrics, "*b*-values" and concentration-discharge variance ratios.

In some watersheds, concentrations may increase during rain or snowmelt events (accretion patterns), while in others, concentrations may decrease (dilution patterns), or remain relatively flat (chemostatic). The relationship between concentration and discharge is commonly understood to be in the empirical form of a power law function (1) (Basu et al., 2010; P. Haygarth et al., 2004; Vogel, Rudolph, & Hooper, 2005). Event-scale patterns can be characterized by the slope-*b* value, with high positive values representing accretion patterns and large negative values indicating dilution patterns. Within this framework, smaller slope-*b* values are associated with more chemostatic behavior (Basu et al., 2010; Godsey et al., 2009), meaning

that concentration remains constant regardless of variations in discharge. Figure 3.14 illustrates examples of selected catchments with accretion, dilution, and stationary patterns for selected nitrate-N catchments. The CV ratio (3) measures the overall variability in concentrations with respect to variations in discharge. Low CV ratios (< 0.3) indicate chemostatic behaviour whereas higher CV ratios illustrate chemodynamic behaviour of the catchment. Histogram plots (Figure 3.15) were constructed to summarize the overall distribution of slope-*b* and CV ratio values for all constituents. Note that catchments with acceptable flux-biases (within ± 15%) and significant slope-*b* magnitudes (p-value < 0.05) are presented. Slope-*b* values in the Great Lakes watersheds ranged between -0.6 – 1.3 for nitrate-N, -0.7 – 1.3 for SRP, and -0.3 – 1.4 for TP. CV ratio magnitudes ranged from 0.1 to 4.0 for nitrate-N, 0.2 to 4.2 for SRP, and 0.2 to 3.3 for TP. Additionally, variation in the slope-*b* and CV ratio among the three nutrients were also found. Specifically, median slope-*b* for TP (0.30) was significantly (p-value < 0.05) higher than nitrate-N (0.22), indicating stronger accretion patterns for phosphorus. Additionally, median CV ratio for nitrate-N (0.41) was significantly lower than both SRP (0.77) and TP (0.63), suggesting more chemostatic behaviour for nitrogen compared to chemodynamic behaviour which is more commonly observed for phosphorus (Basu et al., 2010; Thompson et al., 2011).

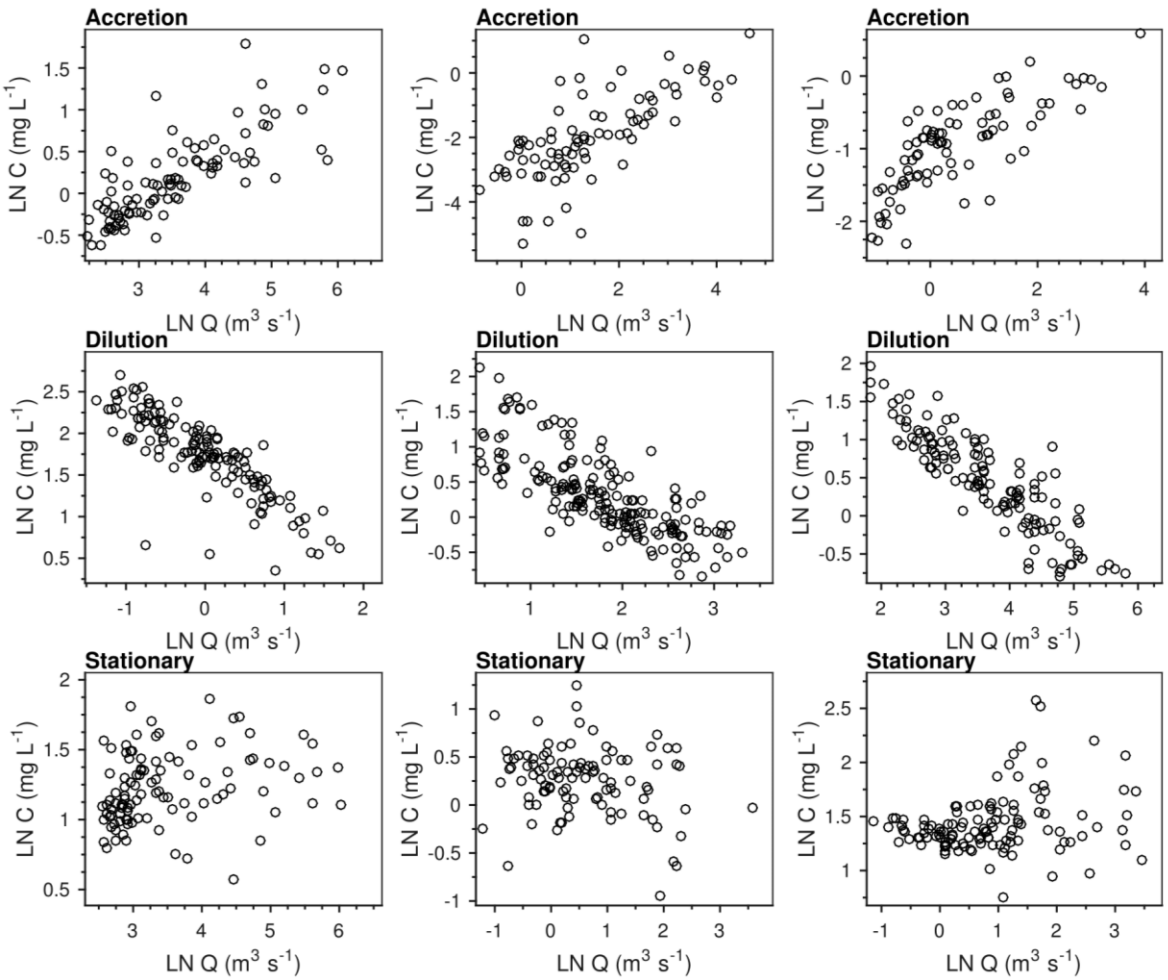

Figure 3.14. Natural-log transformed C-Q plots of selected catchments for nitrate-N. Regression slopes were significant with p-value < 0.05.

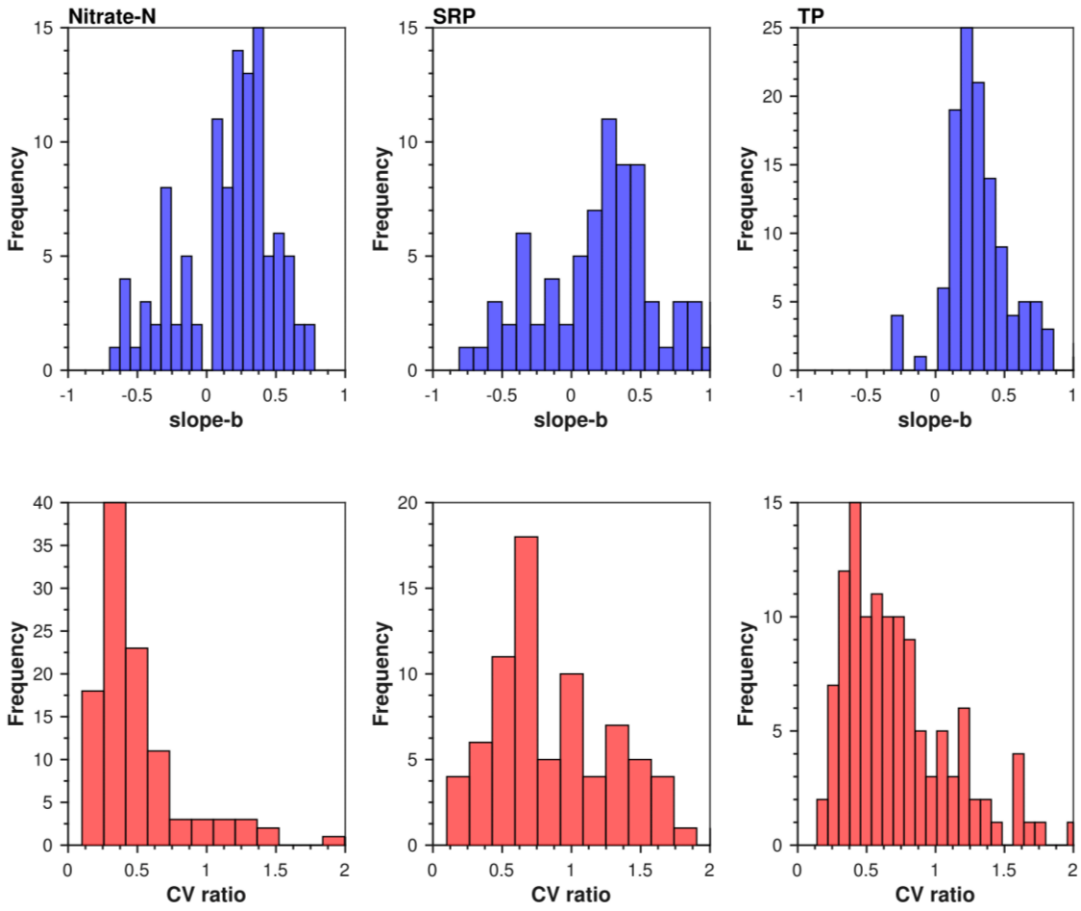

Figure 3.15. Histogram plots of slope-*b* and CV ratio

3.3.2 Slope-b vs. CVR relationship

The degree of correlation between slope-*b* (obtained from lnC – lnQ relationship) and CV ratio can be expressed with Pearson's correlation coefficient (Jawitz & Mitchell, 2011). Musolff et al (2015) proposed a plot which visualizes the biogeochemical signatures of solutes and nutrients by combining the slope-*b* metric and CV ratio. The x-axis shows the CV ratio which describes the variability of concentrations with respect to the variability of discharge. The y-axis shows the slope-*b* magnitudes which describe the type of chemostatic behaviour of the watershed (i.e. accretion behaviour if slope-*b* > 0, dilution behaviour if slope-*b* < 0). Figure 3.16 illustrates the biogeochemical responses of selected watersheds in the Great Lakes region for nitrate-N, SRP and TP.

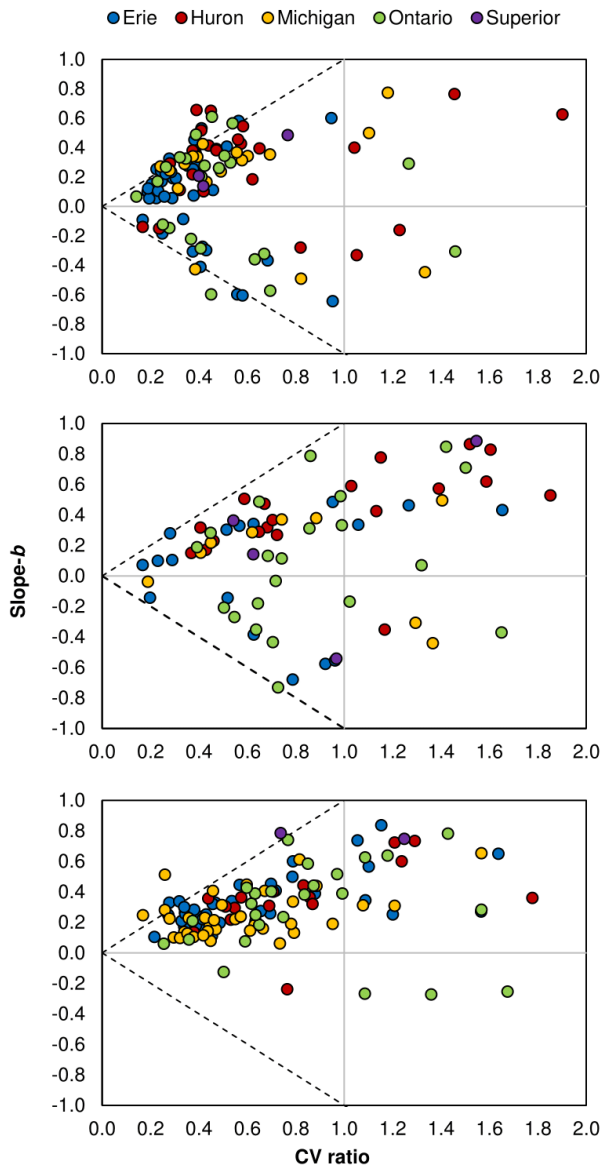

Figure 3.16. Slope-b as a function of CVR correlation plots for nitrate-N, SRP and TP. Blue represents Lake Erie catchments; green represents Lake Ontario catchments; red represents Lake Huron catchments; yellow represents Lake Michigan catchments; purple represents Lake Superior catchments. Only stations with significant slopes (p-value < 0.05) are y shown.

The plots provide a visual aid in understanding the extent to which concentration variability is driven by discharge, and also highlight other potential processes that may influence nutrient export (Musolff et al., 2015). Points that are on the dashed 1:1 line represent watersheds in which the CV ratio is primarily influenced by the slope-*b*. Points that deviate from the boundary line are ones in which other processes may affect CV variability like local denitrification, etc. (Musolff et al., 2015). Figure 3.17 shows a greater number of watersheds with significant

dilution pattern for nitrate-N (p-value < 0.05) and SRP catchments (26% nitrate-N; 27% for SRP); whereas, only 4% of TP catchments exhibit this type of behaviour. Additionally, CV ratios illustrate larger scatter for SRP (average CV ratio = 0.96) and TP (average CV ratio = 0.73), compared to nitrate-N (average CV ratio = 0.56). Differences in slope-*b* and CV ratios were also observed for individual lakes (Table 3.8). For example, median nitrate CV ratio and slope-*b* for Lake Erie were significantly lower than Lakes Huron, Michigan, Ontario, and Superior.

Table 3.8. Median slope-*b* and CV ratios for nitrate-N, SRP and TP based on Lake.

	Nitrate-N		SRP		TP	
	slope-*b*	CV ratio	slope-*b*	CV ratio	slope-*b*	CV ratio
Erie	0.12	0.35	0.28	0.63	0.28	0.48
Ontario	0.20	0.45	0.12	0.80	0.38	0.84
Huron	0.39	0.47	0.40	0.88	0.36	0.76
Michigan	0.30	0.46	0.29	0.85	0.23	0.55
Superior	0.21	0.42	0.25	0.80	0.77	0.99

Lower nitrate CV ratio for Lake Erie was also associated with higher median agricultural land (71%, p-value < 0.05), and higher tile drainage (23%, p-value < 0.05). Significantly lower CV ratio for TP in Lake Erie catchments was also associated with higher agricultural (73%) and tile drainage (34%) percentages. This chemostatic behavior in the intensively managed catchments surrounding Lake Erie is associated with high levels of agricultural production and points to the role of legacy as a buffer mechanism for reducing concentration variability (Basu et al., 2010; Musolff et al., 2015; Thompson et al., 2011). For Lake Ontario, median SRP slope-*b* was significantly lower compared to Lake Huron. Median nitrate-N and SRP slope-*b* values for Ontario were also significantly associated with lower agricultural (nitrate-N, 49%; SRP, 43%) and tile drainage (nitrate-N, 1%; SRP, 1%) areas, higher population densities (nitrate-N, 89 persons/km^2; SRP, 95 persons/km^2), and higher percent slope (nitrate-N, 4%; SRP, 3%). Additionally, lower median slope-*b* for TP in Lake Michigan catchments were associated with

larger urban areas (10%) but lower percent slope (0.7%). For Lake Huron catchments, significantly higher median CV ratio for TP (0.76) was associated with higher forested area (24%), higher percent slope (3%), lower urban area (4%), and lower population density (21 persons/km^2).

4.0 Study limitations and conclusions

Nutrient pollution is a major driver of eutrophication in many water bodies across the Great Lakes Basin. This research study has focused on quantifying dominant controls on stream nutrient concentrations across the GLB at three temporal scales: annual scale, seasonal scale and event scale. Numerous watershed drivers, including land use, soil, climate and other watershed characteristics were analyzed to quantify controls on nutrient export. Regression analyses and other statistical techniques that were used in this study helped identify relationships between multiple variables that became important in identifying key hydrologic and biogeochemical signatures.

The limitations encountered when using regression-based techniques for exploratory analysis include a lack of regularly obtained stream water quality measurements in certain monitoring locations, limited frequency of sampling measurements at certain times of the year (e.g., fewer sampling measurements in the winter versus summer season; low-flow season versus high-flow events, etc.), and the presence of multi-collinearity in the multiple regression analysis. Additionally, data pertaining to catchment characteristics such as land use and climate were static (i.e. changes in land-use over time were not considered).

Future work may include assessing changes in biogeochemical signatures over time, e.g., exploring water quality before, during, and after the establishment of the GLWQA, particularly under changing land use and climate. Uncertainty analysis with regard to the WRTDS estimates (such as extracting the 'standard errors' of the model coefficients or applying Monte Carlo analyses) were beyond the scope of this study; however, it is critical to consider this component of error analysis in future work. Additionally, methods to estimate annual-average flow may also be improved. The current method utilizes a simple single-regression model where annual-average discharge is a function of drainage area only. An alternative approach is to apply the

area ratio method (ARM), in which discharge in an unmonitored area is estimated by multiplying the ratio of the drainage areas for the unmonitored and nearby monitored gauging station, by the annual-average discharge of the nearby monitored discharge station (Emerson, Vecchia, & Dahi, 2005; Fry et al., 2014).

At the annual scale, mean annual flow-weighted nutrient concentrations for selected basins were computed within the Great Lakes Basin. FWC were then individually regressed against selected catchment characteristics, including percent agricultural and urban land use, percent silt and clay content, percent slope, and others. The results from our analysis showed land use (e.g. percent agricultural and urban land, percent wetlands, etc.) as the strongest driver of flow-weighted concentrations for nitrate-N, SRP and TP. Other significant drivers included percent silt and clay content (62%), and percent tile drainage (54%). Multiple regression analysis was used to estimate nutrient concentrations across the Great Lakes watersheds to identify nutrient hotspots. Hotspots for nitrate-N, SRP and TP were found in the Lake Erie watersheds, specifically the lower Maumee and Sydenham River catchments. Lowest nutrient concentrations were observed in Lake Superior watersheds. Moderate concentrations for nitrate-N (0.5 – 3 mg/L), SRP (15 – 40 µg/L) and TP (100-180 µg/L) were found in the Lower Fox catchment of Lake Michigan and the Saginaw Bay catchment of Lake Huron.

Annual average loads were estimated using multiple regression analysis to determine the total annual average export for each lake. Lake Erie was observed to have the highest load for all three nutrients, whereas Lake Superior showed the lowest average annual export, with the exception of total phosphorus. Spatial patterns across the Great Lakes showed Lake Erie Basins consistently generating the highest annual average yields (approximate 13, 0.3, and 0.8 kg/ha/yr for nitrate-N, SRP and TP, respectively). Hotspots for annual average SRP and TP loads were reflected in the human-impacted catchments of Lakes Erie (Lower Maumee and Sydenham), Huron (Ausable and Pigeon-Wiscoggin), and Michigan (Manitowoc-Sheboygan, Milwaukee, and Pike-Root).

Seasonal variations in flow-weighted concentrations were explored based on the seasonality index and regime curve patterns. Findings from our analysis showed significantly higher seasonality for SRP and TP, compared to nitrate-N. Discharge seasonality was found to be much higher (0.43 – 0.77) than FWC seasonality (0.2 – 0.35). The seasonality index for FWC was found to be significantly associated with catchment characteristics. Higher nitrate-N seasonality

index values for example, were found to be linked with lower percent urban and agricultural areas, lower population densities, and lower tile drainage densities. In contrast, higher SI values for phosphorus were associated with larger agricultural area, higher tile drainage density, and lower forested area.

Regime curves for flow-weighted concentrations were characterized based on correlations between monthly FWC and discharge. Three patterns of seasonal behaviour were identified, namely 'in-phase' (positive correlation between monthly FWC and monthly mean discharge), 'out-of-phase' (negative correlation between monthly FWC and monthly mean discharge), and 'stationary' (no significant relationship between monthly FWC and monthly mean discharge). Out-of-phase behaviour was more frequently observed for SRP than for nitrate-N or TP. Additionally, higher concentrations during low-flow periods suggests point-source contributions such as wastewater treatment plants, reservoirs, or wetlands (as a source). Stationary regime curves for nitrate-N may be attributed to lower export in the winter months in relation to lower tile drainage density, but higher export in the summer months from wastewater effluents in catchments with larger population density.

Event-scale concentration-discharge metrics (i.e. slope-*b* and CV ratio) were estimated in order to understand concentration variability as a function of discharge and identify potential controls between concentration and discharge for catchments in the Great Lakes area. In my analysis based on the sampled watersheds within the Great Lakes, I observed significantly higher median slope-*b* values for TP compared to nitrate-N. Additionally, the median CV ratio for nitrate-N was significantly lower than for both SRP and TP, suggesting more chemostatic behaviour for N and chemodynamic behaviour for P. The slope-*b* versus CV ratio plot illustrated a greater number of (significantly) dilution-driven catchments for SRP (35%) and nitrate-N (26%) compared to TP (4%). CV ratios for phosphorus were also observed to be higher compared to nitrate-N. Differences in slope-*b* and CV ratios between individual Lakes showed lower CV ratio for nitrate-N and TP in Lake Erie catchments, which were significantly associated with higher agricultural area and tile drainage densities. Median slope-*b* values for nitrate-N (0.20) and SRP (0.12) in Lake Ontario watersheds were associated with higher population densities and percent slope, as well as lower agricultural and tile drainage areas. Significantly lower slope-*b* and CV ratios for TP in Lake Michigan were associated with lower forest areas and lower percent slope.

Catchments in Lake Huron showed significantly higher median CV ratios for TP (0.76) compared to all other lakes, which was found to be associated with significantly higher forested area (24%).

References

Ahiablame, L. M., Chaubey, I., Smith, D. R., & Engel, B. A. (2011). Effect of tile effluent on nutrient concentration and retention efficiency in agricultural drainage ditches. *Agricultural Water Management*, *98*(8), 1271–1279. https://doi.org/10.1016/j.agwat.2011.03.002

Allan, J. D. (2004). Influence of land use and landscape setting on the ecological status of rivers. *Limnetica*, *23*(3–4), 187–198. https://doi.org/10.1146/annurev.ecolsys.35.120202.110122

Arheimer, B., & Lidén, R. (2000). Nitrogen and phosphorus concentrations from agricultural catchments—influence of spatial and temporal variables. *Journal of Hydrology*, *227*(1–4), 140–159. https://doi.org/10.1016/S0022-1694(99)00177-8

Aronica, G. T., & Candela, A. (2007). Derivation of flood frequency curves in poorly gauged Mediterranean catchments using a simple stochastic hydrological rainfall-runoff model. *Journal of Hydrology*, *347*(1–2), 132–142. https://doi.org/10.1016/j.jhydrol.2007.09.011

Asano, Y., Uchida, T., Mimasu, Y., & Ohte, N. (2009). Spatial patterns of stream solute concentrations in a steep mountainous catchment with a homogeneous landscape. *Water Resources Research*, *45*(10), 1–9. https://doi.org/10.1029/2008WR007466

Aulenbach, B. T., & Hooper, R. P. (2006). The composite method: An improved method for stream-water solute load estimation. *Hydrological Processes*, *20*(14), 3029–3047. https://doi.org/10.1002/hyp.6147

Band, L. E., Tague, C. L., Groffman, P., & Belt, K. (2001). Forest ecosystem processes at the watershed scale: Hydrological and ecological controls of nitrogen export. *Hydrological Processes*, *15*(10), 2013–2028. https://doi.org/10.1002/hyp.253

Basu, N. B., Destouni, G., Jawitz, J. W., Thompson, S. E., Loukinova, N. V., Darracq, A., … Rao, P. S. C. (2010). Nutrient loads exported from managed catchments reveal emergent biogeochemical stationarity. *Geophysical Research Letters*, *37*(23), 1–5. https://doi.org/10.1029/2010GL045168

Basu, N. B., Thompson, S. E., & Rao, P. S. C. (2011). Hydrologic and biogeochemical functioning of intensively managed catchments: A synthesis of top-down analyses. *Water Resources Research*, *47*(10), 1–13. https://doi.org/10.1029/2011WR010800

Beeton, A. M. (2002). Large freshwater lakes: present state, trends, and future. *Environmental Conservation*, *29*(01), 21–38. https://doi.org/10.1017/S0376892902000036

Bennett, J., Mutti, L., Rao, P., & Jones, J. (1989). Interactive effects of nitrogen and water stresses on biomass accumulation, nitrogen uptake, and seed yield of maize. *Field Crops Research*, *19*(8847), 297–311. https://doi.org/10.1016/0378-4290(89)90100-7

Biron, P. M., Roy, A. G., Courschesne, F., Hendershot, W. H., Côté, B., & Fyles, J. (1999). The effects of antecedent moisture conditions on the relationship of hydrology to hydrochemistry in a small forested watershed. *Hydrological Processes*, *13*(11), 1541–1555. https://doi.org/10.1002/(SICI)1099-1085(19990815)13:11<1541::AID-HYP832>3.0.CO;2-J

Blann, K. L., Anderson, J. L., Sands, G. R., & Vondracek, B. (2009). Effects of agricultural

drainage on aquatic ecosystems: A review. *Critical Reviews in Environmental Science and Technology*, *39*(11), 909–1001. https://doi.org/10.1080/10643380801977966

Bruland, G. L., Grunwald, S., Osborne, T. Z., Reddy, K. R., & Newman, S. (2006). Spatial Distribution of Soil Properties in Water Conservation Area 3 of the Everglades. *Soil Science Society of America Journal*, *70*(5), 1662. https://doi.org/10.2136/sssaj2005.0134

Brutsaert, W., & Nieber, J. L. (1977). Regionalized drought flow hydrographs from a mature glaciated plateau. *Water Resources Research*, *13*(3), 637–643. https://doi.org/10.1029/WR013i003p00637

Burt, T. P., & Pinay, G. (2005). Linking hydrology and biogeochemistry in complex landscapes. *Progress in Physical Geography*, *3*, 297–316. https://doi.org/10.1191/0309133305pp450ra

Cambardella, C. a., Moorman, T. B., Jaynes, D. B., Hatfield, J. L., Parkin, T. B., Simpkins, W. W., & Karlen, D. L. (1999). Water Quality in Walnut Creek Watershed: Nitrate-Nitrogen in Soils, Subsurface Drainage Water, and Shallow Groundwater. *Journal of Environment Quality*, *28*(1), 25–34. https://doi.org/10.2134/jeq1999.00472425002800010003x

Canada, & USA. (2013). *Great Lakes Water Quality Agreement*.

Carpenter, S., Caraco, N. F., Correll, D. L., Howarth, R. W., Sharpley, A. N., & Smith, V. H. (1998). Nonpoint Pollution of Surface Waters with Phosphorus and Nitrogen. *Issues in Ecology*, *4*(3), 1–12. https://doi.org/1092-8987

Carpenter, S. R. (2002). Ecological Futures : Building an Ecology of the Long Now. *Ecology*, *83*(8), 2069–2083.

Chanat, J. G., Rice, K. C., & Hornberger, G. M. (2002). Consistency of patterns in concentration-discharge plots. *Water Resources Research*, *38*(8), 22-1-22–10. https://doi.org/10.1029/2001WR000971

Chatterjee, S., & Hadi, A. S. (2006). *Regression Analysis by Example* (4th ed.). New Jersey: John Wiley & Sons, Inc.

Cirmo, C. P., & McDonnell, J. J. (1997). Linking the hydrologic and biogeochemical controls of nitrogen in near-stream zones of temperate-forested catchments A review. *Journal of Hydrology*, *199*, 88–120.

Clark, J. S., Carpenter, S. R., Barber, M., Collins, S., Dobson, A., Foley, J. A., … Wear, D. (2001). Ecological forescasts: an emerging imperative. *Science*, *293*(July), 657–660.

Cochran, W. G. (1977). Sampling Techniques, third edition, 428.

Cohn, T. A. (2005). Estimating contaminant loads in rivers: An application of adjusted maximum likelihood to type 1 censored data. *Water Resources Research*, *41*(7), 1–13. https://doi.org/10.1029/2004WR003833

Cohn, T. A., Caulder, D. L., Gilroy, E. J., Zynjuk, L. D., & Summers, R. M. (1992). The validity of a simple statistical model for estimating fluvial constituent loads: An Empirical study involving nutrient loads entering Chesapeake Bay. *Water Resources Research*. https://doi.org/10.1029/92WR01008

Creed, I. F., & Band, L. E. (1998). Export of nitrogen from catchments within a temperate forest: Evidence for a unifying mechanism regulated by variable source area dynamics. *Water Resources Research*, *34*(11), 3105–3120. https://doi.org/10.1029/98WR01924

De Pinto, J. V., Young, T. C., & McIlroy, L. M. (1986). Great Lakes water quality improvement. *Environmental Science & Technology*, *20*(8), 752–759.

Dolan, D. M., & Chapra, S. C. (2012). Great Lakes total phosphorus revisited: 1. Loading analysis and update (1994-2008). *Journal of Great Lakes Research*, *38*(4), 730–740. https://doi.org/10.1016/j.jglr.2012.10.001

Dolan, D. M., Yui, A. K., & Geist, R. D. (1981). Evaluation of River Load Estimation Methods for Total Phosphorus. *Journal of Great Lakes Research*, *7*(3), 207–214. https://doi.org/10.1016/S0380-1330(81)72047-1

Dove, A., & Chapra, S. C. (2015). Long-term trends of nutrients and trophic response variables for the Great Lakes. *Limnology and Oceanography*, *60*(2), 696–721. https://doi.org/10.1002/lno.10055

Downing, J. A., Watson, S. B., & McCauley, E. (2001). Predicting Cyanobacteria dominance in lakes. *Canadian Journal of Fisheries and Aquatic Sciences*, *58*, 1905–1908. https://doi.org/https://doi.org/10.1139/f01-143

Duan, N. (1983). A Nonparametric Smearing Estimate : Method Retransformation. *Journal of the American Statistical Association*, *78*(383), 605–610.

Duncan, J. M., Welty, C., Kemper, J. T., Groffman, P. M., & Band, L. E. (2017). Dynamics of nitrate concentration-discharge patterns in an urban watershed. *Water Resources Research*, *53*(8), 7349–7365. https://doi.org/10.1002/2017WR020500

Emerson, D., Vecchia, A., & Dahi, A. (2005). Evaluation of Drainage-Area Ratio Method Used to Estimate Streamflow for the Red River of the North Basin , North Dakota and Minnesota Scientific Investigations Report 2005 – 5017 Evaluation of Drainage-Area Ratio Method Used to Estimate Streamflow for th. *Scientific Investigations Report*, 1–13.

Ensign, S. H., & Doyle, M. W. (2006). Nutrient spiraling in streams and river networks. *Journal of Geophysical Research: Biogeosciences*, *111*(4), 1–13. https://doi.org/10.1029/2005JG000114

Environment Canada, & U.S. Environmemntal Protection Agency. (2014). *State of the Great Lakes 2011*. https://doi.org/En161-3/1-2011E-PDF. EPA 950-R-13-00

Evans, C., & Davies, T. D. (1998). Causes of concentration/discharge hysteresis and its potential as a tool for analysis of episode hydrochemistry. *Water Resources Research*, *34*(1), 129–137. https://doi.org/10.1029/97WR01881

Fick, S. E., & Hijmans, R. J. (2017). WorldClim 2: new 1-km spatial resolution climate surfaces for global land areas. *International Journal of Climatology*, *37*(12), 4302–4315. https://doi.org/10.1002/joc.5086

Fiorentino, I., Fahey, T. J., Groffman, P. M., Driscoll, C. T., Eagar, C., & Siccama, T. G. (2003). Initial responses of phosphorus biogeochemistry to calcium addition in a northern hardwood

forest ecosystem. *Canadian Journal of Forest Research*, *33*(10), 1864–1873. https://doi.org/10.1139/x03-111

Fry, L. M., Gronewold, A. D., Fortin, V., Buan, S., Clites, A. H., Luukkonen, C., … Restrepo, P. (2014). The Great Lakes Runoff Intercomparison Project Phase 1: Lake Michigan (GRIP-M). *Journal of Hydrology*, *519*(PD), 3448–3465. https://doi.org/10.1016/j.jhydrol.2014.07.021

Fryefield, C. B. (2013). *The Evolution of the 2012 Great Lakes Water Quality Agreement*. University of Michigan.

Godsey, S. E., Kirchner, J. W., & Clow, D. W. (2009). Concentration–discharge relationships reflect chemostatic characteristics of US catchments. *Hydrological Processes*, *23*, 1844–1864. https://doi.org/10.1002/hyp.7315

Graham, M. H. (2003). Confronting multicollinearity in cological multiple regression. *Ecology*, *84*(11), 2809–2815. https://doi.org/10.1890/02-3114

Grimaldi, S., Petroselli, A., Tauro, F., & Porfiri, M. (2012). Time of concentration: a paradox in modern hydrology. *Hydrological Sciences Journal*, *57*(2), 217–228. https://doi.org/10.1080/02626667.2011.644244

Guo, Y., Markus, M., & Demissie, M. (2002). Uncertainty of nitrate-N load computations for agricultural watersheds. *Water Resources Research*, *38*(10), 3-1-3–12. https://doi.org/10.1029/2001WR001149

Gupta, H. V., Wagner, T., & Yuqiong, L. (2008). Reconciling theory with observations: elements of a diagnostic approach to model evaluation. *Hydrological Processes*, *22*, 3802–3813. https://doi.org/10.1002/hyp.6989

Han, H., & Allan, J. D. (2008). Estimation of nitrogen inputs to catchments: Comparison of methods and consequences for riverine export prediction. *Biogeochemistry*, *91*(2–3), 177–199. https://doi.org/10.1007/s10533-008-9279-3

Harman, C. J., Sivapalan, M., & Kumar, P. (2009). Power law catchment-scale recessions arising from heterogeneous linear small-scale dynamics. *Water Resources Research*, *45*(9), 1–13. https://doi.org/10.1029/2008WR007392

Haygarth, P. M., Condron, L. M., Heathwaite, A. L., Turner, B. L., & Harris, G. P. (2005). The phosphorus transfer continuum: Linking source to impact with an interdisciplinary and multi-scaled approach. *Science of the Total Environment*, *344*(1–3 SPEC. ISS.), 5–14. https://doi.org/10.1016/j.scitotenv.2005.02.001

Haygarth, P., Turner, B. L., Fraser, A., Jarvis, S., Harrod, T., Nash, D., … Beven, K. (2004). Temporal variability in phosphorus transfers: classifying concentration-discharge event dynamics. *Hydrology and Earth System Sciences*, *8*(1), 88–97 ST–Temporal variability in phosphorus tra. https://doi.org/10.5194/hess-8-88-2004

Hedin, L. O., Armesto, J. J., & Johnson, A. H. (1995). Patterns of nutrient loss from unpolluted,old-growth temperate forests: Evaluation of biogeochemical theory. *Ecology*, *76*(November 1993), 493–509.

Helsel, D. R., & Hirsch, R. M. (1992). *Statistical Methods in Water Resources*. *Techniques of Water Resources Investigations, Book 4*. Retrieved from http://pubs.water.usgs.gov/twri4a3

Hill, A. R. (1978). Factors Affecting the Export of Nitrate-Nitrogen from Drainage Basins in Southern Ontario. *Water Research*, *12*, 1045–1057.

Hirsch, R. M. (2014). Large Biases in Regression-Based Constituent Flux Estimates: Causes and Diagnostic Tools. *Journal of the American Water Resources Association*, *50*(6), 1401–1424. https://doi.org/10.1111/jawr.12195

Hirsch, R. M., Alexander, R. B., Smith, A., & Geological, U. S. (1991). Selection of Methods for the Detection and Estimation of Trends in Water Quality. *Water Resour. Res.*, *27*(5), 803–813.

Hirsch, R. M., & De Cicco, L. (2015). *User guide to Exploration and Graphics for RivEr Trends (EGRET) and dataRetrieval: R packages for hydrologic data*. *Techniques and Methods book 4*. https://doi.org/http://dx.doi.org/10.3133/tm4A10

Hirsch, R. M., Moyer, D. L., & Archfield, S. A. (2010). Weighted regressions on time, discharge, and season (WRTDS), with an application to chesapeake bay river inputs. *Journal of the American Water Resources Association*, *46*(5), 857–880. https://doi.org/10.1111/j.1752-1688.2010.00482.x

IJC. (2016). Canada , US Set Lake Erie Algae Reduction Targets : What Happens Next ? Retrieved from http://www.ijc.org/en_/blog/2016/03/15/canada_us_set_lake_erie_algae_reduction_targets/

Jawitz, J. W., & Mitchell, J. (2011). Temporal inequality in catchment discharge and solute export. *Water Resources Research*, *47*(10), 1–16. https://doi.org/10.1029/2010WR010197

Johnson, L., Richards, C., Host, G., & Arthur, J. (1997). Landscape influences on water chemistry in Midwestern stream ecosystems. *Freshwater Biology*, *37*(1), 193–208. https://doi.org/10.1046/j.1365-2427.1997.d01-539.x

Kirchner, J. W. (2009). Catchments as simple dynamical systems: Catchment characterization, rainfall-runoff modeling, and doing hydrology backward. *Water Resources Research*, *45*(2), 1–34. https://doi.org/10.1029/2008WR006912

Lee, C. J., Hirsch, R. M., Schwarz, G. E., Holtschlag, D. J., Preston, S. D., Crawford, C. G., & Vecchia, A. V. (2016). An evaluation of methods for estimating decadal stream loads. *Journal of Hydrology*, *542*, 185–203. https://doi.org/10.1016/j.jhydrol.2016.08.059

Likens, G. E., & Buso, D. C. (2006). Variation in streamwater chemistry throughout the Hubbard Brook Valley. *Biogeochemistry*, *78*(1), 1–30. https://doi.org/10.1007/s10533-005-2024-2

Litke, D. W. (1999). Review of Phosphorus Control Measures in the United States and Their Effects on Water Quality. *Water-Resources Investigations Report 99-4007*, 1–38. Retrieved from http://www.msue.msu.edu/waterqual/WQWEB/ReviewPUSGS.pdf

Maccoux, M. J., Dove, A., Backus, S. M., & Dolan, D. M. (2016). Total and soluble reactive phosphorus loadings to Lake Erie: A detailed accounting by year, basin, country, and tributary. *Journal of Great Lakes Research*, *42*(6), 1151–1165.

https://doi.org/10.1016/j.jglr.2016.08.005

Macdonagh-Dumler, J., Pebbels, V., & Gannon, J. (2005). Great Lakes (North American) Experience and Lessons Learned Brief.

Matzner, E., & Borken, W. (2008). Do freeze-thaw events enhance C and N losses from soils of different ecosystems? A review. *European Journal of Soil Science*, *59*(2), 274–284. https://doi.org/10.1111/j.1365-2389.2007.00992.x

McMillan, H., Gueguen, M., Grimon, E., Woods, R., Clark, M., & Rupp, D. E. (2014). Spatial variability of hydrological processes and model structure diagnostics in a 50 km ^{2} catchment. *Hydrological Processes*, *28*(18), 4896–4913. https://doi.org/10.1002/hyp.9988

Medalie, L., Hirsch, R. M., & Archfield, S. A. (2012). Use of flow-normalization to evaluate nutrient concentration and flux changes in Lake Champlain tributaries, 1990-2009. *Journal of Great Lakes Research*, *38*(SUPPL. 1), 58–67. https://doi.org/10.1016/j.jglr.2011.10.002

Merz, R., & Blöschl, G. (2009). A regional analysis of event runoff coefficients with respect to climate and catchment characteristics in Austria. *Water Resources Research*, *45*(1), 1–19. https://doi.org/10.1029/2008WR007163

Michalak, A. M., Anderson, E. J., Beletsky, D., Boland, S., Bosch, N. S., Bridgeman, T. B., … Zagorski, M. A. (2013). Record-setting algal bloom in Lake Erie caused by agricultural and meteorological trends consistent with expected future conditions. *Proceedings of the National Academy of Sciences*, *110*(16), 6448–6452. https://doi.org/10.1073/pnas.1216006110

Molenat, J., Gascuel-Odoux, C., Ruiz, L., & Gruau, G. (2008). Role of water table dynamics on stream nitrate export and concentration in agricultural headwater catchment (France). *Journal of Hydrology*, *348*(3–4), 363–378. https://doi.org/10.1016/j.jhydrol.2007.10.005

Moyer, D., Hirsch, R., & Hyer, K. (2012). *Comparison of Two Regression-Based Approaches for Determining Nutrient and Sediment Fluxes and Trends in the Chesapeake Bay Watershed: U.S. Geological Survey Scientific Investigations Report*. Retrieved from http://pubs.usgs.gov/sir/2012/5244/pdf/sir2012-5244.pdf

Musolff, A., Schmidt, C., Selle, B., & Fleckenstein, J. H. (2015). Catchment controls on solute export. *Advances in Water Resources*, *86*, 133–146. https://doi.org/10.1016/j.advwatres.2015.09.026

Neff, B. P., Day, S. M., Piggott, A. R., & Fuller, L. M. (2005). *Base flow in the Great Lakes basin*. *U.S. Geological Survey Scientific Investigations Report*.

Paul, M. J., & Meyer, J. L. (2001). Streams in the Urban Landscape, *32*, 333–365.

Piñol, J., Ávila, A., & Rodà, F. (1992). The seasonal variation of streamwater chemistry in three forested Mediterranean catchments. *Journal of Hydrology*, *140*(1–4), 119–141. https://doi.org/10.1016/0022-1694(92)90237-P

Pionke, H. B., Gburek, W. J., Schnabel, R. R., Sharpley, A. N., & Elwinger, G. F. (1999). Seasonal flow, nutrient concentrations and loading patterns in stream flow draining an agricultural hill-land watershed. *Journal of Hydrology*, *220*(1–2), 62–73.

https://doi.org/10.1016/S0022-1694(99)00064-5

Preston, S. D., Bierman, V. J., & Silliman, S. E. (1989). An evaluation of methods for the estimation of tributary mass loads. *Water Resources Research*, *25*(6), 1379–1389. https://doi.org/10.1029/WR025i006p01379

Price, K. (2011). Effects of watershed topography, soils, land use, and climate on baseflow hydrology in humid regions: A review. *Progress in Physical Geography*, *35*(4), 465–492. https://doi.org/10.1177/0309133311402714

Qin, B., Zhu, G., Gao, G., Zhang, Y., Li, W., Paerl, H. W., & Carmichael, W. W. (2010). A drinking water crisis in Lake Taihu, China: Linkage to climatic variability and lake management. *Environmental Management*, *45*(1), 105–112. https://doi.org/10.1007/s00267-009-9393-6

Reddy, K. R., Diaz, O. A., Scinto, L. J., & Agami, M. (1995). Phosphorus dynamics in selected wetlands and streams of the lake Okeechobee Basin. *Ecological Engineering*, *5*(2–3), 183–207. https://doi.org/10.1016/0925-8574(95)00024-0

Robertson, D. M., & Saad, D. A. (2011). Nutrient Inputs to the Laurentian Great Lakes by Source and Watershed Estimated Using Sparrow Watershed Models. *Journal of the American Water Resources Association*, *47*(5), 1011–1033. https://doi.org/10.1111/j.1752-1688.2011.00574.x

Runkel, R. L., Crawford, C. G., & Cohn, T. a. (2004). Load Estimator (LOADEST): A FORTRAN program for estimating constituent loads in streams and rivers. *Techniques and Methods. U.S. Geological Survey. U.S. Department of the Interior*, *4*, 69.

Scavia, D., David Allan, J., Arend, K. K., Bartell, S., Beletsky, D., Bosch, N. S., … Zhou, Y. (2014). Assessing and addressing the re-eutrophication of Lake Erie: Central basin hypoxia. *Journal of Great Lakes Research*, *40*(2), 226–246. https://doi.org/10.1016/j.jglr.2014.02.004

Schindler, D. W. (2006). Recent advances in the understanding and management of eutrophication. *Limnology and Oceanography*, *51*(1), 356–363. https://doi.org/10.4319/lo.2006.51.1_part_2.0356

Schindler, D. W., Hecky, R. E., & McCullough, G. K. (2012). The rapid eutrophication of Lake Winnipeg: Greening under global change. *Journal of Great Lakes Research*, *38*(SUPPL. 3), 6–13. https://doi.org/10.1016/j.jglr.2012.04.003

Schwientek, M., Osenbrück, K., & Fleischer, M. (2013). Investigating hydrological drivers of nitrate export dynamics in two agricultural catchments in Germany using high-frequency data series. *Environmental Earth Sciences*, *69*(2), 381–393. https://doi.org/10.1007/s12665-013-2322-2

Seibert, J., Grabs, T., Köhler, S., Laudon, H., Winterdahl, M., & Bishop, K. (2009). Linking soil- and stream-water chemistry based on a Riparian Flow-Concentration Integration Model. *Hydrology and Earth System Sciences*, *13*(12), 2287–2297. https://doi.org/10.5194/hess-13-2287-2009

Sharpley, A. N., Chapra, S. C., Wedepohl, R., Sims, J. T., Daniel, T. C., & Reddy, K. R. (1994).

Managing Agricultural Phosphorus for Protection of Surface Waters: Issues and Options. *Journal of Environment Quality*, *23*(3), 437–451.

Sinha, E., & Michalak, A. M. (2016). Precipitation Dominates Interannual Variability of Riverine Nitrogen Loading across the Continental United States. *Environmental Science & Technology*, *50*(23), 12874–12884. https://doi.org/10.1021/acs.est.6b04455

Sivapalan, M. (2005). Pattern, Process and Function: Elements of a Unified Theory of Hydrology at the Catchment Scale. *Encyclopedia of Hydrological Sciences*, (APRIL 2006), 193–219. https://doi.org/10.1002/0470848944

Smith, V. H., Joye, S. B., & Howarth, R. W. (2006). Eutrophication of freshwater and marine ecosystems. *Limnol. Oceanogr*, *51*(2), 351–355. https://doi.org/10.4319/lo.2006.51.1_part_2.0351

Sprague, L. A., Hirsch, R. M., & Aulenbach, B. T. (2011). Nitrate in the mississippi river and its tributaries, 1980 to 2008: Are we making progress? *Environmental Science and Technology*, *45*(17), 7209–7216. https://doi.org/10.1021/es201221s

Sprugel, D. G. (1983). Correcting for Bias in Log-Transformed Allometric Equations. *Ecology*, *64*(1), 209–210.

Stenback, G. A., Crumpton, W. G., Schilling, K. E., & Helmers, M. J. (2011). Rating curve estimation of nutrient loads in Iowa rivers. *Journal of Hydrology*, *396*(1–2), 158–169. https://doi.org/10.1016/j.jhydrol.2010.11.006

Stoelzle, M., Stahl, K., & Weiler, M. (2013). Are streamflow recession characteristics really characteristic? *Hydrology and Earth System Sciences*, *17*(2), 817–828. https://doi.org/10.5194/hess-17-817-2013

Thompson, S. E., Basu, N. B., Lascurain, J., Aubeneau, A., & Rao, P. S. C. (2011). Relative dominance of hydrologic versus biogeochemical factors on solute export across impact gradients. *Water Resources Research*, *47*(7), 1–20. https://doi.org/10.1029/2010WR009605

Tian, S., Youssef, M. A., Richards, R. P., Liu, J., Baker, D. B., & Liu, Y. (2016). Different seasonality of nitrate export from an agricultural watershed and an urbanized watershed in Midwestern USA. *Journal of Hydrology*, *541*, 1375–1384. https://doi.org/10.1016/j.jhydrol.2016.08.042

US Environmental Protection Agency, E., & Government of Canada, E. (1995). *The Great Lakes - An Environmental Atlas and Resource Book* (Vol. 3). Chicago, Illinois.

Valett, H. M., Crenshaw, C. L., & Wagner, P. F. (2002). Stream nutrient uptake, forest succession, and biogeochemical theory. *Ecology*, *83*(10), 2888–2901. https://doi.org/10.1890/0012-9658(2002)083[2888:SNUFSA]2.0.CO;2

Van Meter, K. J., & Basu, N. B. (2015). Catchment legacies and time lags: A parsimonious watershed model to predict the effects of legacy storage on nitrogen export. *PLoS ONE*, *10*(5), 1–22. https://doi.org/10.1371/journal.pone.0125971

Vogel, R. M., & Kroll, C. N. (1992). Regional Geohydrologic-Geomorphic Relationships for the Estimation of Low-Flow Statistics. *Water Resour. Res.*, *28*(9), 2451–2458.

Vogel, R. M., Rudolph, B. E., & Hooper, R. P. (2005). Probabilistic Behavior of Water-Quality Loads. *Journal of Environmental Engineering*, *131*(7), 1081–1089. https://doi.org/10.1061/?ASCE?0733-9372?2005?131:7?1081? CE

Von Schiller, D., Martí, E., Riera, J. L., Ribot, M., Argerich, A., Fonollà, P., & Sabater, F. (2008). Inter-annual, annual, and seasonal variation of P and N retention in a perennial and an intermittent stream. *Ecosystems*, *11*(5), 670–687. https://doi.org/10.1007/s10021-008-9150-3

Walsh, R. P. D., & Lawler, D. M. (1981). Rainfall Seasonality: Description, Spatial Patterns and Change Through Time. *Weather*, *36*(7), 201–208. https://doi.org/10.1002/j.1477-8696.1981.tb05400.x

Wolock, D. M., Winter, T. C., & McMahon, G. (2004). Delineation and Evaluation of Hydrologic-Landscape Regions in the United States Using Geographic Information System Tools and Multivariate Statistical Analyses. *Environmental Management*, *34*(S1), S71–S88. https://doi.org/10.1007/s00267-003-5077-9

Yang, X., Wu, X., Hao, H., & He, Z. (2008). Mechanisms and assessment of water eutrophication. *Journal of Zhejiang University SCIENCE B*, *9*(3), 197–209. https://doi.org/10.1631/jzus.B0710626

Ye, S., Yaeger, M., Coopersmith, E., Cheng, L., & Sivapalan, M. (2012). Exploring the physical controls of regional patterns of flow duration curves Part 2: Role of seasonality, the regime curve, and associated process controls. *Hydrology and Earth System Sciences*, *16*(11), 4447–4465. https://doi.org/10.5194/hess-16-4447-2012

Zhang, Q., Brady, D. C., & Ball, W. P. (2013). Long-term seasonal trends of nitrogen, phosphorus, and suspended sediment load from the non-tidal Susquehanna River Basin to Chesapeake Bay. *Science of the Total Environment*, *452–453*, 208–221. https://doi.org/10.1016/j.scitotenv.2013.02.012

Zhang, Q., Harman, C. J., & Ball, W. P. (2016). An improved method for interpretation of riverine concentration-discharge relationships indicates long-term shifts in reservoir sediment trapping. *Geophysical Research Letters*, *43*(19), 10,215-10,224. https://doi.org/10.1002/2016GL069945

Zhu, Q., Schmidt, J. P., & Bryant, R. B. (2012). Hot moments and hot spots of nutrient losses from a mixed land use watershed. *Journal of Hydrology*, *414–415*(3), 393–404. https://doi.org/10.1016/j.jhydrol.2011.11.011

Appendices

Appendix A – Summary of water quality stations and associated error metrics for WRTDS

Table A.1. Summary of sampled water quality stations across the Great Lakes. FluxB, PBS, and NSE are the Flux-bias, Percent Bias, and Nash-Sutcliffe, respectively.

WQ station	River Name	Drainage Area (km^2)	LAT	LONG	Nitrate-N			SRP			TP		
					FluxB	PBS	NSE	FluxB	PBS	NSE	FluxB	PBS	NSE
16018401602	CANAGAGIGUE CREEK	111.46	43.58	-80.53	0.01	0.01	0.76	0.38	-0.20	-0.05	0.06	-0.02	0.33
16018403602	SPEED RIVER	631.43	43.48	-80.28	0.08	-0.08	0.66	0.07	-0.21	0.42	0.02	-0.07	0.47
16018410102	SPEED RIVER	778.00	43.40	-80.37	0.00	-0.03	0.59	-0.09	-0.02	0.19	-0.10	-0.01	0.19
16018403202	NITH RIVER	550.54	43.38	-80.68	0.19	-0.08	0.39	0.40	-0.34	0.22	-0.06	-0.02	0.71
16018400902	NITH RIVER	1130.91	43.19	-80.38	0.04	0.02	0.61	0.63	-0.50	-2.48	0.36	-0.07	0.03
16018409302	FAIRCHILD CREEK	384.45	43.15	-80.17	0.27	-0.14	0.03	-0.03	-0.08	0.33	-0.06	-0.02	0.52
16018401202	GRAND RIVER	2582.20	43.39	-80.39	0.02	-0.01	0.32	0.07	-0.04	0.66	0.12	-0.06	0.59
16018401002	GRAND RIVER	3581.16	43.28	-80.34	0.01	0.00	0.51	0.16	-0.11	0.39	-0.01	0.00	0.70
16018402702	GRAND RIVER	5233.45	43.11	-80.24	0.12	-0.11	0.33	0.39	-0.20	-0.05	0.11	0.00	0.64
16018403702	GRAND RIVER	789.29	43.72	-80.34	0.05	-0.06	0.46	0.23	-0.10	0.18	0.00	0.00	0.21
16018407702	CONESTOGO RIVER	573.81	43.65	-80.70	0.04	-0.02	0.47	0.16	-0.16	0.09	-0.01	0.01	0.17
16018410302	GRAND RIVER	1158.65	43.59	-80.47	0.00	0.02	0.66	0.15	-0.07	0.70	-0.10	0.01	0.62
16018409902	SPEED RIVER	177.00	43.64	-80.27	-0.06	0.00	0.32	-0.04	0.12	0.10	0.02	0.07	0.06
16018410202	ERAMOSA RIVER	232.84	43.55	-80.18	-0.03	0.03	0.36	-0.33	0.06	0.34	-0.01	-0.02	0.36
16018410602	WHITEMANS CREEK	398.90	43.13	-80.38	0.00	0.00	0.34	0.18	-0.15	0.25	0.00	0.00	0.66
16018409602	MCKENZIE CREEK	174.98	43.03	-79.95	0.29	-0.16	0.43	0.17	-0.14	0.18	0.05	-0.01	0.56
16016400102	NANTICOKE CREEK	179.73	42.81	-80.08	0.38	-0.19	0.10	-0.28	0.02	0.27	-0.18	0.01	0.23
16015900302	LYNN RIVER	141.27	42.82	-80.29	0.08	-0.04	0.30	0.03	-0.02	0.00	-0.06	0.00	0.19
16010900702	BIG OTTER CREEK	99.52	42.97	-80.54	0.03	0.03	-0.07	0.19	-0.19	0.52	-0.04	0.01	0.77
16012401102	BIG CREEK	568.02	42.69	-80.54	0.01	0.00	0.02	0.10	-0.14	0.26	0.03	0.00	0.19
16010900802	BIG OTTER CREEK	658.43	42.71	-80.84	0.03	0.01	0.41	0.37	-0.20	-0.15	0.17	-0.08	0.45
16008700502	DODD CREEK	101.39	42.79	-81.27	0.12	0.02	-0.11	-0.13	-0.01	-0.12	0.02	-0.02	0.29
04001308002	SOUTH THAMES RIVER	150.85	43.22	-80.69	0.67	-0.65	-1.50	0.67	-0.52	-3.71	0.20	-0.02	0.25
04001304402	NORTH THAMES RIVER	318.05	43.45	-81.21	0.17	-0.07	-0.17	-0.06	-0.05	0.30	-0.30	0.04	0.17
10000200202	CANARD RIVER	176.83	42.16	-83.02	0.68	-0.52	-1.64	0.44	-0.27	-0.32	0.12	-0.06	0.33
04002701202	SYDENHAM RIVER	706.91	42.83	-81.85	0.06	0.00	0.38	0.14	-0.03	0.32	-0.04	0.00	0.51
04002701602	SYDENHAM RIVER	1152.87	42.65	-82.01	0.12	-0.01	0.54	0.25	-0.13	0.43	-0.01	0.03	0.35
04001305802	THAMES RIVER	4569.45	42.51	-82.07	0.06	0.01	0.39	0.34	-0.37	-0.67	-0.04	-0.02	0.56
16018406702	GRAND RIVER	665.67	43.86	-80.27	0.12	0.01	0.55	-0.28	0.09	0.64	-0.45	0.04	0.52
16018403402	SPEED RIVER	568.27	43.53	-80.25	-0.03	0.01	0.64	-0.36	0.07	-0.18	-0.04	-0.01	0.00
16018407402	NITH RIVER	318.02	43.48	-80.84	0.41	-0.35	-1.12	0.59	-0.60	-1.59	0.37	-0.15	0.40

Table A.2. Summary of sampled water quality stations across the Great Lakes. FluxB, PBS, and NSE are the Flux-bias, Percent Bias, and Nash-Sutcliffe, respectively.

WQ station	River Name	Drainage Area (km^2)	LAT	LONG	Nitrate-N			SRP			TP		
					FluxB	PBS	NSE	FluxB	PBS	NSE	FluxB	PBS	NSE
16012401202	BIG CREEK	146.77	42.99	-80.44	0.04	0.00	0.04	0.17	-0.21	0.37	-0.42	0.07	0.26
04001308302	THAMES RIVER	3844.99	42.73	-81.58	0.03	0.01	0.39	0.14	-0.13	-0.54	-0.07	-0.02	0.16
04001308102	MCGREGOR CREEK	202.86	42.38	-82.09	0.51	-0.08	-0.27	-	-	-	-	-	-
16018404102	GRAND RIVER	2492.24	43.42	-80.41	-0.03	0.01	0.68	0.08	0.11	0.30	0.26	-0.03	-0.24
04001306402	TROUT CREEK	141.48	43.27	-81.08	0.28	-0.31	-0.64	-0.13	0.07	0.01	0.05	-0.01	0.02
06001700702	TWELVE MILE CREEK	47.86	43.11	-79.27	0.15	-0.03	0.06	0.54	-0.29	-1.49	0.42	-0.19	-0.21
06002400102	TWENTY MILE CREEK	293.23	43.15	-79.37	0.82	-0.84	-5.93	-0.15	-0.06	0.55	-0.10	-0.01	0.65
09000800502	SPENCER CREEK	159.31	43.27	-79.96	-0.08	0.29	-0.02	-0.07	-0.11	-0.08	-0.07	0.00	0.08
09000902402	GRINDSTONE CREEK	81.15	43.30	-79.87	-0.03	0.03	0.65	0.21	-0.26	-1.16	-0.19	0.00	0.19
09000800602	SPENCER CREEK	126.12	43.28	-80.05	-0.03	0.00	0.20	0.29	-0.09	-0.35	0.02	0.00	-0.02
06006301102	EAST OAKVILLE CREEK	198.64	43.50	-79.78	0.35	-0.29	0.01	0.13	-0.14	0.51	-0.08	0.02	0.53
06007600302	CREDIT RIVER	635.86	43.65	-79.86	-0.01	0.01	0.71	-0.11	-0.02	0.38	-0.10	0.01	0.53
06007600402	SILVER CREEK	131.39	43.65	-79.87	0.00	0.00	0.82	0.06	-0.10	0.21	-0.09	0.02	0.03
06007601002	CREDIT RIVER	439.45	43.72	-79.93	-0.02	0.02	0.79	0.13	-0.06	0.34	-0.12	0.04	0.44
06007602302	CREDIT RIVER	59.65	43.89	-80.06	-0.01	0.00	0.49	-0.13	0.12	0.03	-0.08	0.06	0.04
06008310402	CENTREVILLE CREEK	42.04	43.92	-79.83	-0.01	0.01	0.38	0.08	-0.13	0.59	-0.12	0.03	0.17
06008300902	COLD CREEK	63.56	43.89	-79.72	-3.37	0.86	-0.02	0.04	-0.02	0.33	-0.03	0.01	0.44
06008310302	HUMBER RIVER WEST	142.70	43.76	-79.68	0.10	-0.05	0.44	0.17	-0.06	0.43	-0.14	0.03	0.34
06008000602	ETOBICOKE CREEK	216.08	43.61	-79.56	0.10	-0.01	0.35	0.07	-0.03	0.35	-0.02	0.03	0.35
06008200302	MIMICO CREEK	71.60	43.63	-79.49	0.05	-0.03	0.27	0.09	-0.06	0.06	-0.09	0.07	0.13
06008501402	DON RIVER	314.47	43.69	-79.36	0.01	-0.03	0.10	0.04	-0.07	0.09	-0.05	0.00	0.35
06010400102	DUFFINS CREEK	278.56	43.84	-79.04	0.07	0.02	0.67	0.26	-0.01	-0.03	-0.24	0.25	-0.03
06012900202	GANARASKA RIVER	72.34	44.02	-78.44	-0.01	0.00	0.31	0.10	-0.10	0.05	-0.10	0.04	0.70
06011700302	WILMOT CREEK	85.65	43.91	-78.61	0.01	0.00	0.12	0.13	-0.11	0.46	-0.09	0.02	0.86
06012900502	GANARASKA RIVER	239.89	43.99	-78.33	0.01	0.01	0.82	0.16	-0.14	0.39	-0.38	0.13	0.51
06013300502	COBOURG CREEK WEST	33.61	43.99	-78.21	0.02	-0.01	0.62	-0.18	-0.10	-0.08	-0.26	0.07	0.19
06013300402	COBOURG CREEK	123.66	43.96	-78.18	0.02	-0.01	0.22	0.04	-0.11	-0.03	-0.06	0.01	-0.01
17003700302	WILTON CREEK	106.87	44.24	-76.85	0.19	-0.19	0.60	-0.13	0.01	0.05	-0.11	0.00	0.12
06018000402	MILLHAVEN CREEK	131.44	44.26	-76.73	0.09	-0.29	-0.06	-0.06	0.11	0.14	-0.03	0.03	0.18
17003500402	NAPANEE RIVER	748.99	44.32	-76.88	0.08	-0.02	0.22	0.04	-0.04	0.08	-0.02	0.00	0.26
06018300202	COLLINS CREEK	160.52	44.26	-76.61	-0.06	0.10	0.00	-0.08	0.00	0.52	-0.03	0.11	0.07
17002600602	MOIRA RIVER	1767.84	44.48	-77.31	0.04	0.38	-0.03	-0.01	0.03	-0.10	-0.02	-0.01	0.35
17002601002	BLACK RIVER	424.11	44.54	-77.37	0.05	0.32	-0.02	0.09	0.02	0.14	-0.04	0.00	0.14

Table A.3. Summary of sampled water quality stations across the Great Lakes. FluxB, PBS, and NSE are the Flux-bias, Percent Bias, and Nash-Sutcliffe, respectively.

WQ station	River Name	Drainage Area (km^2)	LAT	LONG	Nitrate-N			SRP			TP		
					FluxB	PBS	NSE	FluxB	PBS	NSE	FluxB	PBS	NSE
08005603802	NORTH MAITLAND RIVER	556.99	43.89	-81.28	0.38	-0.12	0.22	-0.22	0.08	0.87	-0.38	0.01	0.64
03005703102	INNISFIL CREEK	483.55	44.13	-79.80	-0.73	0.13	0.04	0.10	-0.11	0.59	-0.52	0.06	0.29
03013400102	WANAPITEI RIVER	2960.03	46.40	-80.80	-0.03	0.01	0.43	0.00	-0.02	-0.03	0.03	0.00	0.06
03013301902	CHIPPEWA CREEK	38.94	46.30	-79.46	-0.04	0.01	0.14	-0.23	0.05	0.00	-0.03	0.15	-0.05
03005702502	NOTTAWASAGA RIVER	2728.62	44.48	-80.01	-0.01	0.00	0.36	-0.15	0.23	-0.01	-0.06	0.07	0.03
08012303082	SAUGEEN RIVER	3981.28	44.46	-81.33	0.00	0.00	0.78	0.08	-0.09	0.77	-0.08	0.02	0.80
03005300102	PRETTY RIVER	68.04	44.50	-80.20	0.09	-0.01	0.33	0.48	-0.37	-1.53	-1.05	0.26	0.59
03007703502	UXBRIDGE BROOK	40.34	44.14	-79.11	-0.01	0.00	-0.10	-0.06	-0.05	0.06	0.24	-0.10	-0.21
03007703602	HAWKESTONE CREEK	40.55	44.50	-79.47	-0.02	-0.05	0.36	-0.03	-0.05	0.30	-0.05	0.03	0.00
13001100202	ROOT RIVER	103.46	46.57	-84.32	-0.15	0.05	0.20	-0.02	0.01	0.05	0.07	0.02	-0.05
01006700102	LITTLE PIC RIVER	1350.03	48.80	-86.63	0.24	-0.12	0.45	0.07	-0.03	0.21	0.28	-0.03	0.22
01006000102	PIC RIVER	4277.28	48.71	-86.28	0.12	-0.08	0.46	0.20	-0.09	0.20	0.03	0.03	0.32
01010800102	KAMINISTIQUIA RIVER	7784.47	48.36	-89.29	-0.01	-0.01	-0.20	0.01	-0.17	0.15	-0.20	-0.01	-0.38
04095090	PORTAGE-BURNS WATERWAY	856.02	41.62	-87.18	0.01	0.00	0.67	0.06	-0.03	0.44	0.01	0.00	0.53
04040000	ONTONAGON RIVER	3498.66	46.72	-89.21	0.24	-0.03	0.48	0.14	-0.02	0.13	0.22	0.03	0.21
04059500	FORD RIVER	1184.49	45.75	-87.20	-0.14	0.01	0.30	-0.04	0.03	0.15	-0.07	0.01	0.38
04101500	ST. JOSEPH RIVER	9642.67	41.83	-86.26	0.00	0.00	0.56	0.07	-0.11	0.21	-0.02	-0.02	0.52
04108660	KALAMAZOO RIVER	5039.77	42.65	-86.11	0.01	0.01	0.64	0.11	-0.05	0.05	-0.01	0.00	0.32
04119400	GRAND RIVER	13849.74	43.02	-86.03	0.00	0.00	0.49	0.09	-0.09	0.26	-0.01	0.00	0.38
04121970	MUSKEGON RIVER	5850.56	43.43	-85.67	0.00	0.00	0.64	-0.02	0.01	0.15	-0.03	0.01	0.04
04137500	AU SABLE RIVER	4534.27	44.44	-83.43	0.01	-0.01	0.63	-0.03	0.02	0.36	-0.01	0.00	0.21
04142000	RIFLE RIVER	872.01	44.07	-84.02	-0.02	0.01	0.52	0.02	0.02	0.25	0.03	0.03	0.44
041482663	ALGER CREEK	51.30	42.94	-83.85	0.26	-0.07	0.17	0.13	-0.05	0.12	0.00	0.01	0.34
04157005	SAGINAW RIVER	15500.61	43.42	-83.95	0.01	0.00	0.15	0.05	-0.01	0.21	0.04	0.00	0.29
04161820	CLINTON RIVER	788.69	42.61	-83.03	0.01	0.01	0.60	0.01	-0.03	0.45	-0.02	-0.03	0.30
04165500	CLINTON RIVER	1911.79	42.60	-82.91	0.00	-0.01	0.49	-0.01	-0.01	0.12	0.03	0.05	0.12
04166500	RIVER ROUGE	490.59	42.37	-83.25	-0.01	0.00	0.43	0.12	-0.10	0.36	0.18	0.00	0.40
04167150	MIDDLE RIVER ROUGE	253.94	42.33	-83.25	0.01	0.00	0.64	0.10	-0.11	-0.11	0.08	0.01	0.48
04168400	LOWER RIVER ROUGE	232.45	42.31	-83.25	0.02	-0.02	0.65	0.02	0.00	0.63	0.03	-0.02	0.24
04174500	HURON RIVER	1934.02	42.29	-83.73	0.04	0.00	0.35	-0.07	-0.01	0.22	0.00	0.05	0.05
04175600	RIVER RAISIN	352.16	42.17	-84.08	-0.01	0.00	0.80	0.01	-0.01	0.13	-0.06	0.01	0.47
04176500	RIVER RAISIN	2756.08	41.96	-83.53	0.12	0.02	0.35	0.25	-0.11	0.10	0.17	-0.06	0.31
04024000	ST. LOUIS RIVER	8863.15	46.70	-92.42	0.00	0.01	0.52	0.04	-0.01	0.22	-0.16	0.02	0.68

Table A.4. Summary of sampled water quality stations across the Great Lakes. FluxB, PBS, and NSE are the Flux-bias, Percent Bias, and Nash-Sutcliffe, respectively.

WQ station	River Name	Drainage Area (km^2)	LAT	LONG	Nitrate-N			SRP			TP		
					FluxB	PBS	NSE	FluxB	PBS	NSE	FluxB	PBS	NSE
04213500	CATTARAUGUS CREEK	1150.81	42.46	-78.93	-0.01	0.00	0.57	0.04	0.00	0.44	0.34	-0.30	0.09
04231600	GENESEE RIVER	6401.64	43.14	-77.62	-0.02	0.01	0.31	0.03	-0.02	0.19	-0.10	0.03	0.61
04240180	NINEMILE CREEK	111.73	42.92	-76.33	0.01	0.02	0.28	0.04	-0.04	0.01	0.15	-0.14	-0.92
04249000	OSWEGO RIVER	13662.99	43.45	-76.51	0.01	0.00	0.45	0.06	-0.03	0.16	0.03	-0.04	0.26
04183500	MAUMEE RIVER	5372.59	41.20	-84.74	0.14	-0.15	0.08	0.23	-0.21	-0.04	0.11	0.03	0.28
04186500	AUGLAIZE RIVER	862.10	40.95	-84.27	0.40	-0.15	0.20	0.16	-0.12	0.30	0.12	-0.03	0.38
04188100	OTTAWA RIVER	908.40	40.99	-84.23	0.03	0.01	0.25	0.03	-0.02	0.62	0.07	-0.01	0.20
04188496	EAGLE CREEK	132.11	40.98	-83.65	0.37	-0.17	0.03	0.03	-0.03	0.43	0.01	-0.02	0.39
04190000	BLANCHARD RIVER	1879.67	41.04	-84.23	0.07	-0.01	0.36	0.08	-0.05	0.41	0.11	0.02	0.10
04191500	AUGLAIZE RIVER	5990.36	41.24	-84.40	0.15	-0.02	0.33	0.27	-0.17	0.04	0.00	0.00	0.45
04192500	MAUMEE RIVER	14174.02	41.29	-84.28	0.17	-0.06	0.29	0.44	-0.39	-0.57	-0.01	0.00	0.54
04193500	MAUMEE RIVER	15942.45	41.50	-83.71	0.47	-0.46	-0.49	0.51	-0.36	-0.59	0.06	-0.03	0.63
04195500	PORTAGE RIVER	1090.83	41.45	-83.36	0.06	0.04	0.41	0.08	-0.07	0.53	0.07	-0.02	0.66
04199500	VERMILION RIVER	672.67	41.38	-82.32	0.47	-0.18	-0.61	0.53	-0.28	-1.99	0.27	-0.08	0.22
04200500	BLACK RIVER	1027.55	41.38	-82.10	0.16	0.00	0.12	0.27	-0.07	0.26	0.14	-0.02	0.45
04208000	CUYAHOGA RIVER	1807.88	41.40	-81.63	-0.01	0.00	0.77	0.01	-0.01	0.53	-0.01	0.01	0.16
04027000	BAD RIVER	1621.15	46.49	-90.70	0.01	0.02	0.32	0.05	0.04	0.03	0.11	0.02	0.25
04063700	POPPLE RIVER	340.68	45.76	-88.46	0.03	-0.06	0.23	0.00	0.00	0.16	-0.01	0.01	0.44
04067500	MENOMINEE RIVER	10129.35	45.33	-87.66	0.02	0.01	0.54	-0.10	0.10	0.04	0.00	0.02	0.08
04072150	DUCK CREEK	279.17	44.53	-88.13	0.51	-0.42	-0.66	0.11	-0.14	-0.07	-0.10	0.03	0.13
04085108	EAST RIVER	121.02	44.37	-88.09	0.27	-0.04	0.19	0.05	0.00	0.47	-0.15	0.01	0.23
040851385	FOX RIVER	16046.69	44.53	-88.01	0.06	-0.06	0.24	0.06	-0.13	0.03	-0.04	-0.01	0.37
04085427	MANITOWOC RIVER	1368.78	44.11	-87.72	0.05	-0.02	0.55	0.11	-0.06	0.41	-0.04	0.02	0.23
040857005	OTTER CREEK	24.67	43.79	-87.92	0.06	0.00	0.43	-	-	-	0.09	0.00	0.30
04086000	SHEBOYGAN RIVER	1152.92	43.74	-87.75	0.13	-0.07	0.08	-	-	-	0.04	0.02	0.25
04086139	WEST BRANCH MILWAUKEE RIVER	146.72	43.54	-88.25	-0.07	0.02	0.80	-0.04	0.02	0.53	-0.05	0.01	0.18
04087000	MILWAUKEE RIVER	1777.68	43.10	-87.91	0.17	-0.12	0.55	0.13	-0.03	0.19	0.04	-0.01	0.22
04087204	OAK CREEK	65.43	42.93	-87.87	0.02	0.04	0.40	-0.13	-0.02	0.46	-	-	-
04144032	THREEMILE CREEK	24.24	42.88	-83.98	0.15	-0.05	0.18	0.12	-0.08	0.48	0.02	0.02	0.35
04185318	TIFFIN RIVER	1402.79	41.38	-84.42	0.19	-0.04	0.36	0.15	-0.07	0.25	0.12	-0.01	0.25
04086110	WEST BRANCH MILWAUKEE RIVER	4.79	43.66	-88.42	0.14	-0.05	0.48	0.00	0.02	0.47	0.01	-0.01	0.21
04086120	WEST BRANCH MILWAUKEE RIVER	29.80	43.62	-88.40	-0.01	-0.01	0.60	0.07	0.02	0.16	-0.01	0.03	0.09
04087050	LITTLE MENOMONEE RIVER	22.31	43.21	-88.04	-0.08	0.02	0.13	-	-	-	0.16	-0.07	0.24

Table A.5. Summary of sampled water quality stations across the Great Lakes. FluxB, PBS, and NSE are the Flux-bias, Percent Bias, and Nash-Sutcliffe, respectively.

WQ station	River Name	Drainage Area (km^2)	LAT	LONG	Nitrate-N			SRP			TP		
					FluxB	PBS	NSE	FluxB	PBS	NSE	FluxB	PBS	NSE
17002600902	SKOOTAMOTTA RIVER	682.19	44.55	-77.33	0.03	0.42	-0.02	-0.04	0.07	-0.05	-0.07	0.01	0.00
17002601302	MOIRA RIVER	297.15	44.50	-77.62	0.37	-0.08	0.18	0.00	-0.04	0.13	-0.27	0.00	0.16
17002103802	JACKSON CREEK	116.90	44.30	-78.32	-0.05	-0.05	0.56	0.15	-0.13	0.07	-0.02	0.03	0.05
06007605002	CREDIT RIVER	844.24	43.55	-79.63	0.01	-0.01	0.68	0.10	-0.08	0.91	-0.55	0.10	0.39
06007602402	CREDIT RIVER	57.82	43.90	-80.05	-0.01	0.01	0.43	-0.02	0.05	0.04	-0.04	0.02	-0.01
06006100102	FOURTEEN MILE CREEK	22.53	43.42	-79.73	0.11	0.05	0.40	0.48	-0.25	-1.11	0.36	-0.08	-0.32
06008301802	HUMBER RIVER	166.35	43.93	-79.80	-0.02	0.01	0.22	0.15	0.06	0.02	-0.10	0.01	0.19
17002113302	COLD CREEK	160.59	44.13	-77.79	0.10	-0.08	0.19	0.06	-0.07	0.21	-0.01	0.00	0.11
06011600102	BOWMANVILLE CREEK	89.30	43.89	-78.68	0.00	0.00	0.48	0.17	-0.12	-0.13	0.05	-0.03	0.08
08002202002	AUSABLE RIVER	864.30	43.07	-81.66	0.27	-0.02	0.32	0.02	-0.14	0.75	-0.18	0.01	0.57
08002201002	LITTLE AUSABLE RIVER	141.95	43.18	-81.45	0.64	-0.39	-2.82	-0.12	-0.09	0.52	-0.46	0.03	0.44
08002201602	AUSABLE RIVER	113.68	43.36	-81.51	0.09	-0.03	0.09	0.00	0.01	-0.02	-0.10	0.05	-0.01
08004000802	BAYFIELD RIVER	462.02	43.55	-81.59	0.19	-0.01	0.57	0.38	-0.21	-0.12	-0.43	0.13	0.42
08005603702	SOUTH MAITLAND RIVER	372.57	43.68	-81.54	0.36	-0.01	0.24	-0.04	0.03	0.79	-0.61	0.06	0.38
08005603902	MIDDLE MAITLAND RIVER	656.04	43.84	-81.32	0.61	-0.37	-1.97	0.54	-0.63	-2.86	-0.28	0.02	0.72
08012303002	SAUGEEN RIVER	3941.28	44.46	-81.33	0.01	0.01	0.58	-0.02	0.02	0.41	-0.07	0.04	0.41
08012305102	SOUTH SAUGEEN RIVER	613.11	44.10	-80.99	-0.01	0.04	0.69	0.00	-0.08	0.06	-0.44	0.06	0.28
08012305702	SAUGEEN RIVER	312.77	44.19	-80.79	-0.03	-0.02	-0.06	-0.07	0.04	0.49	-0.07	0.00	0.31
08013500502	SAUBLE RIVER	312.91	44.54	-81.18	0.79	-1.47	-8.09	0.11	-0.15	0.78	-0.30	0.02	0.79
08013500302	SAUBLE RIVER	911.13	44.68	-81.26	0.03	-0.09	0.22	-0.79	0.11	0.17	-0.47	0.04	0.19
03001600302	SYDENHAM RIVER	182.58	44.52	-80.93	-0.26	0.02	-0.13	-0.07	-0.05	-0.08	-0.05	0.01	0.18
03003000202	BIGHEAD RIVER	294.33	44.57	-80.65	-0.13	0.03	0.63	-0.50	0.08	0.00	-0.35	0.02	0.39
03003601002	BEAVER RIVER	603.28	44.52	-80.47	0.08	-0.21	0.33	0.00	-0.02	0.24	-0.13	0.05	0.25
03003600902	BEAVER RIVER	279.32	44.35	-80.54	-0.02	0.00	0.74	-0.01	0.02	-0.06	0.00	-0.01	-0.21
03005702802	NOTTAWASAGA RIVER	175.97	44.02	-79.97	-0.03	0.01	0.17	-0.05	0.10	0.04	0.21	-0.05	-0.08
03005702902	NOTTAWASAGA RIVER	1230.39	44.25	-79.82	-0.04	0.09	0.00	0.24	-0.17	0.48	0.10	-0.05	0.36
03007000402	WYE RIVER	122.80	44.65	-79.90	0.01	0.01	0.40	-0.05	-0.02	0.53	-0.05	-0.02	0.59
03007300202	HOG CREEK	58.98	44.73	-79.78	-0.17	0.00	0.25	-0.11	0.00	0.39	-0.11	0.06	0.35
03007600302	COLDWATER RIVER	169.55	44.71	-79.64	0.04	-0.01	0.47	0.46	-0.17	-1.02	0.49	-0.22	-1.73
03007600502	NORTH RIVER	244.25	44.77	-79.58	-0.01	0.02	0.39	0.01	-0.02	0.35	-0.02	0.00	0.46
03007703902	HOLLAND RIVER	174.73	44.09	-79.49	-0.04	0.02	0.72	-0.08	0.04	0.05	-0.16	-0.01	0.31
14002800302	JUNCTION CREEK	204.40	46.43	-81.10	0.05	-0.04	0.17	0.01	-0.07	0.53	-0.06	0.04	0.00
08005600302	MAITLAND RIVER	1653.62	43.90	-81.35	0.30	-0.02	0.44	0.21	-0.13	0.62	-0.27	-0.01	0.62

Table A.6. Summary of sampled water quality stations across the Great Lakes. FluxB, PBS, and NSE are the Flux-bias, Percent Bias, and Nash-Sutcliffe, respectively.

WQ station	River Name	Drainage Area (km^2)	LAT	LONG	Nitrate-N			SRP			TP		
					FluxB	PBS	NSE	FluxB	PBS	NSE	FluxB	PBS	NSE
040854592	FISHER CREEK	27.61	43.83	-87.83	0.08	-0.05	0.30	-	-	-	-0.03	0.01	0.06
WIDNR_WQX-343033	WOLF RIVER	1220.51	45.19	-88.73	-0.01	-0.02	0.73	-	-	-	-	-	-
STOCKBRIDGE_MUNSEE-RR3	RED RIVER GAGE	309.14	44.90	-88.84	0.00	0.01	0.89	-	-	-	-	-	-
WIDNR_WQX-383001	PESHTIGO WI	2940.37	45.05	-87.75	-0.04	0.01	0.77	-	-	-	-	-	-
WIDNR_WQX-243020	FOX RIVER	3419.13	43.95	-88.95	-0.05	-0.01	0.86	-	-	-	-	-	-
WIDNR_WQX-313038	KEWAUNEE RIVER	322.62	44.46	-87.56	0.27	0.00	0.29	-	-	-	-	-	-
WI_MMSD-RI-01S	MILW. RIVER	1548.54	43.28	-87.94	-0.01	0.00	0.45	-	-	-	-	-	-
WI_MMSD-RI-16S	MENOM. RIVER	78.52	43.19	-88.13	0.02	0.02	0.68	-	-	-	-	-	-
WI_MMSD-ML-02S	GOOD HOPE RD.	47.26	43.15	-88.03	0.35	-0.22	-0.04	-	-	-	-	-	-
WI_MMSD-RI-09S	MENOM. RIVER	319.76	43.05	-88.00	0.07	0.00	0.34	-	-	-	-	-	-
WI_MMSD-RI-11B	MENOM. RIVER	357.68	43.03	-87.93	-0.08	-0.03	0.62	-	-	-	-	-	-
WI_MMSD-RI-13S	KINICK. RIVER	51.83	43.00	-87.92	0.28	-0.11	0.14	-	-	-	-	-	-
WI_MMSD-RI-35S	WILSON PARK CREEK	29.65	42.99	-87.95	0.19	-0.04	0.05	-	-	-	-	-	-
INSTOR_WQX-2004	-	4965.22	41.08	-85.02	0.06	-0.02	0.07	-	-	-	-	-	-
21OHIO_WQX-500040	-	900.35	41.06	-83.69	0.08	-0.02	-0.03	-	-	-	-	-	-
MNPCA-S005-115	-	1132.46	46.63	-92.09	0.02	0.00	0.45	-	-	-	-	-	-
04219768	EIGHTEENMILE CREEK	219.23	43.31	-78.72	-	-	-	0.00	-0.01	0.45	-0.17	0.01	0.38
04220045	OAK ORCHARD CREEK	351.39	43.17	-78.39	-	-	-	0.09	-0.12	0.36	0.15	-0.17	0.20
0422016550	OAK ORCHARD CREEK	505.53	43.30	-78.31	-	-	-	0.01	-0.01	0.39	-0.06	0.00	0.55
0422026250	NORTHRUP CREEK	26.34	43.25	-77.74	-	-	-	0.17	-0.16	0.43	0.08	-0.04	0.07
04229500	HONEOYE CREEK	505.30	42.96	-77.59	-	-	-	-0.04	-0.01	0.18	-0.17	0.03	0.24
04230500	OATKA CREEK	524.84	43.01	-77.79	-	-	-	-0.04	0.03	0.28	0.04	0.02	0.19
04231000	BLACK CREEK	353.75	43.10	-77.88	-	-	-	-0.04	-0.01	0.47	-0.08	0.01	0.14
04232034	IRONDEQUOIT CR	100.83	43.03	-77.48	-	-	-	0.02	0.02	0.03	0.03	0.08	0.00
04232050	ALLEN CREEK	78.22	43.13	-77.52	-	-	-	-0.01	-0.06	0.44	-0.42	0.05	0.12
0423205010	IRONDEQUOIT CR	357.09	43.15	-77.51	-	-	-	-0.12	0.03	0.12	0.11	-0.01	0.21
0423205025	IRONDEQUOIT CREEK	382.02	43.18	-77.53	-	-	-	-0.02	0.03	0.20	0.01	-0.01	0.42
04250200	SALMON RIVER	621.25	43.53	-76.04	-	-	-	0.00	0.02	-0.09	0.10	-0.01	-0.14
04083420	PARSONS CREEK	13.05	43.69	-88.47	-	-	-	0.14	-0.13	0.13	-0.05	0.03	0.38
04083425	PARSONS CREEK	14.00	43.70	-88.48	-	-	-	0.09	-0.04	-0.09	-0.02	0.02	0.32
MAUMEE	MAUMEE RIVER	17057.00	41.29	-84.28	-	-	-	0.00	-	-	0.00	-	-
04099000	ST. JOSEPH RIVER	4883.62	41.80	-85.76	-	-	-	-	-	-	-0.04	-0.01	0.13
04116000	GRAND RIVER	7580.48	42.97	-85.07	-	-	-	-	-	-	-0.02	-0.01	0.58

Table A.7. Summary of sampled water quality stations across the Great Lakes. FluxB, PBS, and NSE are the Flux-bias, Percent Bias, and Nash-Sutcliffe, respectively.

WQ station	River Name	Drainage Area (km^2)	LAT	LONG	Nitrate-N			SRP			TP		
					FluxB	PBS	NSE	FluxB	PBS	NSE	FluxB	PBS	NSE
04122500	PERE MARQUETTE RIVER	1813.54	43.95	-86.28	-	-	-	-	-	-	0.00	0.00	0.16
04145000	SHIAWASSEE RIVER	1615.19	43.25	-84.11	-	-	-	-	-	-	-0.06	-0.01	0.79
04149000	FLINT RIVER	3096.74	43.31	-83.95	-	-	-	-	-	-	-0.05	0.01	-0.04
04073458	ROY CREEK	12.70	43.77	-89.02	-	-	-	-	-	-	-0.08	-0.01	0.18
040734605	GREEN LAKE	39.29	43.78	-89.06	-	-	-	-	-	-	0.04	0.00	0.24
04073462	WHITE CREEK	6.73	43.82	-88.93	-	-	-	-	-	-	-0.40	0.20	0.26
04073466	SILVER CREEK	124.67	43.84	-88.91	-	-	-	-	-	-	-0.06	-0.01	0.27
04073468	GREEN LAKE	149.40	43.82	-88.93	-	-	-	-	-	-	-0.09	0.00	0.15
04073500	FOX RIVER	3419.13	43.95	-88.95	-	-	-	-	-	-	-0.03	0.00	0.62
04085046	APPLE CREEK	121.91	44.35	-88.19	-	-	-	-	-	-	-0.09	0.03	0.29
04085068	ASHWAUBENON CREEK	51.50	44.41	-88.13	-	-	-	-	-	-	0.09	0.04	0.01
040851325	BAIRD CREEK	58.06	44.50	-87.94	-	-	-	-	-	-	0.07	0.04	0.09
04086500	CEDAR CREEK	300.96	43.32	-87.98	-	-	-	-	-	-	0.01	0.02	0.61
04086600	MILWAUKEE RIVER	1548.54	43.28	-87.94	-	-	-	-	-	-	0.02	0.06	0.10
04087030	MENOMONEE RIVER	87.96	43.17	-88.10	-	-	-	-	-	-	0.08	0.05	0.07
04087088	UNDERWOOD CREEK	47.90	43.05	-88.05	-	-	-	-	-	-	0.09	0.08	0.06
04087119	HONEY CREEK	27.65	43.04	-88.01	-	-	-	-	-	-	0.15	-0.02	0.08
04087120	MENOMONEE RIVER	319.78	43.05	-88.00	-	-	-	-	-	-	0.08	0.00	0.12
04087159	KINNICKINNIC RIVER	48.13	43.00	-87.93	-	-	-	-	-	-	-0.02	0.08	0.03
04084911	PLUM CREEK	55.41	44.31	-88.17	-	-	-	-	-	-	-0.04	-0.01	0.30
04087142	MENOMONEE RIVER	356.08	43.03	-87.93	-	-	-	-	-	-	-0.17	0.06	0.24
04083545	FOND DU LAC RIVER	456.17	43.79	-88.46	-	-	-	-	-	-	0.09	-0.02	0.72
04072845	MONTELLO RIVER	334.21	43.82	-89.37	-	-	-	-	-	-	-0.02	0.02	0.30
04073473	PUCHYAN RIVER	277.92	43.86	-88.95	-	-	-	-	-	-	0.00	-0.01	0.29
04073970	WAUKAU CREEK	218.91	44.02	-88.79	-	-	-	-	-	-	0.01	0.03	0.29
040851378	EAST RIVER	381.57	44.52	-88.01	-	-	-	-	-	-	0.06	0.09	-0.04
04085119	BOWER CREEK	36.00	44.42	-87.94	-	-	-	-	-	-	0.01	0.00	0.52

Appendix B – Summary of Gridded Data Sources

Table B.1. Summary of Data Sources for selected catchment characteristics

Data Variable(s)	Title	Spatial Coverage	Author(s)/Organization
Land-use (Agriculture, Forested, Urban, Wetlands, etc.)	Annual Crop Inventory (2015)	Ontario	Agriculture and Agri-Food Canada
Land-use (Agriculture, Forested, Urban, Wetlands, etc.)	National Land Cover Database (2011)	U.S.	Multi-Resolution Land Characteristics (MRLC) Consortium
Soil Texture (Percent Sand, Silt, and Clay)	Harmonized World Soil Database	Global	Food and Agriculture Organization of the United Nations (FAO), International Institute for Applied Systems Analysis (IIASA), ISRIC-World Soil Information, Institute of Soil Science – Chinese Academy of Sciences (ISSCAS), Joint Research Centre of the European Commission (JRC)
Soil Texture (Percent Sand, Silt and Clay)	Detailed Soil Survey (DSS)	Ontario	National Soil Database (NSDB)
Soil Texture (Percent Sand, Silt and Clay)	Area- and Depth-Weighted Averages of Selected SSURGO Variables for the Conterminous United States and District of Columbia	U.S.	Michael E. Wieczorek, USGS-WRD MDWSC, Geographer
Tile Drainage Percentages	Tile Drainage Area shapefile	Ontario	Ontario Ministry of Agriculture, Food and Rural Affairs (OMAFRA)
Tile Drainage Percentages	Tile Drainage Area shapefile	U.S.	USDA, NASS, 2012 Census of Agriculture
Climate (Precipitation and Temperature)	Worldclim 2: New 1-km spatial resolution climate surfaces for global land areas (1970-2000)	Global	Fick, S.E. and R.J. Hijmans, 2017
Slope	Ontario Flow Assessment Tool (OFAT)	Ontario	Ministry of Natural Resources and Forestry
Slope	Hydrologic Landscape Regions of the US	U.S.	Wolock, D.M., Thomas, C.W., Gerard, M.
Population Density	Ontario Population 2011 Census data	Ontario	UWaterloo Geospatial Center Library
Population Density	Sub-County 2010 Census data	U.S.	United States Census Bureau

Appendix C – Normal probability plots of residuals from MLR models used to estimate FWC across the Great Lakes Watersheds

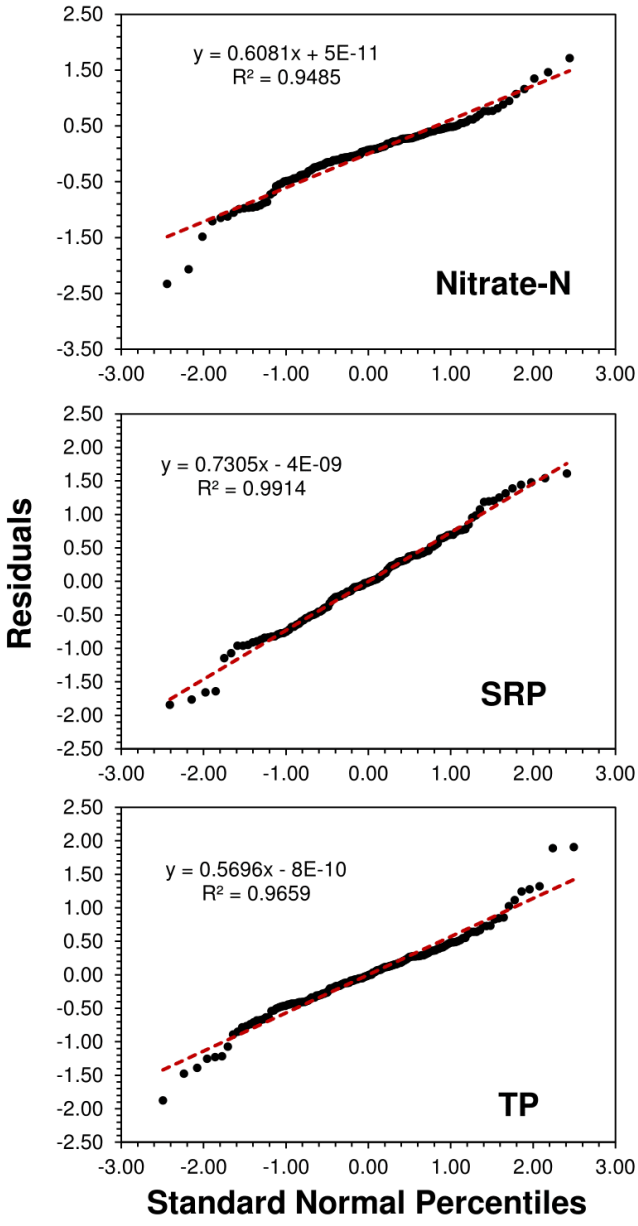

Figure C.1 Normal probability plots of MLR model residuals for nitrate-N, SRP and TP.